UNIVERSIDAD DE SEVILLA

TESIS DOCTORAL

Statistical analysis of different seismogenic zonings of the Iberian Peninsula and adjacent areas through a Geographic Information System

José Lázaro Amaro Mellado

Programa de Doctorado en Arquitectura (RD 99/2011)

Sevilla, junio de 2019

UNIVERSIDAD DE SEVILLA

Departamento de Estructuras de Edificación e Ingeniería del Terreno

Statistical analysis of different seismogenic zonings of the Iberian Peninsula and adjacent areas through a Geographic Information System

Memoria que presenta José Lázaro Amaro Mellado

para optar al grado de doctor por la Universidad de Sevilla

Directores:

Dr. Antonio Morales Esteban

Dpto. de Estructuras de Edificación e Ingeniería del Terreno

Universidad de Sevilla

Dr. Francisco Martínez Álvarez

Data Science & Big Data Lab

Universidad Pablo de Olavide

Sevilla, junio de 2019

Dr. Antonio Morales Esteban, profesor Contratado Doctor adscrito al Departamento de Estructuras de Edificación e Ingeniería del Terreno de la Universidad de Sevilla y **Dr. Francisco Martínez Álvarez**, profesor Titular de Universidad **adscrito** al Data Science & Big Data Lab de la Universidad Pablo de Olavide,

CERTIFICAN QUE:

José Lázaro Amaro Mellado, ha realizado bajo su supervisión el trabajo de investigación titulado:

STATISTICAL ANALYSIS OF DIFFERENT SEISMOGENIC ZONINGS OF THE IBERIAN PENINSULA AND ADJACENT AREAS THROUGH A GEOGRAPHIC INFORMATION SYSTEM

Una vez revisado, autorizan la presentación del mismo como tesis doctoral en la Universidad de Sevilla y estiman oportuna su presentación al tribunal para su valoración. Dicha tesis ha sido realizada dentro del Programa de Doctorado en Arquitectura.

Igualmente, autorizan la presentación para obtener la Mención de Doctorado Internacional.

Sevilla, junio de 2019

Antonio Morales Esteban

Francisco Martínez Álvarez

Tesis doctoral parcialmente subvencionada por la Unión Europea a través del Proyecto Interreg 0313 ”Projetos de Escolas Resilientes aos Sismos no Território do Algarve e de Huelva – PERSISTAH” y el Data Science and Big Data Lab de la Universidad Pablo de Olavide.

Agradecer al *Centro de Investigaçao Marinha e Ambiental* de la *Univerdade do Algarve* por haberme invitado a realizar una estancia de investigación en Portugal.

Finalmente, agradecer las facilidades que me ha concedido para el desarrollo de esta tesis doctoral al Instituto Geográfico Nacional, organismo en el que desarrollo mi actividad desde 2005.

AGRADECIMIENTOS

El camino que desemboca en el depósito de este trabajo se ha hecho más llevadero, e incluso diría que ha sido posible, gracias a colaboración y ayuda de un gran número de personas, entre las que se incluyen todas las olvidadas en estas líneas, que ruego me perdonen.

En primer lugar me gustaría manifestar gratitud a mi tutor, Dr. Percy Durand Neyra, y profundamente a mis directores, Dr. Antonio Morales Esteban y Dr. Francisco Martínez Álvarez que me han educado y guiado en el mundo de la publicación científica a través de la cual llego a este documento. Su ánimo, capacidad crítica, inconformismo y tesón no solo me han ayudado para desarrollar esta tesis sino que su huella perdurará para vislumbrar un horizonte científico halagüeño.

Por otro lado, no sería justo obviar el apoyo recibido por mis compañeros del Instituto Geográfico Nacional, tanto en el Servicio Regional en Andalucía como en los Servicios Centrales. Mención especial para los jubilados Antonio Nuevo, mi compañero de Sevilla, por ser siempre un apoyo fundamental en el día a día matutino; y Antonio Jesús Martín Martín, por su sabio asesoramiento así como por su cariño y paciencia conmigo.

El apoyo y ánimo de mis compañeros del Departamento de Ingeniería Gráfica de la Universidad de Sevilla me ha resultado muy útil y reconfortante a lo largo de estos años de investigación.

También me gustaría agradecer al *Centro de Investigaçao Marinha e Ambiental* de la *Univerdade do Algarve.* En especial al Dr. João Manuel Carvalho Estêvão por acogerme y darme la oportunidad de tener otro enfoque sobre la investigación desarrollada que espero pronto dé sus frutos en forma de publicaciones.

Además, dar las gracias al Dr. Peláez de la Universidad de Jaén por los consejos dados. En el lado más personal y menos académico, el cariño, aliento y apoyo de mis amigos ha servido de refuerzo para no cejar en mi empeño de desarrollar

y concluir esta tesis doctoral. Leo, Pedro, Isa, Jesús, Miguel Ángel, Ana, Dani, etc.

Finalmente, quisiera pedir perdón a mis mujeres y mujercitas por haberos hurtado tanto tiempo a lo largo de estos años de investigación. Gracias hermana, gracias tita-madre Alicia y sobre todo a vosotras, mi día a día, a mi mujer Elisa y a mis hijas Lucía y Alicia.

Desafortunadamente, a mis padres no les he podido robar nada de este tiempo, como me habría y te habría gustado, papá. El horizonte que definiste me acompaña desde que te fuiste, aunque yo no me haya dado cuenta durante gran parte del tiempo.

De nuevo, gracias.

ABSTRACT

The knowledge of the seismic hazard in the Iberian Peninsula (IP) and its neighboring area is important to address the mitigation of damage that earthquakes could cause in it. The occurrence of earthquakes in the area is quite frequent because it is in the contact zone between the Eurasian Plate and the African Plate.

The general objective of this document is the calculation, representation and analysis of a set of seismic parameters (*b*-value, maximum magnitude and annual rate of earthquakes per unit area) of the Iberian Peninsula and its adjacent area, considering geographic information systems (GIS) as a basic working tool. These systems allow the integration of data from different information sources, as well as rigorous and quality analysis and graphical representations.

To achieve this goal, having a quality seismic catalog is essential. Therefore, one has been compiled for the area as complete, rigorous and extensive in the time possible, and further, revised, homogeneous in size (magnitude) and with independent events. This has served as the basis for the works exposed here. For the generation of this catalog, the database of earthquakes of the National Geographic Institute of Spain has been consider as a starting point, that has been revised (especially the magnitude) and completed with other databases and specific studies. In addition, the catalog of work has included earthquakes for which only macroseismic (and reliable) information is available as well as those recorded during the instrumental period according to the scientific advances of each moment. Then, the size of all the events has been transformed to moment magnitude (M_w) in order to compare it, taking into account only the events with M_w greater or equal to 3.0. Subsequently, a process of elimination of non-main shocks (foreshocks, aftershocks and swarms) has been carried out. Finally, a completeness date has been considered for each magnitude.

In this thesis, the *b*-value, the annual rate of earthquakes per unit area and the maximum magnitude have been calculated, represented and analyzed. In

addition, it has been done through two approaches. The first deals with zoning related to Spanish seismic regulations and are based on both geological characteristics and seismicity of the area; and others that are based on objective and mathematically robust criteria and considers only seismicity. In the second approach, a set of multiresolution grids have been established, in which zonings are defined according to a purely geographic criterion. The size of the cells (zones) has been 0.5º x 0.5º for the calculation of the maximum magnitude recorded and 1º x 1º and 2º x 2º for the b-value and the annual rate normalized with the area.

In both types of zoning, after the calculations and the representation of the seismic parameters, an analysis of them has been carried out. From this analysis it can be deduced that in some areas there has not been a quantity of events that allows to derive seismic parameters with solidity from a statistical point of view. It can also be concluded that earthquakes with maximum recorded magnitude have a marine epicenter and are located in the SW of the IP. Moreover, the *b*-value takes a value of 1.0 or somewhat lower in the contact zone between the Eurasian and African plates (a value that decreases further to the east), while in the mainland, 1.2 can be considered an approximate value, with somewhat higher values in some areas. Finally, regarding the annual rate, it should be noted that the highest values (close to 1E-3 events / km^2) appear in the Granada basin and in the Pyrenees Region and to a lesser extent, to the SW of Cabo de San Vicente, in Galicia and a large part of the southeast of the IP where values greater than 1E-4 are exceeded.

RESUMEN

El conocimiento de la peligrosidad sísmica en la península ibérica y su entorno es importante para abordar la mitigación de los daños que los terremotos podrían causar en la misma. La ocurrencia de terremotos en el área es bastante frecuente porque se encuentra en la zona de contacto entre la placa euroasiática y la africana.

El objetivo general de esta tesis doctoral es el cálculo, representación y análisis de un conjunto de parámetros que intervienen en la definición de la peligrosidad sísmica de la península ibérica y su área adyacente, considerando como herramienta básica de trabajo los sistemas de información geográfica. Estos permiten la integración de datos de distintas fuentes de información, así como el análisis y representaciones gráficas rigurosas y de calidad.

Para la consecución de este objetivo, el disponer de un catálogo sísmico de calidad es fundamental. Por tanto, se ha compilado uno para la zona lo más completo, riguroso y extenso en el tiempo posible y además, revisado, homogéneo en tamaño (magnitud) y con eventos independientes. Este ha servido como base para los trabajos que aquí se exponen. Para la generación del mismo, se ha partido de la base de datos de terremotos del Instituto Geográfico Nacional de España, que se ha visto revisada (sobre todo la magnitud) y completada con otras bases de datos y estudios específicos. Además, en el catálogo del trabajo se han incluido, desde terremotos de los que únicamente se dispone de información macrosísmica (y fiable) como los registrados durante la época instrumental según los avances científicos de cada momento. Luego, se ha transformado el tamaño de todos los eventos a magnitud momento (M_w) para poder compararlo, tomando solo los eventos con M_w mayor o igual a 3,0. Posteriormente, se ha llevado a cabo un proceso de eliminación de terremotos no principales (premonitores, réplicas y enjambres). Finalmente, se ha considerado una fecha de completitud para cada magnitud.

En esta tesis se han calculado, representado y analizado el parámetro *b-value*, la tasa anual de terremotos por unidad de área y la magnitud máxima. Además, se

ha hecho a través de dos aproximaciones. La primera versa sobre zonificaciones relacionadas con la normativa sismorresistente española y basadas tanto en las características geológicas como en la sismicidad de la zona; y por otras que parten de criterios objetivos y robustos matemáticamente y están basadas solo en la sismicidad. En la segunda aproximación, se han establecido un conjunto de mallas multirresolución, en las que las zonificaciones son definidas según un criterio puramente geográfico. El tamaño de las celdas (zonas) ha sido de 0,5º x 0,5º para el cálculo de la magnitud máxima registrada y de 1º x 1º y 2º x 2º para el del *b-value* y la tasa anual normalizada con el área.

En ambos tipos de zonificaciones, tras los cálculos y la representación de los parámetros sísmicos, se ha llevado a cabo un análisis de los mismos. De este se deduce que en algunas zonas no ha ocurrido una cantidad de eventos que permita extraer parámetros sísmicos con solidez desde un punto de vista estadístico. También se puede concluir que los terremotos con magnitud máxima registrada tienen epicentro marino y se encuentran al suroeste de la península ibérica. Por otro lado, el *b-value* toma un valor de 1,0 o algo menor en la zona de contacto entre las placas euroasiática y africana (valor que disminuye más al este), mientras que en tierra firme como valor aproximado se puede considerar 1,2, con valores algo mayores en algunas zonas. Finalmente, respecto a la tasa anual de terremotos, cabe comentar que los valores más altos (cercanos a 1E-3 eventos / km^2) aparecen en la cuenca de Granada y en la región de los Pirineos y, en menor medida al SO del Cabo de San Vicente, en Galicia y gran parte del sureste peninsular donde se superan valores mayores a 1E-4.

Table of contents

List of figures

List of tables

Chapter 1.
Introduction

The aim of this doctoral thesis is the calculation, representation and analysis of some of the main parameters that intervene in the definition of the seismic hazard of the Iberian Peninsula and its closest environment. This knowledge is relevant for the mitigation of damage caused by earthquakes in the Iberian Peninsula. To this end, a specific geographic information system (GIS) has been designed that allows, by means of georeferencing, an optimum integration and management of geographic and seismotectonic data. Before presenting these works, the general framework within which they are framed is set out.

1.1. BACKGROUND

In the study of earthquakes, it is possible to distinguish between the analysis and the parameters corresponding to their area of origin (focal region), which is what is called seismicity. This is the study of the size and spatial distribution of ground movement caused by the earthquake (displacement, speed and acceleration), known as seismic hazard and generally expressed by its maximum values, and the study of the effects of this movement on the population, the infrastructure and the environment, which is what is called seismic risk.

The action produced by some natural phenomena means a risk that can give rise to physical, human, economic and environmental damage and losses. One of the phenomena that cause the greatest damage, both material and personal, are earthquakes. These are brought about by a sudden rupture along crustal faults, which causes the consequent release of energy. Part of this takes the form of elastic waves that produce ground movements, which is what is commonly referred to as an earthquake. Usually, these ruptures take place in the areas close to the contact between tectonic plates, although in some cases they occur within the same plate (intra-plate phenomena). The occurrence of these ruptures is linked to the area's seismotectonic framework.

In order to determine an area's seismic risk, it is necessary to perform the convolution between seismic hazard, vulnerability and exposure. One way of

expressing risk is in terms of cost, such as the probability that an earthquake will cause certain economic losses and loss of life. So:

Risk = Hazard * Exposure * Vulnerability (*Cost)

Of these factors, exposure refers to the number and value of exposed elements that can therefore be damaged by seismic hazard, which is linked to spatial planning and urban planning. These elements can be the population, the infrastructure, the environment, buildings, etc.

Next, vulnerability concerns the ability of these elements to withstand seismic excitation. In the case of buildings and infrastructures, this depends on their calculation and design, both in terms of materials and the geometric configuration of the structural elements.

To finish with the factors, the last that intervenes in the seismic risk is the seismic hazard, the only one that does not depend on human action (except in the case of induced seismicity). This thesis focuses on the study of some parameters that characterize seismic hazard in the geographical area of the Iberian Peninsula and its adjacent area.

After treating seismic risk and its factors, it becomes necessary to address how the size of earthquakes is expressed, given their importance within seismic parameter studies. The size is normally defined either by the magnitude, the seismicity parameter linked to the energy released at the rupture, or by the macroseismic intensity, the risk parameter thus related to the effects of the earthquake. These two parameters refer to two different concepts and are sometimes misinterpreted by the non-specialized literature, which tends to express non-integer values of intensity, such as "intensity 5.1 earthquake". As will be seen later, this is not correct. In addition, another way to measure the size of earthquakes is the seismic energy itself (contained in the seismic waves), which has a special implication in the study of seismic series, since it is possible to add that of several events and thus calculate the accumulated seismic energy.

The magnitude is a focal parameter, unique for each earthquake, proportional to the released energy whose size, registered and measured instrumentally, responds to continuous and theoretically unlimited values, although until now no earthquake has surpassed that of Chile in 1960, whose magnitude reached 9.5 (M9.5). This is measured by means of various magnitude

scales, depending on the waves on which it is based and on how it is determined and calculated. Thus, one can speak of the magnitude of internal waves, local waves, surface waves, etc. At present, the most suitable is the so-called moment magnitude (M_w) (Hanks and Kanamori, 1979), directly linked to the energy released at the rupture. This moment magnitude is especially recommended for large earthquakes, since it has the advantage that its value is not saturated as a function of the energy released, as is the case with the generality of other magnitude scales.

As has been mentioned before, the intensity alludes to the measurement of the effects caused by the earthquake, which depend on the movement of the ground (hazard). This is quantified by means of the so-called intensity degree scales which, unlike magnitude scales, are discrete (represented by Roman numerals), empirical and of a limited number of degrees. In addition, the same earthquake causes different effects depending on the location considered, on the distance to the epicenter (vertical projection on the terrestrial surface of the earthquake focus), the attenuation of seismic waves, the ground effect, etc. In principle, the closer the epicenter is to the point under consideration, the greater the observed intensity will be, with the epicenter generally being the maximum. The intensity assigned to an earthquake in the catalogs corresponds to the maximum recorded, generally in the epicenter (epicentral intensity). Of special importance for earthquakes with a marine epicenter is the consideration of corrections based on attenuation (in which the maximum intensity recorded on land will in most cases be lower than the hypothetical epicentral intensity) since it is not possible to quantify the effects of the earthquake in the sea (López-Casado et al., 2000).

The devastating effects of earthquakes worldwide are well known. Although not exhaustive, regions that have suffered strong seismic shocks in recent years can be cited. In 2017, Mexico M7.1; in 2016, Ecuador M7.8; in 2015, Nepal M7.8; in 2011, Japan M9.0 with tsunami and nuclear disaster. In 2010, Haiti M7.0 and in 2004, Sumatra-Andamán M9.1 (with tsunami) events took place that caused more than 200,000 deaths. Closer to the area of study of this paper are several relatively high magnitude earthquakes that occurred recently in Italy, in 2009 M6.3 and 2016 M6.2.

The Iberian Peninsula, with an approximate extension of 580,000 km^2, is located in the southwest of the continental zone of the Eurasian plate. Its southernmost area is in contact with the African plate with which it presents a relative movement between the two with an estimated displacement rate of between 2 and 5 mm per year, according to a NW-SE to WNW-ESE (IGN-UPM WG, 2013), which conditions the seismotectonic framework. Figure 1.1 presents the seismotectonic context map.

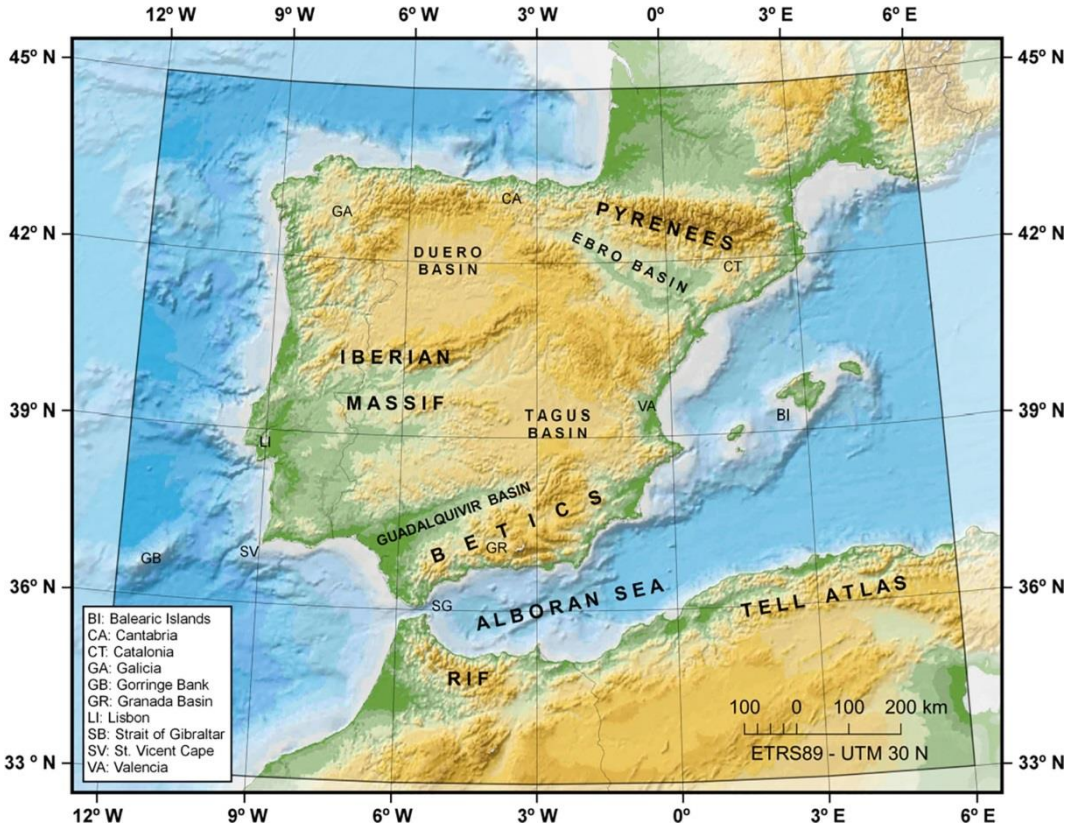

Figure 1.1. Context map. Source: Amaro-Mellado et al. (2017)

The seismic activity of the Peninsula and adjacent areas is considered moderate-low, despite which, historically, some very important earthquakes have occurred. These have taken place both in the interior of the Peninsula and in the surrounding sea. Some have been really catastrophic, especially in the southwest of the Peninsula, as for example the earthquake of Lisbon 1755 M8.7 and, more recently, another also to the southwest of Cape St. Vincent in 1969 M7.9. Also noteworthy are others closer, such as the earthquakes in the north of Algeria in 2003 M6.8 or Al Hoceima in the north of Morocco 2004 M6.3. Even with an

epicenter in the mainland, historically quite harmful events have taken place (IGN, 2019a), such as the earthquake of Andalusia in 1884 M6.8, Torrevieja in 1829 M6.6, Malaga in 1680 M6.5 or the earthquake of Carmona in 1504 M6.8. Very recently, in 2011, an earthquake took place in Lorca (Murcia) with a moderate magnitude M5.1 but which caused the lives of nine people, and also losses of millions of euros.

When carrying out a seismic hazard analysis, it would be ideal to have a good knowledge of the seismotectonic framework, made up of the seismicity and of the distribution of faults.

In the case of the Iberian Peninsula, despite the invaluable effort that is being made in the knowledge of faults that generate seismic activity, the information relating to these elements is still definitely incomplete at a peninsular level. Especially relevant are the works promoted by the Geological and Mining Institute of Spain (*Instituto Geológico y Minero de España*, *IGME*), specifically the compilation Quaternary Active Faults database of Iberia (QAFI). Its latest public version of which is QAFI v.3 (IGME, 2015), in which the *Laboratorio Nacional de Energia e Geologia* (*LNEG*, Portugal), among others, has collaborated.

After studying the available research, it has been considered convenient to conduct a deeper analysis of some of the most influential seismic parameters of several seismic zonings proposed by various researchers, as well as to obtain the parameters according to a zoning in the form of a purely geometric grid. Thus, the body of this thesis includes two different approaches to address the issue. Previously a rigorous, revised and homogeneous catalog must be compiled, from the National Geographic Institute of Spain (hereinafter, NGIS) (*Instituto Geográfico Nacional, IGN*) earthquake database. As general tool a GIS is used, among other tasks, to integrate heterogeneous geographical data, make high quality representations and performing analysis.

On the one hand, seismic parameters are calculated, represented and analyzed starting from the seismic zoning considered most relevant. On the other hand, the calculation and representation of those same seismic parameters is carried out starting in this case, instead of with a predefined zoning, with a zoning in the form of a pseudorectangular multiresolution grid (0.5º x 0.5º, 1º x 1º, 2º x 2º), by means of a network of parallels and meridians covering the working

environment, in a similar way to that proposed in Mapa Sismotectónico WG (1992).

1.2. OBJECTIVES

The general objective of this work is to calculate, represent and analyze a series of seismic parameters (the *b*-value, maximum magnitude and mean annual seismic activity rate per unit area) for the Iberian Peninsula and its environment using a GIS as a fundamental tool. This general aim can be achieved through several specific objectives.

Therefore, a first specific objective, and a starting point for the rest, is to generate a reviewed seismic catalog, homogeneous in magnitude and with independent events for the Iberian Peninsula and its surroundings. This must include both earthquakes for which only macroseismic information is available, as well as those of the pre-instrumental stage and, finally, those recorded during the purely instrumental period. Given that the recurrence periods of major events in the Iberian Peninsula are at least hundreds of years, valuable information on the size of ancient earthquakes (provided it is of sufficient quality to be considered reliable) cannot be discarded from the calculation. In order for events to be comparable, the magnitude of all of them must be homogeneous, so to convert the size of all earthquakes to M_w has been chosen for the reasons noted above. This aim will be treated in Chapter 3.

The second objective is to calculate and represent the parameters of seismic hazard of different seismic zoning proposed for the Iberian Peninsula and its environment. As a source of information, in addition to the geometry of these seismic zonings and the seismic catalog, the QAFI database has been used. In order to achieve this objective, a method must be used that takes into account both the heterogeneity of the seismic detection networks (through geometric sectoring of the completeness year) and the existence of earthquakes throughout the different periods (considering different couples of magnitude-years of completeness). This is fundamental given the importance, both in number and size, of the earthquakes recorded in the catalog of work over time, not only in the instrumental period but also in previous ones. Chapter 4 addresses this and the next one goal.

The third objective consists of analyzing different zonings such as those related to building seismic regulations, based on both the registered seismicity and on geological characteristics, as well as the zonings resulting from the establishment of objective criteria, centered exclusively on seismic catalogs (although validated with geology).

Finally, the fourth specific objective, that will be conducted in Chapter 5, is the calculation and graphical representation of the parameters mentioned continuously in space by means of multiresolution grids (0.5º x 0.5º, 1º x 1º, 2º x 2º) and considering a different minimum number of events per cell, to proceed or not to its calculation, and without pre-established previous zoning.

1.3. OUTLINE

The doctoral thesis is structured in seven chapters:

- ✓ This **Chapter 1** contains an introduction to the basic concepts related to seismic hazard as well as the framework in which it is framed, and presents the objectives, both general and specific, that are pursued with this doctoral thesis.

- ✓ **Chapter 2** deals with the fundamentals required to conduct a rigorous research. Thus, seismic catalogs, seismogenic zonings, fault databases, seismic hazard parameters and GIS concepts are treated.

- ✓ **Chapter 3** details the sequence of operations carried out to generate a revised, homogeneous and without non-main earthquakes seismic work catalog from the NGIS earthquake database.

- ✓ In **Chapter 4**, after compiling the working seismic catalog, this will be later used to calculate, represent and analyze different seismic hazard parameters of the seismic zonings of the Iberian Peninsula that have been considered the most relevant. It is based on Amaro-Mellado et al. (2017).

- ✓ **Chapter 5** describes the calculation, representation and analysis of the same hazard parameters considering multiresolution grids (0.5º x 0.5º, 1º x 1º, 2º x 2º) pseudorectangular ones -a network of parallels and meridians- that encompass the working environment instead of pre-defined zoning, from the generated catalog. It is based on Amaro-Mellado et al. (2018).

- ✓ **Chapter 6** lists the conclusions drawn from the work carried out.

- ✓ Finally, **Chapter 7** presents the contributions undertaken during PhD research period.

Chapter 2.
Fundamentals

For the understanding of subsequent chapters, several concepts such as a seismic catalog, seismogenic zones, seismic hazard parameters, fault database and geographic information systems should be presented.

2.1. SEISMIC CATALOGS

Seismic catalogs can be defined as databases in which various relevant parameters of earthquakes are collected, such as their epicentral location, date, time of origin, information on size (magnitude and/or macroseismic intensity depending on the available data), depth, etc. They can also collect information on the phases, focal mechanisms and quality parameters of the calculation, such as the uncertainty of the location, the number of stations considered during the calculation, etc.

In principle, continuous catalogs are available spatially (unlike what happened with the knowledge of faults), prepared by different institutions and at different times, whose quality is closely linked to the configuration and technology of the seismic detection network used for its determination. For a good evaluation of the seismic hazard, it is fundamental to have a quality seismic catalog, since practically all the parameters that are going to define it are going to be derived from it.

Normally, given the breadth of the scope of seismological studies, as well as the different organisms involved in the recording of seismic movements, it is necessary to review various databases in order to compile a catalog that is as complete as possible.

In this work, the catalog of the NGIS has been used as a starting point. This is considered to be the most continuous, homogeneous and stable one on the Iberian Peninsula and its contiguous zone. It contains earthquakes since 1373 (IGN, 2019b), as previous events may lack the reliability necessary for their integration into the catalog, so it covers more than 600 years (although until a few years ago much older earthquakes were also shown in it). However, the consideration of other sources of information, such as the catalogs of other seismic research centers, papers collected in the international scientific literature,

etc., enriches the starting point of the catalog both quantitatively and qualitatively. The way of obtaining the catalog of the work is detailed in Chapter 3.

2.2. SEISMOGENIC ZONES

When conducting a Probabilistic Seismic Hazard Analysis (hereinafter, PSHA), two types of sources or areas where earthquakes originate (or a hybrid of both) can be considered: faults (linear sources) and seismogenic zones (zonal sources). As an approximation, a seismogenic zone is a faulted region with homogeneous seismic and tectonic characteristics. It may consist of one or more faults or seismic structures. Depending on the degree of seismotectonic knowledge of the region and the size of the earthquakes, individualized faults or zones are usually chosen. In the case of large ruptures, the treatment is usually carried out from the thorough knowledge of the system of generating faults since it tends to be more viable. If the seismic activity is less energetic, it is more common to develop studies from seismic zonings.

Seismic source identification is characterized by great uncertainty and subjectivity. This is a problem faced from two sides: depicting the seismic sources and determining their parameters.

First, setting the limits of the seismic sources poses a great uncertainty. Generally, seismogenic zones have been obtained from the geological structures and the distribution of epicenters. In zones of moderate seismic activity, such as the IP, the catalog of earthquakes can be incomplete. Moreover, the geological structures considered cannot be related to the current tectonic regime (Martínez-Álvarez et al., 2015). The efforts of many authors have generated the idea that the same area can have as many different seismogenic zones as studies. The analysis of the thermal and resistant parameters may give a better method for depicting the seismogenic zones. Nevertheless, determining the rheological profiles is greatly uncertain.

Second, there is also a great uncertainty regarding the calculation of the seismic parameters of the seismogenic zones. Insufficient data or inappropriate methods are often used to calculate the seismic parameters.

In the Iberian Peninsula, the use of zoning has so far played a very important role, given that the maps of seismic hazard considered in Spanish Building Seismic Regulations have been defined from seismogenic zones. As an example, there are the proposals of García-Mayordomo et al. (2012b), of Bernal (2011) and, with slight modifications, of Martín (1984).

As commented before, in the fourth chapter the zones defined by different authors have been considered and, in the fifth, some zonings have been defined with a purely geographical criterion, by means of regular grid cells (0.5º x 0.5º, 1º x 1º, 2º x 2º).

The use of zonings with exclusively geographical criteria implies an objective contribution to the calculation of parameters, since these are not conditioned by limits defined a priori in a subjective manner. Thus, four 2º x 2º grids have been considered (the original one; one displaced 1º to the east; another 1º to the south; and finally, one displaced to the east and south); four grids of 1º x 1º, with displacements of 0.5º instead of 1º; and a grid of 0.5º x 0.5º, without overlaps. When working with overlaps between the different grids, the result shown is a combination of what was obtained with each one, so that the border effect between cells is mitigated. For more details see Chapter 5.

2.3. THE IBERIAN PENINSULA AND EXISTING PROPOSAL FOR SEISMOGENIC ZONINGS

As previously stated, the IP is on the border of the Eurasian Plate. The seismicity of this complex boundary is mainly due to the convergence between this plate and the African one. The ocean-ocean contact between these plates changes to a continent-continent collision through the Betics and Atlas structures, with the Alboran Sea in between (Mezcua et al., 2011). Morales-Esteban et al. (2013) showed that this seismicity is moderate with few events of magnitude equal to or larger than 5.0.

The ocean-ocean contact area begins at the E-W Gloria Fault. It moves to the east towards an area centered at the Gorringe Bank where reverse faulting with a horizontal pressure axis in NW-SE direction motions produces large earthquakes. Recently, the M7.9 Cape St. Vincent Earthquake (1969) and, long ago, the 1755 Lisbon Earthquake (M8.7) hit within this area (Peláez et al., 2007).

Besides, the continent-continent collision takes place in the north of Morocco, Algeria, south Iberia and the Alboran Sea. It is interesting to note that, although focal mechanisms of shallow earthquakes show stress regime compatible with a horizontal N-S to NW-SE convergence of Eurasian and African plates, in the Betics-Alboran region an E-W horizontal extension happens (Buforn et al., 2004). Furthermore, there is a relevant seismicity in the Pyrenees, particularly, and in Galicia. The latter extends to the Atlantic Ocean. There are other zones of seismicity, such as the strip between Cantabria and the south of Valencia, and the Cordoba-Lisbon zone that also extends to the Atlantic Ocean (Carreño et al., 2003). The earliest references corresponding to some of the largest earthquakes suffered by the IP: peninsular earthquake are from 24 August 1356 (Justo and Gentil, 1990); the 1504 Carmona earthquake (Gentil and Justo, 1983; Justo and Gentil, 1983); the 1531 Lisbon earthquake (Justo and Salwa, 1998); the 1680 Malaga earthquake (Gentil and Justo, 1985); and the 1884 Andalusia earthquake (López-Arroyo et al., 1981).

Likewise, it is interesting to highlight that the contact area between the African and the Eurasian Plates produces frequent and large earthquakes that affect the IP. Nevertheless, the seismicity within the Iberian Plate is moderate. Despite this, earthquakes of significant magnitude have been produced. This seismicity has been observed in the Tagus Basin and in Galicia (Teves-Acosta et al., 2017; Giner-Robles et al., 2012; Martín-González et al., 2012; Carreño et al., 2008).

Most earthquake hypocenters are located at a shallow depth (< 30 km) and at an intermediate depth (30–150 km). It is of interest to note that there are some shocks that hit at great depth (≅650 km) (Buforn et al., 1995).

Three main parts can be distinguished regarding the geology of the IP. First, the Hercynian Block –or Iberian Massif– which is the core of the IP. To its southeast, the Betic Foldchain can be found. The Pyrenean Fold is to the northeast. Both these are part of the Alpine Belt. The IP is bounded to the west by the Atlantic Continental Margin off Portugal and Spain. Figure 1.1 shows a general schema including, some remarkable sites.

The first relevant seismic zoning for the IP was proposed by Martín (1984) who defined 27 seismogenic zones. As stated by Mezcua et al. (2011), NCSE-02

is due with minor changes to Martín (1984) and is based on seismic distribution and on structural and tectonic characterizations.

López-Casado et al. (1995) used four different zonings for their *b*-value study: one for the Betics Cordillera and three for the Betics-Rif Region. Jiménez-Peña et al. (1998) depicted a map based on seismic and geological data. Ten zones were delimited for the south-east of the IP. Also, Molina (1998) evaluated the seismic hazard in the contact area between the African Plate and Iberian Peninsula Sub-plate. He defined 25 shallow zones ($h < 30$ km), five intermediate ($30 < h \leq 60$ km) and two deep zones ($60 < h \leq 90$ km). Later, Secanell et al. (1999) did a specific study for Catalonia. This research was based on the Gutenberg-Richter law and the usual mathematical methods for seismic-studies. Peláez and López-Casado (2002) did a seismic hazard analysis for the IP. Only shallow and intermediate seismicity ($h \leq 30$ km; $30 < h \leq 60$ km, respectively) was considered. García-Mayordomo (2007) presented a hybrid model, based on the spatial distribution of the epicenters and the geological structures, for defining seismogenetic sources. He presented an example of his method to zone the southeastern IP. Mezcua et al. (2011) proposed a new seismogenetic zoning for Spain which is a sum of existing partial zonings. The authors defined 36 zones based on several regional seismic zonings.

Recently, IGN-UPM WG (2013) presented a new probabilistic seismic hazard analysis for Spain. It is based on the seismic zonings of García-Mayordomo et al. (2012b) and Bernal (2011). The zoning by García-Mayordomo et al. (2012b) is based on a previous model named Iberfault (García-Mayordomo et al., 2010). It was later adjusted to the seismic zonings of Portugal and France with the collaboration of experts from both countries (Stucchi et al., 2013). Finally, it was modified by the Project Following Committee and the Working Group. The work by Bernal (2011) is based on various seismic hazard studies undertaken by the authors in the period of 1990–2009. The geology, tectonics and a thorough analysis of the seismicity have been considered.

Morales-Esteban et al. (2014) proposed a method for seismic zoning based on an effective adaptive Mahalanobis k-means algorithm. This method was used for the IP and adjacent areas. These zones were also checked with the geology.

Martínez-Álvarez et al. (2015) defined 34 zones for the IP and adjacent areas. The zones were delimited using a triclustering algorithm. The zones were later validated with the geology.

A detailed description of recent zonings for the IP, regions of the IP, France, Portugal and northern Africa can be found in IGN-UPM WG (2013).

2.4. THE FAULT DATABASE OF THE GEOLOGICAL AND MINING INSTITUTE OF SPAIN (IGME)

The QAFI is constructed by the IGME (info.igme.es/qafi, last accessed March 2015). This database collects only active faults during the Quaternary period. These are considered the only faults capable of generating seismic activity nowadays. It is necessary to point out that, although it is constantly updated, not all the Quaternary faults are known. This leads to an inevitable lack of information. It contains information related to location, geometry and kinematics (length, sense of movement, depth), Quaternary activity (geomorphic evidence, age of the youngest deposits affected by the fault, slip rate, maximum slip per event, number of seismic events, evidence of aseismic creep), seismic parameters (maximum magnitude, recurrence period, date of the last maximum event), associated seismicity and extended data. The maximum expected magnitude is obtained from equations that consider the length and/or width of the faults (García-Mayordomo et al., 2012a). For further details on uncertainties related to these transformations (García-Mayordomo et al., 2012a) can be checked out. In this work, the QAFI v.2.0 release has been used. Figure 2.1 depicts a map of the QAFI.

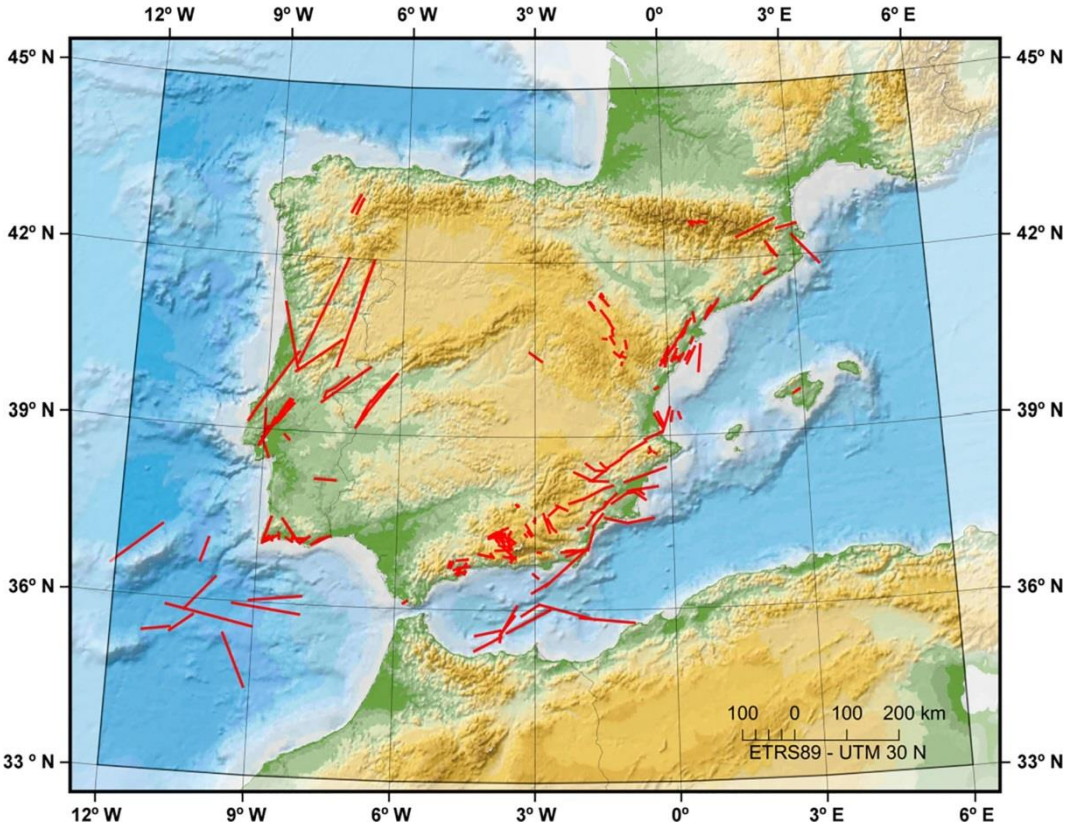

Figure 2.1. Map of the Quaternary active faults database of Iberia. QAFI v.2.0 (www.igme.es). Source: Amaro-Mellado et al. (2017)

2.5. SEISMIC HAZARD PARAMETERS

The seismic hazard can be defined by means a series of parameters, where some of the most common are the following: the size distribution of earthquakes (*b*-value), the annual rate of earthquakes and the maximum magnitude. All of them will be calculated, represented and analyzed in this work.

2.5.1. The size-distribution (*b*-value)

Earthquake size distribution has been studied since the beginning of the 20th Century. First, Ishimoto and Iida (1939) and, later, Gutenberg and Richter (1941) noticed that the rate of earthquakes, *N*, of magnitude larger than or equal to a threshold magnitude, M_{min}, follows a power law distribution:

$$N(M) = \alpha M_{min}^{-\beta} \qquad \text{(Eq. 2.1)}$$

where α and β are the adjustment parameters.

Gutenberg and Richter (1944) and Gutenberg and Richter (1954) transformed this equation into a linear law which is known as the Gutenberg-Richter frequency-magnitude relation:

$$\log_{10} N(M) = a - bM \qquad \text{(Eq. 2.2)}$$

By means of this law, the cumulative (or absolute) number of earthquakes (of magnitude ≥ M_{min}) is related to the *a* and *b* parameters. The *a*-parameter is a measure of the seismic activity (earthquake productivity) (Cheng and Sun, 2018). Parameter *b*, known as the *b*-value, reflects the relationship between earthquakes of different sizes (larger or smaller magnitudes and it is an outstanding parameter in seismic studies as is of capital importance to understand a territory's seismic hazard.

On a global scale, 0.9–1.0 is considered as the normal *b*-value (Frohlich and Davis 1993; Hiemer et al. 2014; Page et al., 2016). The importance of the *b*-value is due to its relationship with the physical characteristics of an area as well as with its tectonics (Lee and Yang, 2006; Bachmann et al., 2012; Reyes et al., 2013; Martínez-Álvarez et al., 2015). A high *b*-value indicates material heterogeneity and that high stress cannot be held. By contrast, a low *b*-value reflects a high rigidity, so the area can accumulate a higher stress and release it suddenly. This issue is not clear indeed and the variation of the *b*-value is still under discussion among the experts (Kamer and Hiemer, 2015; Singh and Singh, 2015). There are two different theories. The first argues its relation to the physics. The second states that the *b*-value must be around 1.0 and its variations are due to miscalculations, lack of data, inhomogeneous detection network, etc. (Frohlich and Davis, 1993; Amorese et al., 2010).

Over time, multiple methods to calculate the *b*-value and its uncertainty have been proposed-non exhaustive (Aki, 1965; Utsu 1965; Weichert 1980; Shi and Bolt, 1982; Bender, 1983; Tinti and Mulargia, 1987; Frohlich and Davis, 1993; Kijko and Smit, 2012; Kamer and Hiemer, 2015). At first, the least square (LS) method was applied but then Maximum-Likelihood Estimate (hereinafter, MLE) has been considered preferable (Aki, 1965; Utsu, 1965; Amorese et al. 2010) and more robust as it does not present interdependency between variables (IGN-UPM WG, 2013).

The MLE method (Aki, 1965; Utsu, 1965) estimates the *b*-value as:

$$\beta = \frac{1}{\overline{M} - M_{min}} \qquad \text{(Eq. 2.3)}$$

where $\beta = b / \log e$; $\overline{M}$ is the average magnitude of the earthquakes larger than or equal to M_{min}; M_{min} is the cut-off magnitude. In this case, M_{min} is equal to the magnitude of completeness (M_c), i.e., the lowest magnitude at which events records are complete.

M_c is a crucial value and is closely related to the earthquake detection network configuration (González, 2017) and obviously predetermines the number of events (*N*). A thorough description of different methods for its calculation such as the Maximum Curvature (*MAXC*) technique, the Goodness-of-Fit Test (*GFT*), the M_c by *b*-value stability (*MBS*), and the M_c from the Entire Magnitude Range (hereinafter, *EMR*), among others, can be found in Mignan and Woessner (2012). Recently, the method by Stepp (1972) was used in IGN-UPM WG (2013) and the linear method was employed by Mezcua et al., (2011), both of them in the area of this research.

As stated above, in González (2017) a detailed research on the evolution of the magnitude of completeness for Spain applying the *EMR* method, focused on the instrumental era, was conducted.

One of the most crucial steps is to define the computation of M_c, as this value has a direct impact on the results of the *b*-value.

Regarding its temporality: (a) using a unique value of M_c and just an interval of time (beginning and end) (Morales-Esteban et al., 2014; Scitovski, 2018); (b) using one M_c for different intervals of time (one M_c for every interval) (Mezcua et al., 2011).

With regards to its spatiality: (a) one M_c value for the whole area of interest, as in Mezcua et al. (2011; (b) different M_c values depending on the location: either a local value for small areas (González, 2017) or a regional value (for a seismogenic zonation, for instance) (IGN-UPM WG, 2013).

Regarding the *b*-value calculation methods, most of them compute it considering just one M_c for the whole catalog. In the Iberian Peninsula, the impact of historical, pre-instrumental and early instrumental events is relevant. So, using a method with different cut-off magnitudes is advisable.

Kijko and Smit (2012) proposed dividing the catalog into sub-catalogs with different years of completeness. Also, the method suggested by Weichert (1980) allows splitting the catalog into sub-catalogs. Moreover, this has been used in several investigations for the same region (Mezcua et al., 2011; IGN-UPM WG 2013). Kijko and Smit's method is simpler and easier to drive and it is not based on an iterative process. This allows computing the mean seismic activity rate easily, once the *b*-value has been obtained.

The generalized Aki–Utsu $\hat{\beta}$ estimator dealing with sub-catalogs with different levels of completeness is (Kijko and Smit, 2012):

$$\hat{\beta} = \left(\frac{r_1}{\hat{\beta}_1} + \frac{r_2}{\hat{\beta}_2} + \cdots + \frac{r_s}{\hat{\beta}_s} \right)^{-1} \quad \text{(Eq. 2.4)}$$

where $r_i = n_i/n$, $n = \sum_{i=1}^{s} n_i$ is the total number of earthquakes of magnitude equal to or larger than the M_c for the years of completeness of the full catalog. $\hat{\beta}_i$ are the Aki–Utsu β-values estimators calculated for individual sub-catalogs according to (Eq. 2.3). The sample standard deviation is defined as:

$$\hat{\sigma}_{\hat{\beta}} = \frac{\hat{\beta}}{\sqrt{n}} \quad \text{(Eq. 2.5)}$$

Kijko and Smit (2012) also suggested applying the formula provided by Ogata and Yamashina (1986) to correct the slight overestimation of the *b*-value, for small samples:

$$\tilde{b} = \frac{(n-1)b}{n} \quad \text{(Eq. 2.6)}$$

Hereinafter, when referring to the *b*-value in this research it will relate to the $\tilde{b}$-value, calculated from (Eq. 2.6).

One key point is to establish the minimum number of events to obtain a meaningful *b*-value. This is a matter of debate among experts: Bender (1983) and Bachmann et al. (2012) proposed 25 events; Amorese et al. (2010), Singh and Singh (2015) and Mousavi (2017) suggested 50 events; González (2017) used 60; and Roberts et al. (2015) established a minimum of 200. Shi and Bolt (1982) gave a general method to estimate the *b*-value calculation error and Nava et al. (2017) studied the precision for different nominal values of the *b*-value by means of the *MLE*. A summary of Nava et al. (2017) can be found in Table 2.1Table 2.1.

b-value estimate and its precision for b = 0.8; b = 1.0; b = 1.2 versus the number of events (Nava et al. 2017).

Table 2.1. b-value estimate and its precision for b = 0.8; b = 1.0; b = 1.2 versus the number of events (Nava et al. 2017)

N	*b nom* = 0.8 *sigma*	*b nom* = 0.8 *b est*	*b nom* = 1.0 *sigma*	*b nom* = 1.0 *sigma*	*b nom* = 1.2 *b est*	*b nom* = 1.2 *sigma*
10	0.885	0.310	1.103	0.385	1.321	0.458
25	0.831	0.172	1.037	0.214	1.241	0.255
50	0.814	0.117	1.015	0.145	1.216	0.174
200	0.802	0.057	1.001	0.071	1.198	0.084
5000	0.798	0.011	0.996	0.014	1.193	0.012

The *b*-value is spatially variable, so, in order to assess its value the area must be divided into smaller parts. A seismogenic zonation is a kind of division. When not considering a zonation, the sampling process is usually as follows: a grid is considered, being the sample distance (not exhaustive) between 1 km x 1 km for California-USA (Wiemer and Wyss 2002); 0.025º x 0.025º (Ghosh et al. 2008) for Costa Rica; 0.05º x 0.05º (Mignan et al. 2011) for Taiwan; 10 km x 10 km for Alaska-USA (Wiemer and Wyss 2000); 0.1º x 0.1º (Zhao and Wu 2008) for China; 0.3º x 0.3º for Iran (Mousavi 2017); to 1º x 1º, (Mapa Sismotectónico WG 1992). Then, one of these options (Tormann et al. 2014) must be selected:

- ✓ Fixed *R*: a fixed radius (or geographical distance) is considered. All events located in this "circle" (centered in the grid node) are used to calculate a local *b*-value—just if there are enough earthquakes (N_{min}).
- ✓ Nearest *N*: for every grid node, the closest *N* events ($N \geq N_{min}$) are used for the computation of the *b*-value, considering a maximum radius, R_{max}. Centered in this node, a surface is created (a circle or a trapezoid). The radius and minimum number of events required are pretty variable.

- ✓ *DEW* (Distance Exponential Weighted) method: this employs decay functions, considering the distance between the grid node and every event.

Regarding the *b*-value mapping, different issues must be considered. As stated above, it may be used as a crude stress-meter to obtain the relative stress distribution in the Earth's crust (Schorlemmer et al. 2005; Bachmann et al. 2012; Tormann et al. 2014).

It is clear that the lower the number of events (*N*), the greater the uncertainty of the *b*-value calculation. On the one hand, there is a trade-off between accuracy and coverage. On the other hand, the larger the radius, the smaller the spatial resolution is.

2.5.2. The maximum magnitude

The maximum magnitude is another key parameter in a seismic hazard study as it warns of the most energetic event in the study area. The value of this can refer to either recorded values or potential values (as from QAFI database), and even both could be exceeded in the future given the long periods of recurrence of major earthquakes. Publications related to paleoseismology (from thousands to millions of years) (Ferrater et al., 2017; Masana et al., 2018; Gómez-Novell et al., 2019) or archaeoseismology (from hundreds to around 4000 years BC) (Rodríguez-Pascua et al., 2016) of the Iberian Peninsula are becoming more and more frequent.

Yet, different methods to estimate the maximum possible magnitude and its uncertainty can be found in the literature. Some are based on the width and/or length of the faults (IGN-UPM WG, 2013). Others use the Bayesian procedure (Kijko, 2012).

2.5.3. The annual rate

Finally, within the parameters of seismic hazard, this study has chosen to also obtain the annual rate of earthquakes normalized according to the surface in square kilometers.

Kijko and Smit (2012) stated that after calculating the $\hat{\beta}$-value, the mean seismic activity rate $\lambda(M_{min})$ can be determined. Kijko and Sellevoll (1989, 1992)

asserted that the maximum likelihood estimation of $\lambda(M_{min})$ can be calculated from the following equation:

$$\lambda(M_{\min}) = \frac{n}{\sum_{i=1}^{s} t_i \exp\left[-\hat{\beta}\left(M_{min}^{i} - M_{min}\right)\right]} \qquad \text{(Eq. 2.7)}$$

where, M_{min} is the minimum magnitude considered, n is the total number of earthquakes equal to or larger than the cut-off magnitude, t_i is time-lapse and M_j^i is the sample of n_i earthquake magnitudes registered during the time-lapse of the i-th subcatalog and $\hat{\beta}$ is the maximum likelihood estimation of the β-value. The mean seismic activity rate is more significant if it is related to the area of every zone (km^2).

It should be noted that the area of a surface given in conformal projection (where shapes and angles are kept, but not distances or areas), such as the Universal Transverse Mercator (UTM) coordinate system is not accurate. This fact is more important when the zones considered are far away from the first meridian of the projection. In this study, long distances (19° longitude) are considered. This causes more than a 1% error. This has led to the choice of an equivalent projection (where the area of a surface is maintained, but neither distances nor shapes are) in order to determine an accurate value of the area of every zone. INSPIRE recommendation (Council of the European Union European Parliament, 2007) has been followed and the ETRS89-LAEA (Lambert Azimuthal Equal-Area) for statistical purposes has been chosen to calculate the area of every zone. The impact of the improvement generated by the use of equivalent projections compared to the UTM projection for the calculation of zonal parameters can be consulted in Pérez-Romero and Amaro-Mellado (2014). Finally, the annual rate of earthquakes per square kilometer (hereinafter, *AR*) has been defined as the quotient between the mean seismic activity rate and the area, in square kilometers, of every zone (A_i):

$$AR = \frac{\lambda(M_{min})}{A_i} \qquad \text{(Eq. 2.8)}$$

Obviously, where there are not enough events to a proper *b*-value calculation, *AR* is not rigorous.

2.6. GEOGRAPHIC INFORMATION SYSTEMS

Finally, the use of GIS is very useful to be able to adequately manage the purely geometric or geographical information and the information coming from databases (seismic catalogs, information on faults, etc.).

GIS are computer-based tools for collecting, storing, processing, analyzing and visualizing geographic information. They are tools that improve the efficiency and effectiveness of handling information about objects and events located in geographic spaces (Longley et al. 2015).

The power of this tool, both to carry out calculations and to generate latent information (the result of the combination and analysis of the initial data), as well as to represent it, makes it possible to obtain results or data outputs that would not otherwise be viable.

The transfer of data to georeferenced files, visually very intuitive, not only facilitates operations with them, but sometimes makes them possible, since otherwise to do so would not always be feasible.

As a strong point of the use of these systems, it is worth mentioning that they allow a fairly agile adaptation to a change in the initial data, such as the catalog, zoning or other parameters involved in the seismic hazard, which allows new results to be obtained quickly.

For these reasons, the use of geographic information systems has been fundamental both in the approach and in the attaining of the works that are framed in this doctoral thesis.

In this study a GIS has been used to integrate the final catalog, the background information, the seismogenic zonings (in case of multiresolution grid have even been created with a GIS) and the QAFI. This information has been previously treated in order to ensure coherence, including depuration of the associated databases. The geometries have been edited in order to avoid conflation problems (misalignment due to the use of different systems of reference or coordinates, etc.).

Chapter 3.
Seismic catalog generation

3.1. INTRODUCTION

This chapter shows the generation of a seismic catalog for the Iberian Peninsula. The use of a reliable and homogenous catalog is a need for seismicity studies since its compilation is a crucial step.

Firstly, the generation of the seismic catalog of work will be dealt with given its capital importance for the rest of the subsequent analysis, since from this the different parameters related to seismic hazard have been calculated, represented and analyzed, i.e., the *b-value*, maximum magnitude and annual rate (Figure 3.1). Therefore, the results obtained are presented below, and will be used in both: in the case of using predefined seismic zoning and in the case of using a grid defined on the basis of *exclusively* geographical parameters.

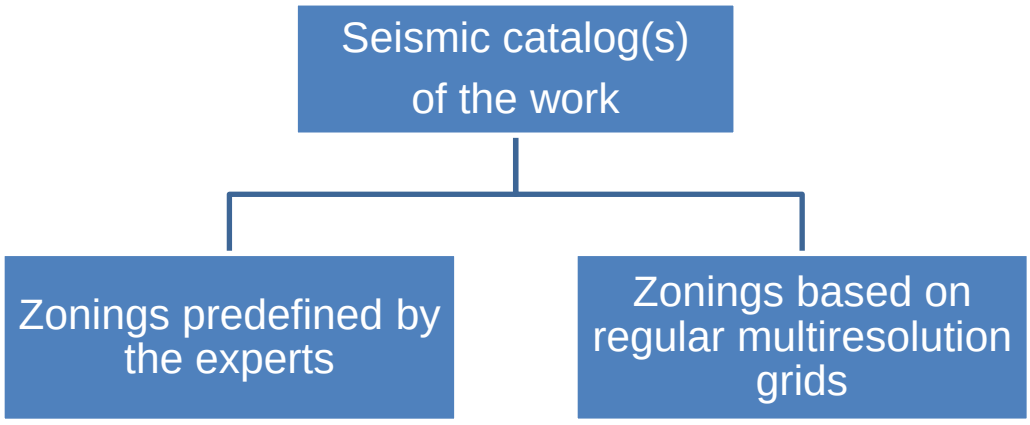

Figure 3.1. Catalog use schema

The seismic catalog is the basis for the rest of the analysis. In this doctoral thesis, a catalog has been compiled from the NGIS database of earthquakes in the area of the Iberian Peninsula and its adjacent area as indicated in Figure 3.2.

3.2. CATALOGS GENERATION

Firstly, the records in the initial catalog have been reviewed (especially earthquakes with a marine epicenter) and supplemented with information from other catalogs and specific studies. Subsequently, the size of the events was homogenized to M_w, establishing the cut-off magnitude in M3.0. Thirdly, non-main earthquakes have been removed (a process called declustering). Then, a completeness date has been considered for each reference magnitude. Finally, the seismic catalog of the work is shown, the result of the processes mentioned.

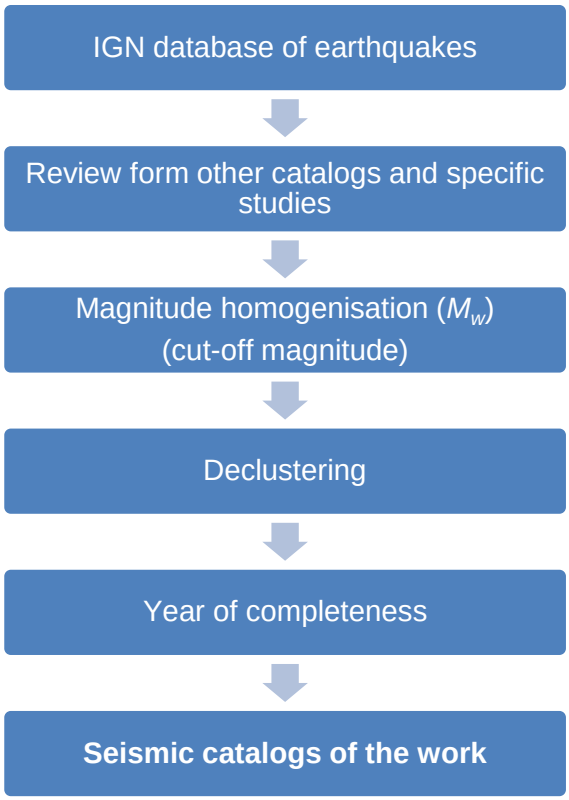

Figure 3.2. Seismic catalog generation workflow

3.2.1. The National Geographic Institute of Spain seismic catalog

The NGIS seismic catalog —freely available at the NGIS website (IGN, 2019b)— has been considered as the basis to define the working catalog of this research study. It is the official earthquake catalog of Spain and has kept records with reliable information from 1373 until nowadays, thus spanning more than 600

years. It comprises parallels 26ºN to 45ºN and meridians 20ºW to 6ºE. A thorough study of its evolution, precision and completeness can be found in González (2017).

As shown in Figure 3.3. Earthquakes of th NGIS catalog form 1373 to 2015. Source: Amaro-Mellado et al. (2018), there are two separated regions of interest: the IP and adjacent areas, and the Canary Islands and surroundings. The events which occurred outside of these two zones are not recorded in the NGIS catalog. This database has eleven fields: event ID, date, hour (UTC and local), latitude (°), longitude (°), depth (km), macroseismic intensity, magnitude, magnitude type and administrative location. As a first approach, all earthquakes with a recorded magnitude larger than or equal to 2.5 have been considered, as well as events with I_{max} greater than or equal to “II” from 1373 to December 2015. Figure 3.3 illustrates all earthquakes gathered in the catalog considered.

In this study, only shakes that affect the IP and adjacent areas have been considered. So, the whole catalog has been limited to 33°N to 45°N latitude and from 12°W to 6°E longitude. Moreover, earthquakes whose hypocentral depth is over 65 km have been removed. Deeper events are not considered relevant to seismic hazard (IGN-UPM WG, 2013).

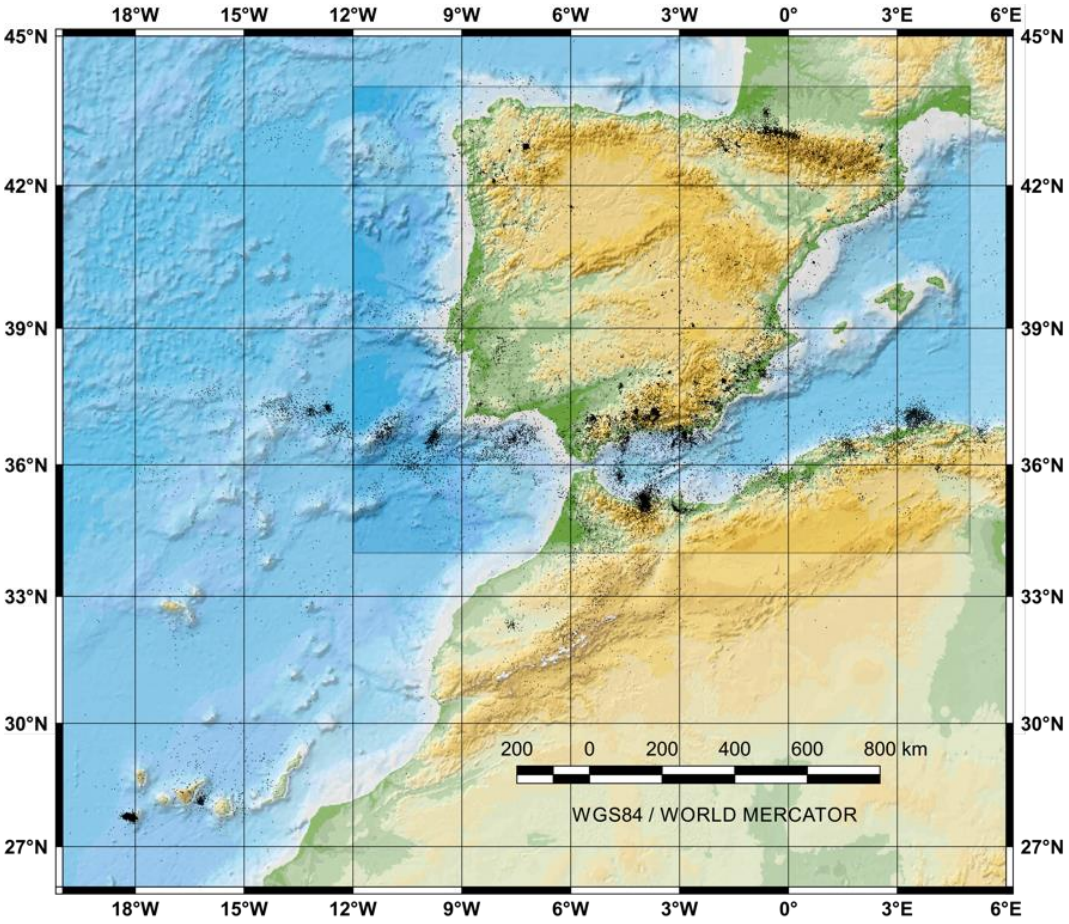

Figure 3.3. Earthquakes of th NGIS catalog form 1373 to 2015. Source: Amaro-Mellado et al. (2018)

3.2.2. Review from other catalogs and specific studies

In order to update and improve the NGIS catalog, the information from other catalog reviews and specific studies have also been considered. These reviews are particularly important in order to decide upon the magnitude of some historical earthquakes. More than 350 events have been reviewed or added (note that these events are available as supplementary material in Amaro-Mellado et al., 2017).

Here below, modifications to the catalog are listed, considering that those written later in this text prevail over those written earlier, and M_w over other types of magnitude.

First of all, earthquakes with a marine epicenter and with only macroseismic information have been separately computed. For this purpose, the

correction suggested by López-Casado et al. (2000) to determine a better epicentral I_{MAX} estimation, in accordance with the distance to the mainland and the recorded depth have been conducted, just like IGN-UPM WG (2013). Obviously, this leads into a relevant I_{MAX} increase for some marine events. Thus, more than 70 marine events' I_{MAX} have been revised.

Then, in order to avoid any missing information, events from the north of Africa have been added and reviewed.

- ✓ Peláez et al. (2007) compiled a catalog including the main earthquakes in Morocco and adjacent areas from 1045 to 2005. They used different catalogs and other specific reviews.
- ✓ Hamdache et al. (2010) generated a catalog including the main northern Algeria and adjacent areas from 856 until 2008. They extracted information from different catalogs and specific studies.

Then, the database of the Geophysics Institute of Andalusia (*Instituto Andaluz de Geofísica*) was reviewed to assign moment magnitude to some shocks of the instrumental period.

- ✓ Stich et al. (2003a) calculated moment tensor inversion for small and moderate shallow events from IP, northern Morocco and northern Algeria from November 1995 to March 2002.
- ✓ Stich et al. (2005b) established moment magnitude for earthquakes that hit in the Gulf of Cadiz and Cape St. Vincent region from 1964 to 2004.
- ✓ Stich et al. (2010) presented moment tensor solutions for earthquakes in the Ibero-Maghrebian area from mid-2005 to the end of 2008.
- ✓ Martín et al. (2015) performed moment tensor inversion for earthquakes in the Ibero-Maghrebian area from the beginning of 2009 to mid-2014.

Also, the reviews from Martínez-Solares and Mezcua (2002) and Mezcua et al. (2004) have been used to reveal moment magnitude through Bakun and Wentworth's method (Bakun and Wentworth, 1997) for some historical and preinstrumental earthquakes.

Finally, some specific studies have been adopted to improve the catalog (Batlló et al., 2010; 2008; Olivera et al., 2006; Stich et al., 2005a, 2003b).

3.2.3. Magnitude homogenization

It has been previously stated that the NGIS has ancient records (from 1373). This means that the magnitude of the earthquakes has been calculated with different procedures. A detailed description of the equations used in every time-period, as well as further discussion on the same, can be found in IGN-UPM WG (2013). The following periods can be distinguished, with an estimation of uncertainties (1σ), between brackets:

1. Historical seismicity (up to 1923). Epicentral or maximum intensity, I_{MAX}. The most reliable parameter to determine the magnitude of historical events was macroseismic intensity. ($0.5 \leq \sigma \leq 1.5$)

2. Pre- and early instrumental (1924–February 1962). Duration magnitude, $M_D(MMS)$. Both macroseismic intensity and magnitude were recorded (Mezcua and Solares, 1983). ($\sigma = 0.4$)

3. February 1962–March 2002. Surface-wave magnitude, $m_{b,Lg}(MMS)$. For this interval, the equations used for magnitude calculations were based on A/T ratio (amplitude/period of the wave) and the epicentral distance (Mezcua and Solares, 1983). ($\sigma = 0.3$ < 1985); ($\sigma = 0.2$ > 1985)

4. From March 1998. Body-wave magnitude, $m_b(V-C)$. For this period, the magnitude was calculated by means of the formula given by Veith and Clawson (1972). It should be noted that from 1998 onwards, both $m_{b,Lg}$ and m_b were obtained, although the catalog of the NGIS only shows one of them. ($\sigma = 0.2$)

5. From March 2002. Surface-wave magnitude, $m_{b,Lg}$(L). Wideband seismometers appear. The usage of m_b is maintained. From 2002, the equation from López (2008) that depends on A/T ratio and the hypocentral distance was also used. This magnitude was correlated to the Richter scale of local magnitude (Richter, 1935). ($\sigma = 0.2$)

6. The NGIS also started the calculation of the moment magnitude, M_w, for larger events whose value depends on the seismic moment. It was installed in the NGIS by Rueda and Mezcua (2005). ($\sigma = 0.1$)

It must be said that other interesting studies on magnitude calculation exist (by M_D and $M(A/T)$) for earthquakes which occurred during the 20th century: Samardjieva et al. (1999) (1912–1962), Miguel and Payo (1983) (1948–1961) and Miguel and Payo (1980) (1962–1975).

It can be observed that various parameters and equations have been used to calculate the earthquake magnitude. In order to provide an adequate catalog, all events must be characterized in the same magnitude. It is known that moment magnitude has a direct relation with the physics of the source through scalar seismic moments. Moreover, this scale of magnitude does not get saturated by large earthquakes. Due to these reasons, the moment magnitude has been considered as the reference-magnitude in this research.

For that purpose, most records (where the M_w was not provided) have been converted into moment magnitude. Over time, different conversion relations between these macroseismic and magnitude scales have been proposed (Johnston, 1996a, b; Rueda and Mezcua, 2002; Castellaro et al., 2006; Gaspar-Escribano et al., 2008; Cabañas et al., 2015). Finally, the formulae used have been calculated from a reduced major axis regression, just like IGN-UPM WG (2013) for the same area. This model can be assumed to be more robust than least square regression when handling errors in both dependent and independent variables. The equations for these transformations, as well as further discussions on them, can be found in Cabañas et al. (2015) and are listed as follows:

$$M_w = 1.656 + 0.545 I_{MAX} \quad \text{(Eq. 3.1)}$$

$$M_w = 0.290 + 0.973 m_{b,Lg}(MMS) \quad \text{(Eq. 3.2)}$$

$$M_w = -1.528 + 1.213 m_{b,Lg}(V - C) \quad \text{(Eq. 3.3)}$$

$$M_w = 0.676 + 0.836 m_{b,Lg}(L) \quad \text{(Eq. 3.4)}$$

Besides, it is necessary to point out that only earthquakes from 1373 onwards have been considered in this research because this date is a conservative value to find events with a certain epicentral location and macroseismic intensity reliability.

With regard to magnitude cut-off, it must be said that this is a variable which depends on the authors. That is to say, Miguel and Payo (1980, 1983), who determined the magnitude from the epicentral distance and the attenuation of the amplitude/period ratio of the maximum LgV waves recorded by Iberian WWSSSN stations from 1948 to 1975, including 2.5 or I_{MAX} greater or equal than III; Peláez et al. (2007) used 3.0 as cut-off magnitude for their studies on Morocco. Also Morales-Esteban et al. (2010, 2014), did so for the IP and surroundings. Mezcua et al. (2011) and IGN-UPM WG (2013) considered 3.5 for the same area. Martín (1984) computed 4.0 as a cut-off. 4.5 was taken by Jiménez et al. (1999) for events from 1900 to 1989 in the IP, and by Hiemer et al. (2014) to establish a model for Europe, etc.

Finally, the chosen cut-off value has been 3.0, as it had been previously calculated by Morales-Esteban et al. (2010) for the NGIS database. It should be noted that a lower cut-off magnitude can lead to inconsistencies, as the number of small earthquakes can be less than expected from the extrapolation of moderate magnitude earthquakes (Lombardi, 2003).

3.2.4. Declustering

It is known that earthquakes do not occur in an isolated manner. Normally, large magnitude earthquakes trigger subsequent smaller earthquakes (aftershocks). It is also possible for tremors to forewarn larger earthquakes (foreshocks). It may even occur that there is no dominant earthquake (seismic swarm).

In the *b*-value calculation, it is assumed that the occurrence of earthquakes follows the Poisson distribution where earthquakes are independent events. Therefore, it is necessary to previously eliminate dependent earthquakes (aftershocks, foreshocks and swarms) through a process known as declustering.

The results of the subsequent processes would be contaminated or unreliable if the catalog of earthquakes did not follow a Poisson distribution. In this research, although trials have been carried out using the Reasenberg (1985) method, finally the one described by Gardner and Knopoff (1974) has been used due to its clarity, simplicity and stability (IGN-UPM WG, 2013; Hamdache et al., 2010; Talbi and Yamazaki, 2009; Peláez et al., 2007). It establishes windows of both time and space, depending on the magnitude of the principal earthquake.

The windows are defined through logarithmic functions. The original parameters of this method may require modification (personalization) in order to adjust them to the IP. These have been obtained after the corresponding trials and bibliography revisions. In the recent literature two main groups of values (Peláez et al. 2007; IGN-UPM WG 2013) have been used for the Iberian Peninsula.

For the study of seismogenic zones predefined by experts, the values considered by Peláez et al. (2007) have been used. For example, for a 3.0 and an 8.0 M_w earthquake, a space-window of 20 and 100 km has been, respectively, obtained. With regard to the length of the time-window, 10 and 900 days have been, respectively, determined.

Regarding the zonings based on multiresolution grid, the calculations have been done considering both values. Moreover, this allows comparing the results. Peláez et al.'s (2007) values have been also considered by Crespo (2011) for the Iberian Peninsula.

This declustering option and the different temporal and geographical extent (as will be seen later) results in that, actually, three catalogs very slightly different coexist (but are not mix up).

3.2.5. Year of completeness

A catalog is complete only if all records equal or superior to a cut-off magnitude have been recorded. Obviously, it is more likely for larger earthquakes to have been previously registered. Therefore, the year of completeness is more recent for smaller magnitudes. Morales-Esteban et al. (2010) calculated that 1978 is the year of completeness for the catalog of the NGIS for a threshold magnitude of 3.0. The linear method (Mezcua et al., 2011) was used for that purpose.

From a strict point of view, this parameter must be calculated for each zone. In this study approximately 900 zones have been considered including the zones of all the zonings studied. Moreover, some zones are very small which means that not much data are available within it. Another way to face the issue is to consider a global value for the whole area, as in Mezcua et al. (2011). In line with this approach, the year of completeness has been determined for the zones proposed by Martín (1984). Also, the linear method has been used. Then, the

most recent (restrictive) year for every cut-off magnitude considered (3.0, 4.0, 5.0 and 6.0, in this study), for all the zones, has been taken as representative for the entire NGIS catalog. Later, this has been compared with other years of completeness published for the Iberian Peninsula (IGN-UPM WG, 2013; Mezcua et al., 2011). It has been found that the results are conservative and in accordance with these sources. The results are listed in Table 3.1.

Table 3.1. Year of completeness

Magnitude	Completeness
3.0	1980
4.0	1953
5.0	1915
6.0	1522

But, as the results have not been satisfactory due to detection network heterogeneity depending on the location, a regionalization has been applied. In particular, regionalized values considered in IGN-UPM WG (2013) have been finally considered. The division can be seen in Figure 3.4, and the corresponding years of completeness for every magnitude are shown in Table 3.2.

Table 3.2. Regionalized year of completeness

Magnitude	Africa	Azores	SE Spain	Rest
3.0	1987	1987	1978	1985
4.0	1950	1972	1908	1933
5.0	1910	1935	1800	1800
6.0	1578	1720	1370	1370

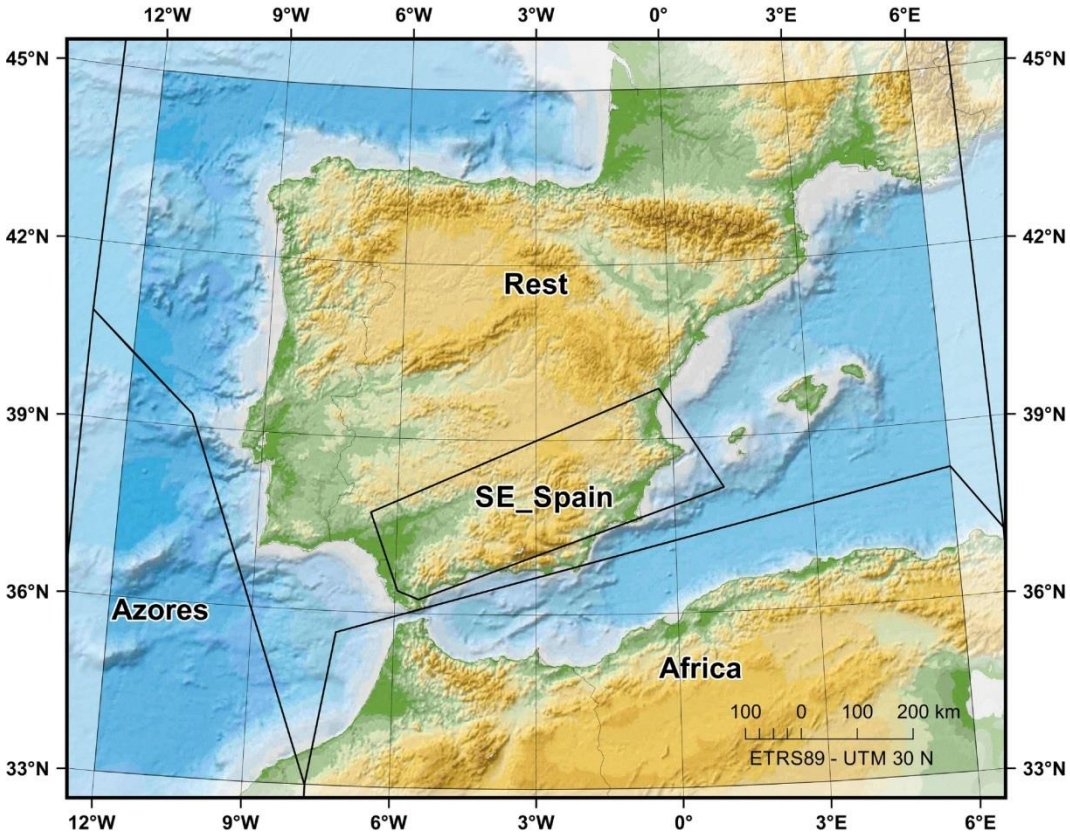

Figure 3.4. Regionalization of completeness adapted from IGN-UPM WG (2013). Source: Amaro-Mellado et al. (2017)

Finally, it has been verified that this choice is consistent with the period in which the Spanish seismic network can be considered to have spread all over the Iberian Peninsula.

3.2.6. Resulting catalogs

The catalogs resulting from this series of processes has been integrated into a GIS.

Figure 3.5 depicts all shocks employed for the analysis of the zonings proposed by the experts. It is comprised by parallels 33ºN and 45ºN and meridians 12ºW and 6ºE. The temporal extension varies from 1373 to June 2014.

Figure 3.6 presents the earthquakes for the seismic parameters in the multiresolution grids. The geographical window includes events from latitude 34ºN to 44ºN and the longitude spans 17º (12ºW - 5ºE). It gathers earthquakes

from 1373 to December 2015. In the case of the multiresolution zoning, visually, both catalogs are almost identical so just one is shown.

As can be seen, the geographic breath of the catalog considered to analyze for the zonings designed by the experts is greater. As will be shown in Chapter 4, some of the zones of these zonations are further away from the IP which justifies this greater geographic extension of the catalog.

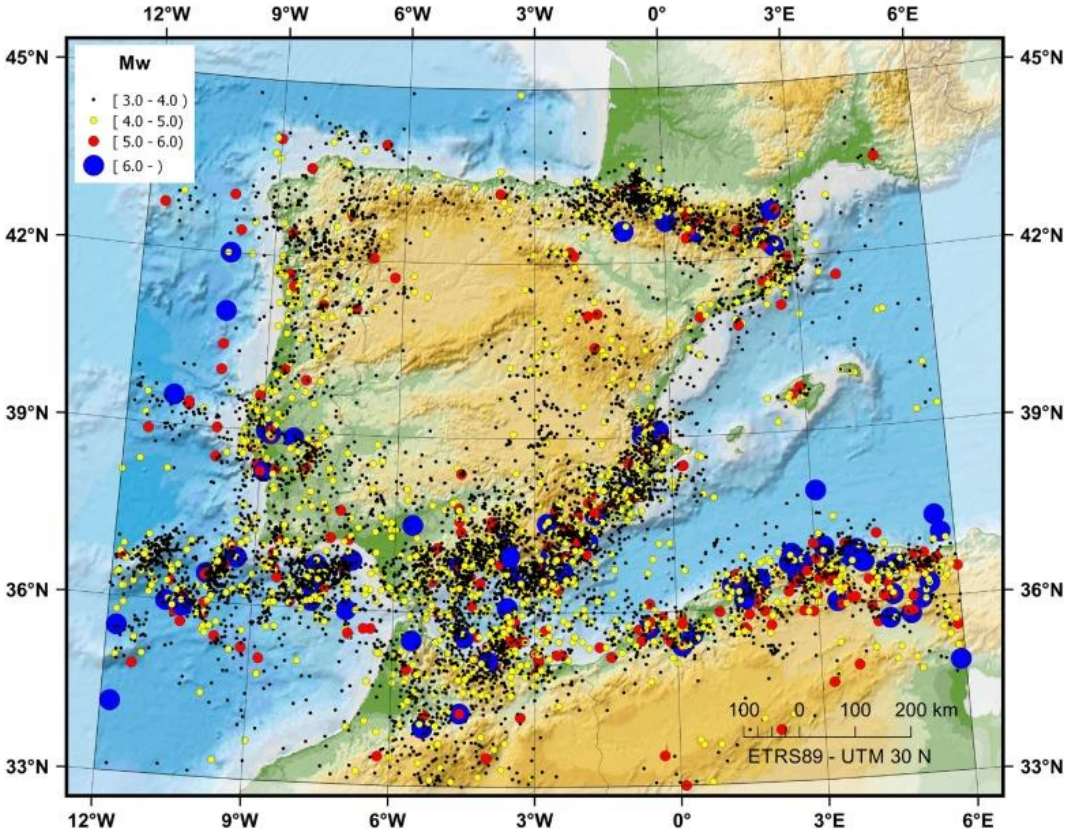

Figure 3.5. Seismic catalog for studying zonings proposed by the experts (from 1373 to June 2014). Decluster parameters: Peláez et al. (2007). Source: Amaro-Mellado et al. (2017)

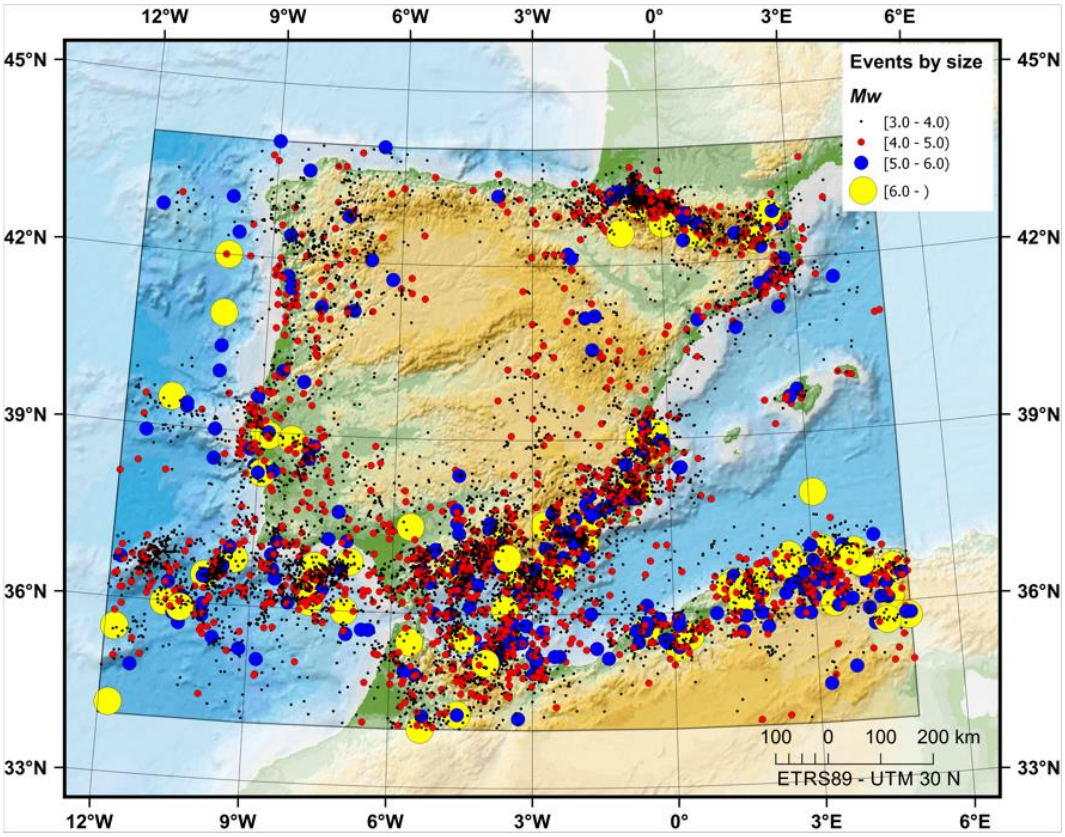

Figure 3.6. Seismic catalog for studying zonings from a multiresolution grid (from 1373 to December 2015). Decluster by IGN-UPM WG (2013). Source: Amaro-Mellado et al. (2018)

Chapter 4.
Seismic parameter analysis of zonings predefined by the experts

This chapter deals with the calculation, representation and analysis of the seismic parameters of different seismic zonings proposed by the experts for the Iberian Peninsula. Firstly, an introduction exposing the issue is given. Then, the seismogenic selected zonings that will be analyzed are shown. Later, the seismic hazard parameters together with the input data are presented. Finally, the results achieved are displayed and analyzed.

4.1. INTRODUCTION

One of the most important issues in a PSHA is depicting the seismic sources. A seismic source must have some relatively uniform seismic parameters and must be different to the adjacent one. Some *b*-value variations can be permitted in a seismic source. By contrast, the maximum magnitude and the annual rate must be uniform (Martínez-Álvarez et al., 2015).

The Iberian Peninsula seismic activity is moderate with infrequent earthquakes of $M \geq 5$. Large earthquakes are infrequent and the recurrence period between events is long. This makes the population unaware of this hazard and inadequately prepared to behave in a safe manner. For this reason, seismogenic zones were used in the last Spanish Building Seismic Regulations (Ministerio de Fomento (Gobierno de España), 2002; Ministerio de Obras Públicas Transporte y Medio Ambiente (Gobierno de España), 1994). According to Mezcua et al. (2011) both are based on the seismogenic zoning defined by Martín (1984) with minor modifications. A new Seismic Regulation is currently being developed. This is based on the seismogenic zonings proposed by García-Mayordomo et al., (2012b) and Bernal (2011).

In this study, from the working catalog compiled in the previous chapter, the statistical parameters have been obtained though methods that use different years of completeness. These methods also allow calculating the statistical parameters (standard errors and confidence limits) of the seismic parameters obtained. This allows using more data for the calculations and avoiding errors due to incomplete data. Also, the Quaternary activity database has been used to complete the data.

This research conducts a critical review of the seismogenic zonings of the IP. This analysis is only based on the seismic parameters calculated from this catalog. A GIS has been used for this goal.

Regarding the review of the seismogenic zonings of the IP, it should be noted that this analysis is based solely on its seismic parameters. Namely, the *b*-value, the annual rate of earthquakes per square kilometer and the maximum magnitude.

The solution proposed by Kijko and Smit (2012) has been used to calculate the *b*-value, as has been explained in Chapter 2. This method has the advantage of using different magnitudes of completeness. This allows the use of more data which provides stronger statistical results. Also, the correction for the *b*-value calculation proposed by Ogata and Yamashina (1986) has been considered.

The annual rate of earthquakes has been obtained from the maximum likelihood estimation of the seismic activity. This has been later divided by the area of every zone. It should be noted that corrections regarding the curvature of the Earth have been assumed to avoid inaccurate data. In this way, the annual rate of earthquakes per square kilometer has been obtained.

The maximum magnitude for every zone has been determined through two methods. The Fault Maximum Magnitude (hereinafter, *FMM*) that considers the maximum magnitude that the faults intersecting the zone can produce according to the information provided by the QAFI, and the Recorded Maximum Magnitude (hereinafter, *RMM*), which is the largest earthquake recorded within the zone. This is particularly relevant due to the long time span (more than 600 years) of the NGIS catalog, making it very probable that the largest earthquake has previously been recorded. All of these parameters have been programmed in the GIS. Therefore, their determination is automatic and lacks human error.

All of the above-mentioned seismic parameters have been calculated for all the zones of five seismogenic zonings selected for this research (Bernal, 2011; García-Mayordomo et al., 2012b; Martín, 1984; Martínez-Álvarez et al., 2015; Morales-Esteban et al., 2014). It is to be mentioned that the zonings by Martín (1984), García-Mayordomo et al. (2012b) and Bernal (2011) have been selected due to their use in the Spanish Seismic Regulations. The zonings by

Morales-Esteban et al. (2014) and Martínez-Álvarez et al. (2015) have been chosen for comparison due to the relevant mathematical and statistical methods that support these works.

Therefore, it is expected that the method exposed in this research will help defining seismogenic zones more objectively. A more robust calculation of the statistical parameters of the seismogenic zones will also be provided.

Finally, it should be noted that all the information and calculations have been integrated into a GIS. This presents some interesting advantages. First, it allows the combination of graphic and alphanumeric data. This is especially relevant for calculation and passing information. Second, the calculations have been programmed on the GIS which facilitates their determination and avoids errors. It has a strong graphical support which allows for the generation of rich graphic results. The preparation and programming can be tedious but it allows for the obtaining of multiple results. This is this case where more than 200 different zones have been used. Finally, it should be noted that new information can be obtained from the GIS.

4.2. SEISMOGENIC ZONINGS SELECTED

In this research, five of the most relevant seismogenic zonings for the Iberian Peninsula have been considered. The first one is the model used, with minor modifications, in current Spanish regulations (Mezcua et al., 2011). The second and the third ones are those proposed for the next regulation. The fourth and the fifth ones have been selected due to the fact that they are based on strong mathematical and statistical methods. Specifically, the fourth one is based on the efficient adaptive Mahalanobis k-means algorithm and the last one is based on triclustering. These zonings are briefly described below, and depicted in Figure 4.1, Figure 4.2, Figure 4.3, Figure 4.4 and Figure 4.5:

- ✓ Martín (1984) proposed 27 zones for the Iberian Peninsula (Figure 4.1). These were based on the seismic catalog and macroseismic activity maps. The zones were limited considering both homogeneous geological and geophysics criteria. This zoning is selected for being the first relevant zonation and for being, with slight modifications, the one included in the last two building regulations for Spain (Earthquake Code Permanent

Commission of Spain 1994, 2002; Mezcua et al., 2011). This zoning has been named in this paper as AJM.

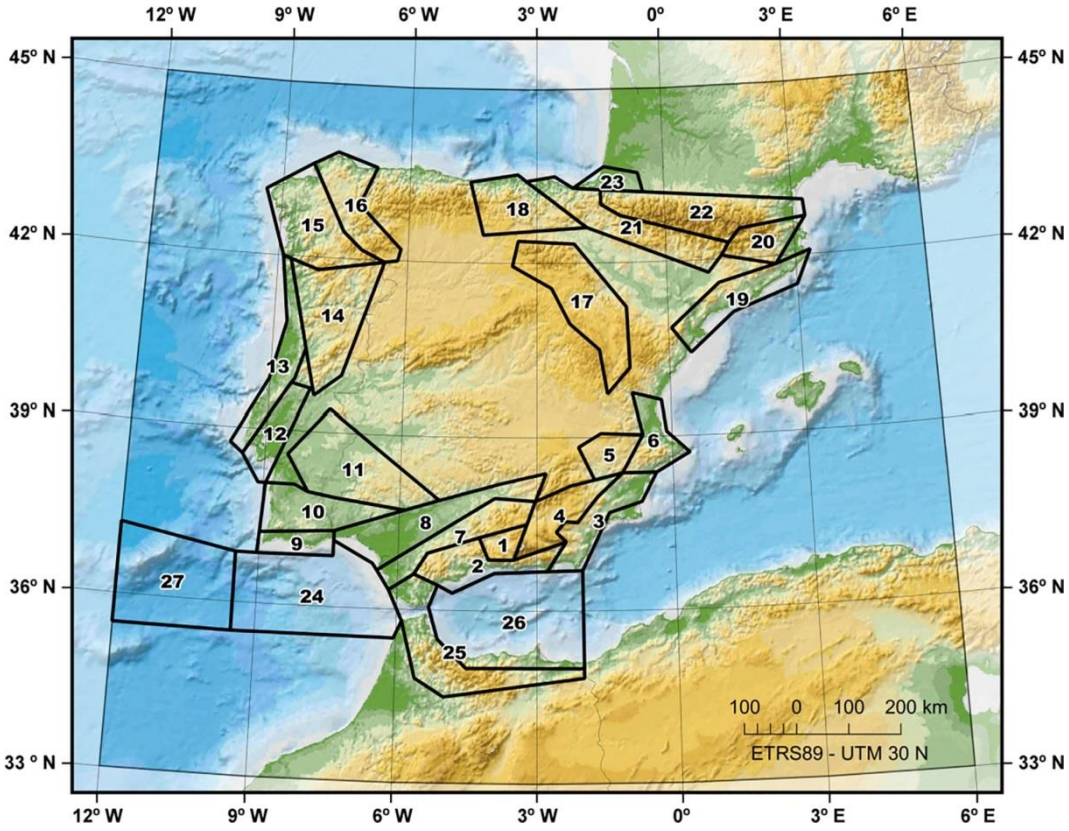

Figure 4.1. AJM zoning for the IP. Source: Amaro-Mellado et al. (2017)

✓ García-Mayordomo et al. (2012b) proposed a first model based on the Iberfault model. This takes into account various aspects, such as tectonic and geological cartography, relief, thickness of the crust, thermal flux, historical and instrumental seismicity. Afterward, this model was improved with the idea of adjusting the Spanish zoning in line with those of neighboring countries. For that purpose, a follow-up commission with experts from Portugal (*Instituto Superior Técnico*) and France (*Institut de Radioprotection et de Sûreté Nucléaire*) was formed (Stucchi et al., 2013). Also the QAFI was used. Finally, the model proposed by García-Mayordomo et al. (2012b) (hereinafter, GM12) has 55 shallow and four deep zones (the latter not being considered in this study), see Figure 4.2.

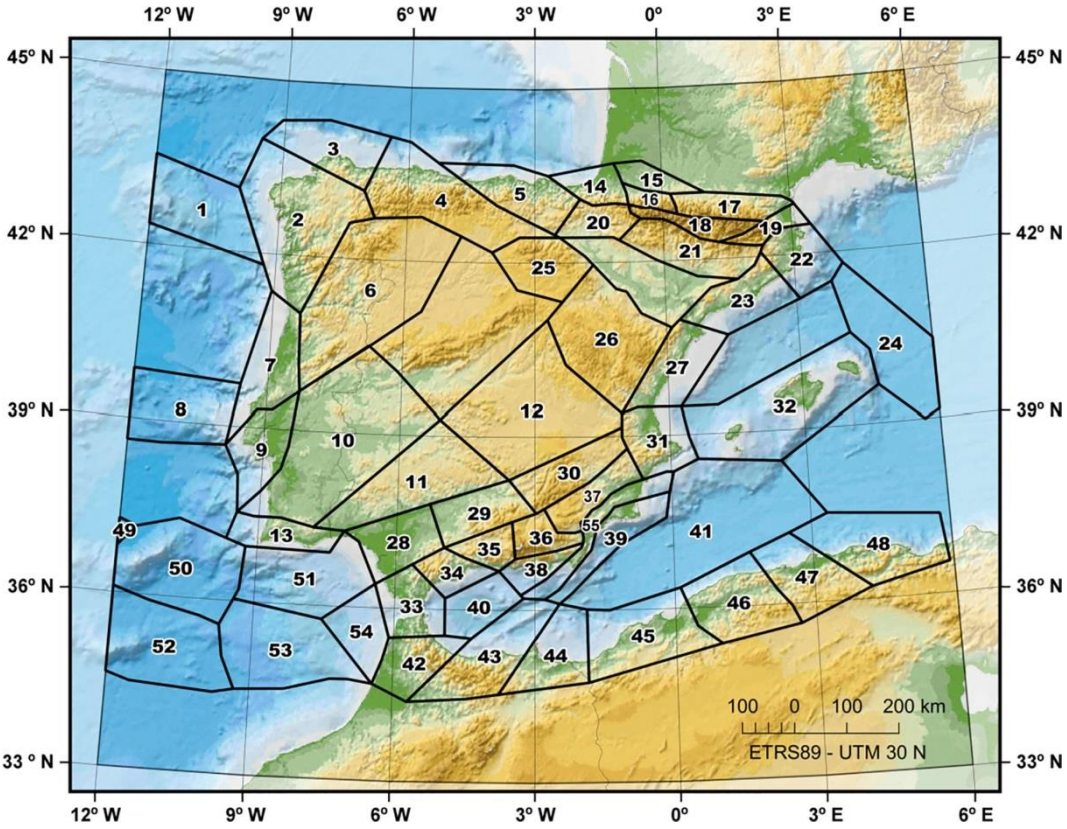

Figure 4.2. GM12 zoning for the IP. Source: Amaro-Mellado et al. (2017)

✓ Bernal (2011) (hereinafter, ByA12) used geology and tectonics as general criteria for each seismogenic zone, including several zones, together with a detailed seismicity analysis. The Iberian Peninsula was split into eight regions, where 72 seismic zonings were established (Figure 4.3).

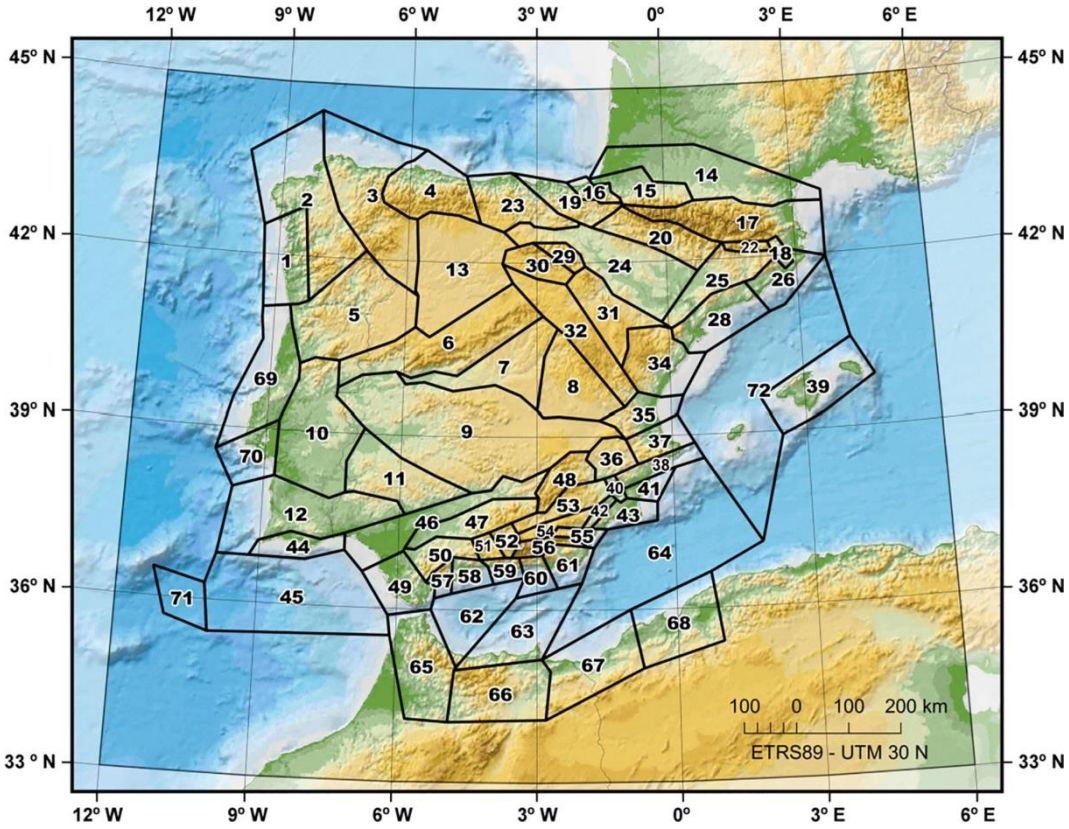

Figure 4.3. ByA zoning for the IP. Source: Amaro-Mellado et al. (2017)

- ✓ Morales-Esteban et al. (2014) (hereinafter, MAH) used an efficient adaptive Mahalanobis *k*-means algorithm for zoning the Iberian Peninsula. The catalog of the NGIS was used. The advantage of this method lies in its ability to discover elliptical zones in any direction. The zones were smoothed according to geology and a good match with the QAFI was found. Finally, 16 zones were defined (Figure 4.4).

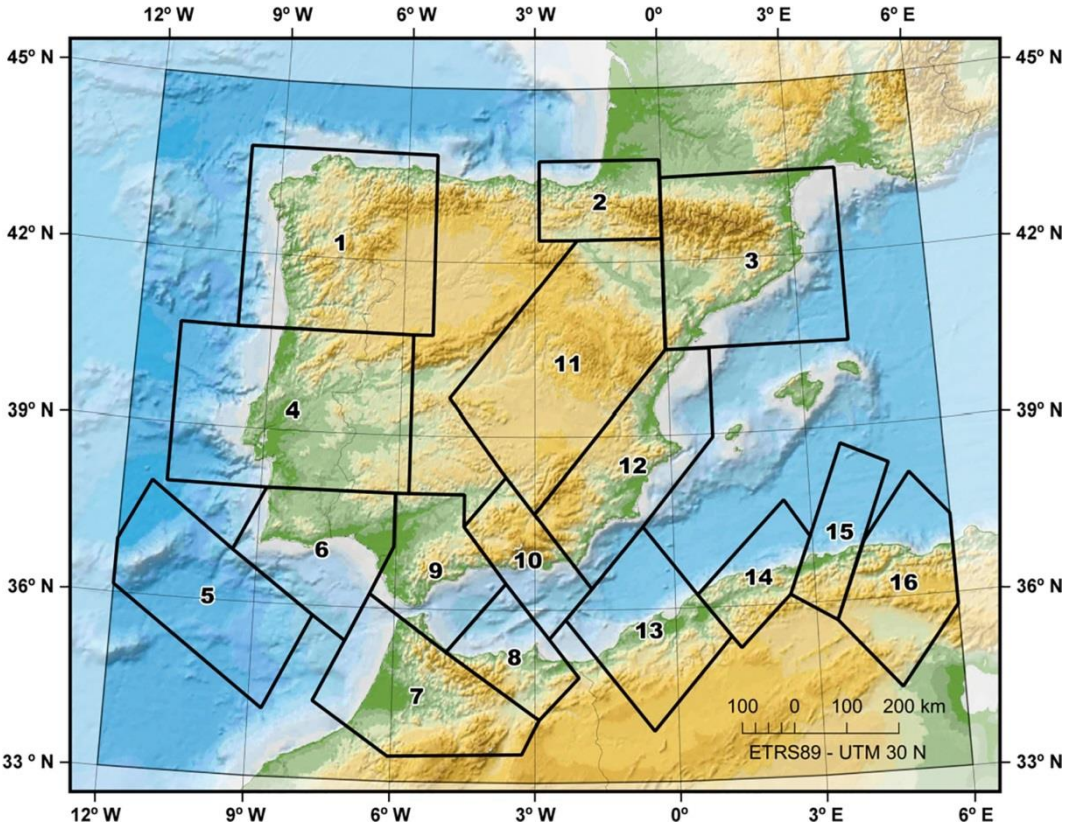

Figure 4.4. MAH zoning for the IP. Source: Amaro-Mellado et al. (2017)

✓ Martínez-Álvarez et al. (2015) (hereinafter, TRIC) proposed 34 zones for the Iberian Peninsula based on a statistical analysis of the seismicity. Triclustering was used for that purpose and the catalog of the NGIS was adopted. The advantage of this method is its impartiality. It is solely based on seismic data and zone depicting is automatic. The zones were later confirmed with the geology (Figure 4.5).

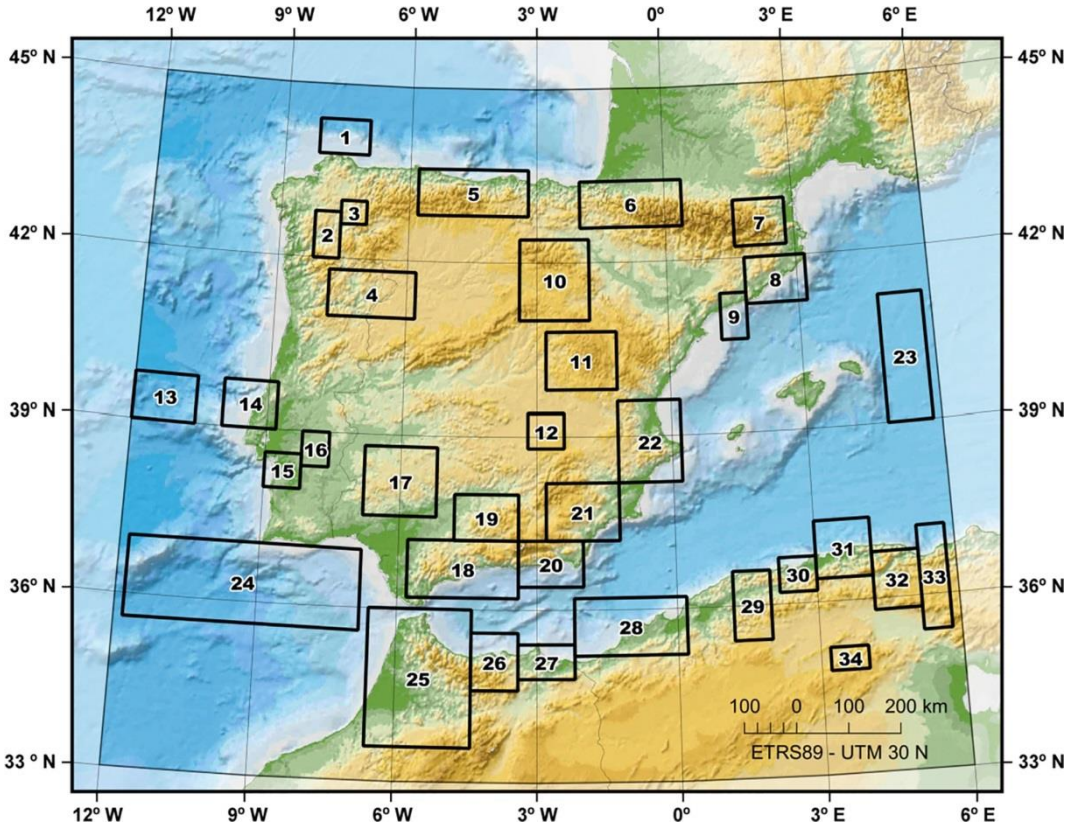

Figure 4.5. TRIC zoning for the IP. Source: Amaro-Mellado et al. (2017)

4.3. SEISMIC STATISTICAL PARAMETERS

In this section, the seismic statistical parameters used in this research are presented. First, the *b*-value has been calculated by the method proposed by Kijko and Smit (2012) that takes into account different periods of completeness is described. The correction proposed by Ogata and Yamashina (1986) has also been used. Next, the normalized annual rate has been calculated (*AR*). The error in the area of every zone due to the curvature of the Earth is also corrected. Finally, two methods for calculating the maximum magnitude are shown. This is determined in consideration of both the largest earthquake registered from the historical data and from the properties of the active Quaternary faults of every zone.

The catalog used for these calculations spans 1373 to June 2014 comprised by parallels 33°N–45°N and meridians 12°W–6°E (Figure 3.5).

The declustering has been applied considering the method proposed by Gardner and Knopoff (1974) with the parameters defined by Peláez et al. (2007) as was mentioned in Chapter 3.

The minimum number of events to compute a proper *b*-value has been set to 30, taking into account the study conducted by Shi and Bolt (1982). This value represents a trade-off between the small amount of data available for some zones and the standard error associated with a significant *b*-value. Thus, *b*-value has been declared "undefined" and is shown as "-" for zones with less than 30 events.

4.4. RESULTS

4.4.1. Results achieved

In this section the results from this study are shown. First, the *AR* is compared to the *b*-value for the five zonings analyzed: Figure 4.6, Figure 4.7, Figure 4.8, Figure 4.9 and Figure 4.10. The axes of these figures have the same length in order to allow a comparison between them. Note that GM12 and ByA12 seismogenic zonings boundary-line files have been provided by the NGIS, upon request.

Later, tables with the zone numbering (*N*), number of events (*NE*), area of the zone (in km^2), $\hat{b}$-value, the $\tilde{b}$-value, the standard deviation of the $\tilde{b}$-value ($\hat{\sigma}_{\tilde{b}}$), the lower and upper endpoint of the 95% confidence interval for the $\tilde{b}$-value, *AR*, *RMM* and *FMM* (when available) are listed. Table 4.1, Table 4.2, Table 4.3, Table 4.4 and Table 4.5 show the results for AJM, GM12, ByA12, MAH and TRIC, respectively.

Finally, regarding with the representations of the parameters: $\tilde{b}$-value are shown in Figure 4.11, Figure 4.12 and Figure 4.13; standard deviation of the $\tilde{b}$-value ($\hat{\sigma}_{\tilde{b}}$) are depicted in Figure 4.14, Figure 4.15 and Figure 4.16; AR is represented in Figure 4.17, Figure 4.18 and Figure 4.19; lastly, in Figure 4.20, Figure 4.21 and Figure 4.22 RMM are presented.

4.4.2. Analysis of the results

This section provides analytical discussion about the results achieved. For a better visualization, illustrate color maps for the $\tilde{b}$-value, its standard deviation, *AR* and *RMM*, for the five studied zonings.

4.4.2.1. AJM zoning (Martín, 1984)

AJM zoning consists of 27 zones that mainly cover the IP. The zone with the lowest number of events is zone 18 (west of the Pyrenees) with 22 events. This ensures an acceptable minimum number of earthquakes for the calculation of the parameters for almost all zones. The smallest zone has 3860 km^2 and the biggest has 48,801 km^2. The $\tilde{b}$-value lies between 0.98 and 1.68. The *AR* varies between 1.4E−03 for zone 1 (Granada Basin) and 4.5E−05 for the west of the Pyrenees. The *RMM* ranges from 4.7 to 8.7 (zone 27) and the *FMM*, similarly, from 5.5 to 8.1 (zone 27). It is important to analyze the Granada Basin (zone 1). This is the zone with the highest *AR* - notably the highest, see Figure 4.6 - and with a $\tilde{b}$-value of 1.16. This means that earthquakes are frequent but large events are not particularly frequent. The *AR* of zones 2, 3 and 22 (Penibetic area, east of the Betics System and north Pyrenees, respectively) is also high. The normalized annual rate, *AR*, presents values between 1.4E-3 for the Granada basin and 4.5E-5 for the Iberian Massif. Figure 4.1 and Figure 4.6 show that zones 2–3 are adjacent and have a very similar *AR* and $\hat{b}$-value and not so dissimilar from 4 and even 1 zones.

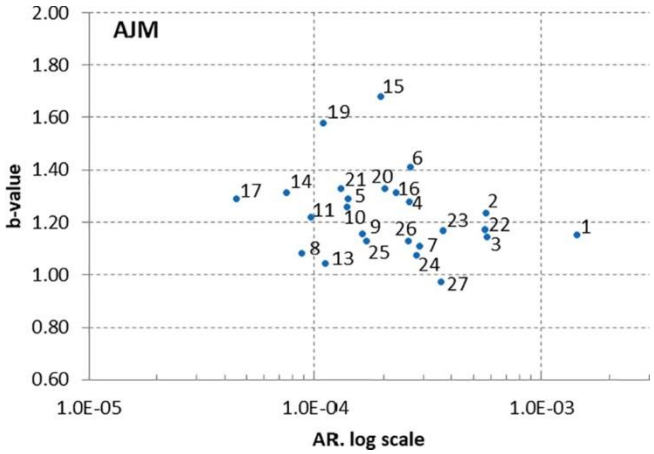

Figure 4.6. Annual rate vs. $\tilde{b}$-value for AJM zoning. Source: Amaro-Mellado et al. (2017)

Table 4.1. Results for AJM zoning

N	*NE*	Area	$\widehat{b}$	$\widetilde{b}$	$\widehat{\sigma}_{\widetilde{b}}$	Lower	Upper	*AR*	*RMM*	*FMM*
1	230	3860	1.16	1.15	0.08	1.00	1.30	1.4E−03	6.7	6.7
2	321	13,888	1.24	1.24	0.07	1.10	1.37	5.7E−04	6.8	6.7
3	315	13,224	1.15	1.15	0.06	1.02	1.27	5.7E−04	6.6	7.4
4	125	12,015	1.29	1.28	0.12	1.05	1.50	2.6E−04	6.3	6.9
5	39	7060	1.32	1.29	0.21	0.87	1.70	1.4E−04	4.7	7.1
6	100	9702	1.42	1.41	0.14	1.13	1.69	2.6E−04	6.7	7.1
7	170	14,023	1.12	1.11	0.09	0.94	1.28	2.9E−04	5.5	5.6
8	82	22,123	1.10	1.08	0.12	0.85	1.32	8.8E−05	6.9	–
9	34	6437	1.19	1.16	0.20	0.76	1.56	1.6E−04	5.2	7.2
10	69	15,57	1.28	1.26	0.15	0.96	1.56	1.4E−04	5.7	7.2
11	88	27,938	1.23	1.22	0.13	0.96	1.48	9.7E−05	5.5	6.9
12	28	9757	–	–	–	–	–	–	6.6	7.5
13	50	13,174	1.06	1.04	0.15	0.75	1.34	1.1E−04	5.5	7.7
14	62	25,837	1.33	1.31	0.17	0.98	1.64	7.5E−05	5.5	7.9
15	134	22,596	1.69	1.68	0.15	1.39	1.97	1.9E−04	5.5	7.9
16	112	15,43	1.33	1.31	0.13	1.07	1.56	2.3E−04	5.9	6.9
17	39	27,111	1.32	1.29	0.21	0.87	1.70	4.5E−05	5.7	7.0
18	22	15,767	–	–	–	–	–	–	5.1	–
19	54	16,023	1.61	1.58	0.22	1.15	2.00	1.1E−04	5.7	7.4
20	53	8222	1.35	1.33	0.19	0.96	1.69	2.0E−04	7.3	7.4
21	82	19,937	1.34	1.33	0.15	1.04	1.62	1.3E−04	6.0	–
22	429	23,04	1.17	1.17	0.06	1.06	1.28	5.6E−04	6.3	7.4
23	50	4139	1.19	1.17	0.17	0.84	1.50	3.7E−04	5.4	–
24	437	46,232	1.08	1.07	0.05	0.97	1.17	2.8E−04	6.9	8.0
25	118	24,549	1.14	1.13	0.10	0.92	1.33	1.7E−04	6.6	5.5
26	359	48,801	1.13	1.13	0.06	1.01	1.25	2.6E−04	6.7	7.5
27	437	38,631	0.98	0.98	0.05	0.88	1.07	3.6E−04	8.7	8.1
Min	22	3860	0.98	0.98	0.05	0.75	1.07	4.5E−05	4.7	5.5
Max	437	48,801	1.69	1.68	0.22	1.39	2.00	1.4E−03	8.7	8.1

4.4.2.2. GM12 zoning (García-Mayordomo et al., 2012b)

This zoning has 55 zones that spread over the IP, the Mediterranean Sea, the north of Africa and the Atlantic Coast to the west of the IP. This plentiful number of zones means that a few zones have less than 30 registers. It should be noted that zone 49 is outside of the area considered in this study. The smaller zone is number 16 (in the Pyrenees) with 3201 km^2 and the biggest is zone 41 (east of the Alboran Sea) with 68,858 km^2. The $\tilde{b}$-value oscillates between 0.73 and 1.96, which may denote the lack of data for a proper calculation of some zones. It should be noted that zone 16 has the highest *AR* (2.6E-3). The *AR* is also significant in zones 35 and 38 (inner Betics System). The *RMM* lies between 4.4 and 8.7 (zone 50). Similarly, the *FMM* ranges from 4.9 to 8.6 (zone 53). There are also many zones with a very low *AR*. Figure 4.2 and Figure 4.7 show that zones 50–51 and 45–46–47–48 are adjacent and have a very similar *AR* and $\tilde{b}$-value.

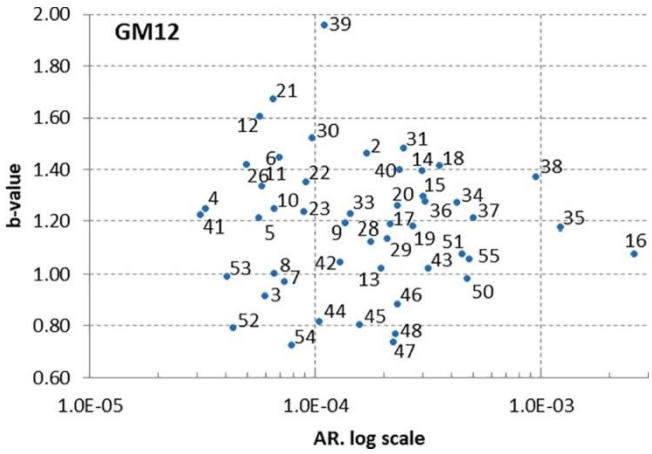

Figure 4.7. Annual rate vs. $\tilde{b}$-value for GM12 zoning. Source: Amaro-Mellado et al. (2017)

Table 4.2. Results for GM12 zoninig

N	*NE*	Area	$\widehat{b}$	$\widetilde{b}$	$\widehat{\sigma}_{\widetilde{b}}$	Lower	Upper	*AR*	*RMM*	*FMM*
1	17	25,367	–	–	–	–	–	–	6.3	–
2	243	46,034	1.47	1.46	0.09	1.28	1.65	1.7E−04	5.5	7.6
3	39	18,438	0.94	0.92	0.15	0.62	1.21	6.0E−05	5.2	–
4	35	33,604	1.29	1.25	0.22	0.82	1.68	3.2E−05	5.5	–
5	32	17,675	1.25	1.21	0.22	0.78	1.65	5.6E−05	5.1	–
6	124	57,525	1.46	1.45	0.13	1.19	1.70	6.9E−05	5.9	7.9
7	51	20,058	0.99	0.97	0.14	0.70	1.25	7.3E−05	5.5	7.9
8	51	25,178	1.03	1.01	0.14	0.72	1.29	6.5E−05	6.3	–
9	69	15,633	1.21	1.20	0.15	0.91	1.48	1.4E−04	6.6	7.7
10	134	63,264	1.26	1.25	0.11	1.04	1.46	6.5E−05	6.0	7.5
11	58	31,676	1.36	1.34	0.18	0.99	1.69	5.8E−05	5.9	–
12	92	52,789	1.62	1.61	0.17	1.27	1.94	5.7E−05	4.9	6.0
13	73	10,997	1.04	1.03	0.12	0.79	1.26	1.9E−04	5.2	7.2
14	71	7647	1.41	1.39	0.17	1.07	1.72	2.9E−04	5.2	–
15	55	5760	1.32	1.30	0.18	0.95	1.64	3.0E−04	4.4	–
16	280	3201	1.08	1.08	0.06	0.95	1.21	2.6E−03	6.3	–
17	69	9858	1.21	1.19	0.15	0.91	1.48	2.1E−04	6.0	–
18	77	6912	1.44	1.42	0.16	1.10	1.74	3.5E−04	6.3	7.4
19	41	4681	1.21	1.18	0.19	0.81	1.55	2.7E−04	7.3	7.4
20	62	8324	1.28	1.26	0.16	0.94	1.58	2.3E−04	6.0	–
21	33	17,215	1.73	1.67	0.30	1.09	2.26	6.5E−05	6.0	–
22	39	13,599	1.39	1.35	0.22	0.92	1.79	9.1E−05	6.3	7.3
23	48	16,739	1.26	1.24	0.18	0.88	1.59	8.9E−05	5.7	7.4
24	14	28,162	–	–	–	–	–	–	4.7	–
25	16	15,76	–	–	–	–	–	–	5.7	–
26	55	35,547	1.45	1.42	0.20	1.04	1.80	4.9E−05	5.2	7.0
27	17	17,212	–	–	–	–	–	–	4.4	7.4
28	114	15,607	1.14	1.13	0.11	0.92	1.34	1.8E−04	6.9	–
29	123	14,326	1.15	1.14	0.10	0.94	1.34	2.1E−04	5.3	5.6
30	55	14,826	1.55	1.52	0.21	1.11	1.93	9.6E−05	4.7	7.1
31	141	14,832	1.49	1.48	0.13	1.24	1.73	2.5E−04	6.7	7.1
32	9	47,978	–	–	–	–	–	–	5.5	4.9
33	80	13,958	1.25	1.23	0.14	0.96	1.50	1.4E−04	5.5	5.5
34	135	8000	1.28	1.27	0.11	1.06	1.49	4.2E−04	6.8	6.7
35	344	6894	1.18	1.18	0.06	1.05	1.30	1.2E−03	6.7	6.7
36	91	7429	1.29	1.28	0.14	1.01	1.54	3.1E−04	6.3	6.9
37	218	10,723	1.22	1.21	0.08	1.05	1.38	5.0E−04	5.7	6.8
38	194	6480	1.38	1.37	0.10	1.18	1.57	9.5E−04	6.5	6.4
39	42	12,739	2.00	1.96	0.31	1.35	2.56	1.1E−04	4.9	6.5
40	77	11,656	1.42	1.40	0.16	1.08	1.72	2.4E−04	6.7	–
41	69	68,858	1.24	1.23	0.15	0.93	1.52	3.1E−05	4.8	–
42	50	13,544	1.07	1.05	0.15	0.75	1.34	1.3E−04	6.6	–
43	223	24,421	1.03	1.02	0.07	0.89	1.16	3.2E−04	6.2	7.5
44	54	17,569	0.83	0.82	0.11	0.60	1.04	1.0E−04	5.8	7.5
45	127	27,4	0.81	0.81	0.07	0.67	0.95	1.6E−04	7.0	7.5
46	160	23,671	0.89	0.88	0.07	0.75	1.02	2.3E−04	7.3	–
47	130	19,446	0.75	0.74	0.07	0.61	0.87	2.2E−04	7.3	–
48	197	29,065	0.77	0.77	0.06	0.66	0.88	2.3E−04	7.1	–
49	1	868	–	–	–	–	–	–	3.4	–
50	520	35,368	0.99	0.99	0.04	0.90	1.07	4.7E−04	8.7	8.1
51	431	28,564	1.08	1.08	0.05	0.98	1.18	4.5E−04	6.9	8.0
52	48	33,387	0.81	0.79	0.12	0.56	1.02	4.3E−05	6.2	7.1
53	47	33,633	1.02	0.99	0.15	0.70	1.28	4.0E−05	5.5	8.6
54	30	12,707	0.75	0.73	0.14	0.46	1.00	7.8E−05	6.7	–
55	220	10,791	1.06	1.06	0.07	0.92	1.20	4.8E−04	6.6	7.4
Min	1	868	0.75	0.73	0.04	0.46	0.87	3.1E−05	3.4	4.9
Max	520	68,858	2.00	1.96	0.31	1.35	2.56	2.6E−03	8.7	8.6

4.4.2.3. ByA12 zoning (Bernal, 2011)

ByA12 is the zoning analyzed with the largest number of zones (72). Therefore, in many zones, less than 30 earthquakes have been registered. This zoning covers the full IP and surrounding area. Zone 40 has just 1144 km^2 (Medium Segura fault zone). By contrast, the largest is zone 72 (coastal zone to the east of Levante) with 69,348 km^2. The $\tilde{b}$-value lies from 0.78 to 1.85. There are a few zones with a high *AR* (greater than 1E-3), especially zone 51 (Loja-Gorda Mountains), zone 52 (Granada), zone 15 (northwestern Pyrenees), zone 60 (Adra-Alhamilla Mountains) and zone 55 (Almanzora Valley). The *RMM* ranges between 3.5 and 8.7 (zone 45) and the *FMM* between 4.9 and 8.0 (zone 45).It should be noted that the 44–45 adjacent zones present not dissimilar $\tilde{b}$-values and *AR* figures. Finally, and again, it must be highlighted that too many zones exist with not enough data to conduct a proper calculation and to look for potential clusters of zones.

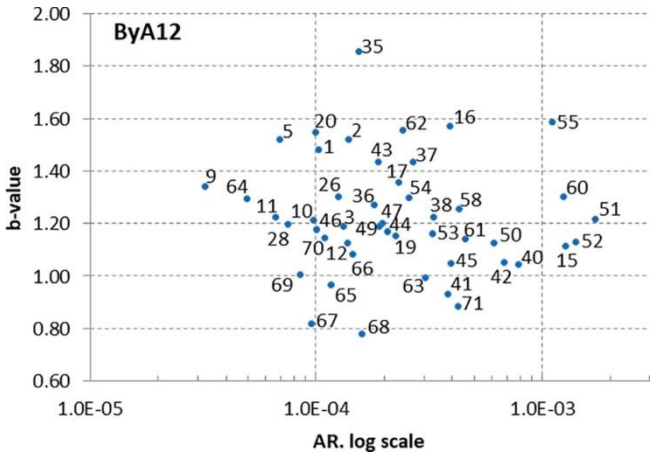

Figure 4.8. Annual rate vs. $\tilde{b}$-value for ByA12 zoning. Source: Amaro-Mellado et al. (2017)

Table 4.3. Results for ByA12 zoning

N	*NE*	Area	$\widehat{b}$	$\widetilde{b}$	$\widehat{\sigma}_{\widetilde{b}}$	Lower	Upper	*AR*	*RMM*	*FMM*
1	46	14,447	1.51	1.48	0.22	1.04	1.92	1.0E−04	5.5	7.6
2	149	34,639	1.53	1.52	0.13	1.27	1.77	1.4E−04	5.5	7.9
3	153	35,278	1.20	1.19	0.10	1.00	1.38	1.3E−04	5.9	7.2
4	19	16,314	–	–	–	–	–	–	4.9	–
5	70	32,581	1.54	1.52	0.18	1.16	1.88	6.9E−05	5.5	7.9
6	7	29,734	–	–	–	–	–	–	3.5	7.5
7	21	17,939	–	–	–	–	–	–	4.4	7.5
8	28	16,72	–	–	–	–	–	–	4.9	–
9	69	67,193	1.36	1.34	0.16	1.02	1.66	3.2E−05	5.9	7.5
10	95	29,982	1.22	1.21	0.13	0.97	1.46	9.7E−05	6.0	7.6
11	39	18,073	1.25	1.22	0.20	0.83	1.62	6.7E−05	4.4	–
12	139	30,178	1.13	1.13	0.10	0.94	1.32	1.4E−04	5.7	7.2
13	2	31,861	–	–	–	–	–	–	4.7	–
14	12	27,401	–	–	–	–	–	–	4.8	–
15	369	8707	1.12	1.12	0.06	1.00	1.23	1.3E−03	6.3	–
16	35	2905	1.62	1.57	0.27	1.04	2.11	3.9E−04	5.2	–
17	176	24,003	1.36	1.35	0.10	1.15	1.56	2.3E−04	7.3	7.4
18	14	1396	–	–	–	–	–	–	6.3	6.9
19	59	8000	1.18	1.16	0.15	0.86	1.46	2.2E−04	4.9	–
20	37	12,072	1.59	1.55	0.26	1.04	2.06	9.9E−05	6.0	–
22	10	1593	–	–	–	–	–	–	5.3	6.9
23	24	13,917	–	–	–	–	–	–	5.1	–
24	4	26,915	–	–	–	–	–	–	4.0	–
25	8	12,054	–	–	–	–	–	–	4.1	–
26	34	8476	1.34	1.30	0.23	0.85	1.75	1.3E−04	5.7	7.3
28	33	13,539	1.24	1.20	0.22	0.78	1.62	7.5E−05	5.2	7.4
29	10	2786	–	–	–	–	–	–	5.7	–
30	0	6030	–	–	–	–	–	–	4.1	–
31	21	12,853	–	–	–	–	–	–	5.2	7.0
32	24	17,005	–	–	–	–	–	–	5.2	–
34	19	15,11	–	–	–	–	–	–	4.4	7.4
35	42	7274	1.90	1.85	0.29	1.28	2.43	1.5E−04	5.5	7.1
36	39	5382	1.30	1.27	0.21	0.86	1.68	1.8E−04	5.5	7.1
37	68	6507	1.45	1.43	0.18	1.09	1.78	2.7E−04	6.7	7.1
38	71	5330	1.24	1.23	0.15	0.94	1.52	3.3E−04	5.2	6.8
39	6	18,419	–	–	–	–	–	–	5.5	4.9
40	38	1144	1.07	1.04	0.17	0.70	1.38	7.8E−04	5.7	6.8
41	53	3138	0.95	0.93	0.13	0.68	1.19	3.8E−04	6.6	6.8
42	39	1357	1.08	1.05	0.17	0.71	1.39	6.8E−04	6.0	7.0
43	37	5045	1.47	1.43	0.24	0.96	1.91	1.9E−04	4.9	6.8
44	46	6758	1.20	1.17	0.18	0.82	1.52	2.1E−04	5.2	7.2
45	643	47,774	1.05	1.05	0.04	0.97	1.13	3.9E−04	8.7	8.0
46	72	17,455	1.19	1.18	0.14	0.90	1.45	1.0E−04	6.9	–
47	86	10,715	1.22	1.20	0.13	0.95	1.46	2.0E−04	5.3	5.6
48	23	6688	–	–	–	–	–	–	4.3	7.1
49	83	10,62	1.20	1.19	0.13	0.93	1.45	1.9E−04	4.9	5.5
50	160	6264	1.14	1.13	0.09	0.95	1.30	6.1E−04	5.5	–
51	146	2081	1.23	1.22	0.10	1.02	1.42	1.7E−03	6.5	6.7
52	135	2300	1.14	1.13	0.10	0.94	1.32	1.4E−03	6.7	6.5
53	92	6855	1.18	1.16	0.12	0.92	1.40	3.3E−04	5.5	6.9
54	36	3516	1.34	1.30	0.22	0.86	1.74	2.6E−04	6.3	6.9
55	97	2297	1.60	1.59	0.16	1.27	1.90	1.1E−03	6.3	6.5
56	25	3045	–	–	–	–	–	–	5.5	6.1
57	24	2264	–	–	–	–	–	–	5.2	6.3
58	72	4175	1.27	1.25	0.15	0.96	1.55	4.3E−04	6.8	6.7
59	24	2906	–	–	–	–	–	–	6.1	6.2
60	160	4016	1.31	1.30	0.10	1.10	1.50	1.2E−03	6.4	7.4
61	88	5810	1.15	1.14	0.12	0.90	1.38	4.6E−04	6.5	7.4
62	98	14,581	1.57	1.55	0.16	1.24	1.87	2.4E−04	6.7	6.9
63	166	18,832	1.00	0.99	0.08	0.84	1.15	3.0E−04	6.2	7.5
64	95	59,723	1.31	1.30	0.13	1.03	1.56	5.0E−05	4.9	7.5
65	71	20,888	0.98	0.97	0.12	0.74	1.20	1.2E−04	6.6	–
66	84	20,258	1.10	1.08	0.12	0.85	1.32	1.4E−04	6.7	–
67	61	21,527	0.83	0.82	0.11	0.61	1.03	9.5E−05	5.7	7.4
68	99	20,73	0.79	0.78	0.08	0.62	0.93	1.6E−04	7.0	7.4
69	63	21,448	1.02	1.00	0.13	0.75	1.26	8.5E−05	5.5	7.7
70	34	9449	1.18	1.15	0.20	0.75	1.54	1.1E−04	6.6	7.5
71	109	7938	0.89	0.89	0.09	0.72	1.05	4.3E−04	7.9	8.0
72	20	69,348	–	–	–	–	–	–	4.9	7.3
Min	0	1144	0.79	0.78	0.04	0.61	0.93	3.2E−05	3.5	4.9
Max	643	69,348	1.90	1.85	0.29	1.28	2.43	1.7E−03	8.7	8.0

4.4.2.4. MAH zoning (Morales-Esteban et al., 2014)

MAH zoning is the zoning with the lowest number of zones (16). All zones possess a great number of events (160–693). This makes the statistical results very robust (0.11 as maximum standard deviation). The smallest zone is zone 14 (northeast of the Tell Atlas) with 29,478 km^2 and the largest is zone 4 (center and coastal zone to the west of Portugal) with 1,384,436 km^2. The smallest $\tilde{b}$-value is 0.70 (zone 16) and the highest is 1.50 (zone 11, Iberian Mountain Mass). It is noteworthy that zones 13–16 have a $\tilde{b}$-value below 1.0. This shows that large earthquakes are quite frequent in the Tell Atlas. No zone can be highlighted for having a very low or very high *AR* (between 5.0E-4 and 4.8E-5) as the areas are quite large and this softens the results. The lowest *RMM* is 5.7 and the lowest *FMM* is 6.7. The largest *RMM* (8.7) is similar to the largest *FMM* (8.6), both in zone 5. Only zones 14, 15 and 16 have a more or less similar $\tilde{b}$-value and *AR* to their neighbors.

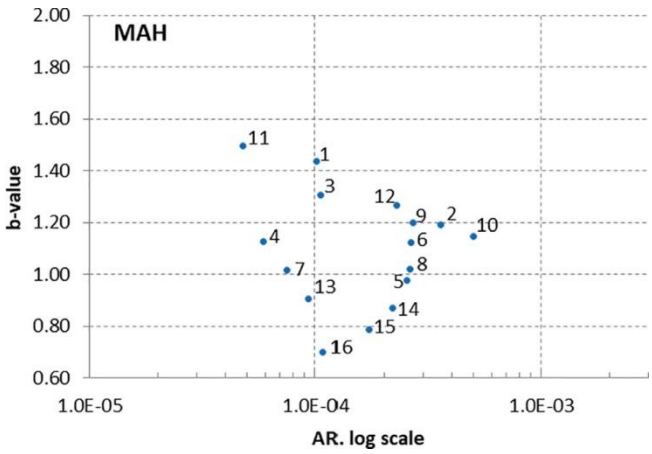

Figure 4.9. Annual rate vs. $\tilde{b}$-value for MAH zoning. Source: Amaro-Mellado et al. (2017)

Table 4.4. Results for MAH zoning

N	*NE*	Area	$\widehat{b}$	$\widetilde{b}$	$\widehat{\sigma}_{\widetilde{b}}$	Lower	Upper	*AR*	*RMM*	*FMM*
1	404	127,115	1.44	1.43	0.07	1.29	1.57	1.0E−04	5.9	7.9
2	418	35,487	1.19	1.19	0.06	1.08	1.31	3.6E−04	6.0	–
3	388	113,716	1.31	1.30	0.07	1.17	1.44	1.1E−04	7.3	7.4
4	273	138,436	1.13	1.13	0.07	0.99	1.26	5.9E−05	6.6	7.9
5	628	78,936	0.98	0.98	0.04	0.90	1.05	2.5E−04	8.7	8.6
6	520	58,867	1.12	1.12	0.05	1.03	1.22	2.6E−04	6.9	8.0
7	164	75,504	1.02	1.02	0.08	0.86	1.17	7.5E−05	6.7	–
8	241	31,997	1.03	1.02	0.07	0.89	1.15	2.6E−04	6.7	7.1
9	522	47,498	1.20	1.20	0.05	1.10	1.30	2.7E−04	6.9	6.7
10	693	33,556	1.15	1.15	0.04	1.06	1.23	5.0E−04	6.7	7.5
11	182	122,376	1.51	1.50	0.11	1.28	1.72	4.8E−05	5.7	7.0
12	692	75,647	1.27	1.26	0.05	1.17	1.36	2.3E−04	6.7	7.4
13	170	62,216	0.91	0.91	0.07	0.77	1.04	9.3E−05	7.0	7.5
14	190	29,478	0.88	0.87	0.06	0.75	1.00	2.2E−04	7.3	–
15	160	31,053	0.79	0.79	0.06	0.66	0.91	1.7E−04	7.3	–
16	187	56,554	0.70	0.70	0.05	0.60	0.80	1.1E−04	7.1	–
Min	160	29,478	0.70	0.70	0.04	0.60	0.80	4.8E−05	5.7	6.7
Max	693	138,436	1.51	1.50	0.11	1.29	1.72	5.0E−04	8.7	8.6

4.4.2.5. TRIC zoning (Martínez-Alvarez et al., 2015)

TRIC zoning has 34 zones. An almost acceptable number of events (between 23 and 27) has been registered for several zones (5, 9, 10, 11, 12, 23) and a very low number of earthquakes for zone 23 (zone to the east of the Balearic Islands) and 34 (south of the Tell Atlas). The smallest zone is zone 3 (east of Galicia) with 2200 km^2 and the largest is zone 24 (Azores-Gibraltar Fault) with 69,726 km^2. Zone 33 (east of the Tell Atlas) can be considered the zone with the lowest $\tilde{b}$-value (0.60). It should be noted that in this zoning quite a few zones with a $\tilde{b}$-value below 1.0 have been identified. Zones 3 (in Galicia) and 6 (west of the Pyrenees) have the highest *AR*. As in the MAH zoning, the *AR* values are also very homogeneous (between 8.7E-4 and 6.8E-5) The *RMM* ranges from 4.4 to 8.7 (zone 24) and the *FMM* from 6.3 to 8.1 (zone 24). The analysis of the Figure 4.10 shows that all the zones are different to those adjacent except for 27–28 and 30–33.

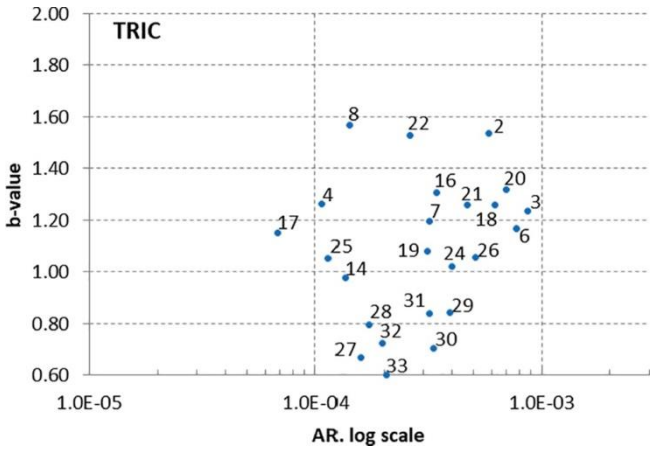

Figure 4.10. Annual rate vs. $\tilde{b}$-value for TRIC zoning. Source: Amaro-Mellado et al. (2017)

Table 4.5. Results for TRIC zoning

N	*NE*	Area	$\widehat{b}$	$\widetilde{b}$	$\widehat{\sigma}_{\widetilde{b}}$	Lower	Upper	*AR*	*RMM*	*FMM*
1	22	6365	–	–	–	–	–	–	4.5	–
2	76	4402	1.56	1.54	0.18	1.19	1.89	5.9E−04	4.4	–
3	62	2200	1.25	1.23	0.16	0.92	1.54	8.7E−04	5.4	6.9
4	51	14,858	1.29	1.26	0.18	0.91	1.62	1.1E−04	5.5	7.9
5	25	18,778	–	–	–	–	–	–	5.1	–
6	443	17,39	1.17	1.16	0.06	1.06	1.27	7.7E−04	6.3	–
7	91	8751	1.21	1.20	0.13	0.95	1.44	3.2E−04	7.3	7.4
8	45	10,37	1.60	1.57	0.24	1.10	2.03	1.4E−04	5.7	6.9
9	24	4485	–	–	–	–	–	–	5.1	–
10	23	20,707	–	–	–	–	–	–	5.7	–
11	23	15,104	–	–	–	–	–	–	5.2	6.8
12	24	4610	–	–	–	–	–	–	4.7	–
13	25	10,71	–	–	–	–	–	–	5.4	–
14	43	9180	1.00	0.98	0.15	0.68	1.27	1.3E−04	6.6	7.7
15	27	4661	–	–	–	–	–	–	6.6	7.0
16	38	3476	1.34	1.31	0.22	0.88	1.73	3.4E−04	5.5	–
17	42	18,666	1.18	1.15	0.18	0.79	1.50	6.8E−05	4.9	–
18	594	23,796	1.26	1.26	0.05	1.16	1.36	6.2E−04	6.8	6.7
19	144	10,977	1.09	1.08	0.09	0.90	1.26	3.1E−04	5.5	6.3
20	246	11,092	1.32	1.32	0.08	1.15	1.48	6.9E−04	6.5	7.4
21	297	15,66	1.26	1.26	0.07	1.11	1.40	4.7E−04	6.3	7.0
22	190	18,873	1.54	1.53	0.11	1.31	1.75	2.6E−04	6.7	7.1
23	10	20,826	–	–	–	–	–	–	4.7	–
24	962	69,726	1.02	1.02	0.03	0.96	1.09	4.0E−04	8.7	8.1
25	176	53,588	1.06	1.05	0.08	0.90	1.21	1.1E−04	6.7	–
26	148	10,115	1.06	1.06	0.09	0.88	1.23	5.1E−04	6.2	6.9
27	35	7283	0.69	0.67	0.12	0.44	0.90	1.6E−04	5.8	–
28	124	24,096	0.80	0.79	0.07	0.65	0.93	1.7E−04	7.0	7.5
29	111	9604	0.85	0.84	0.08	0.68	1.00	3.9E−04	7.3	–
30	48	4772	0.72	0.70	0.10	0.50	0.90	3.3E−04	7.3	–
31	112	11,869	0.85	0.84	0.08	0.68	1.00	3.2E−04	7.0	–
32	59	9966	0.74	0.72	0.10	0.54	0.91	2.0E−04	6.8	–
33	69	10,763	0.61	0.60	0.07	0.46	0.74	2.1E−04	7.1	–
34	4	3241	–	–	–	–	–	–	5.0	–
Min	4	2200	0.61	0.60	0.03	0.44	0.74	6.8E−05	4.4	6.3
Max	962	69,726	1.60	1.57	0.24	1.31	2.03	8.7E−04	8.7	8.1

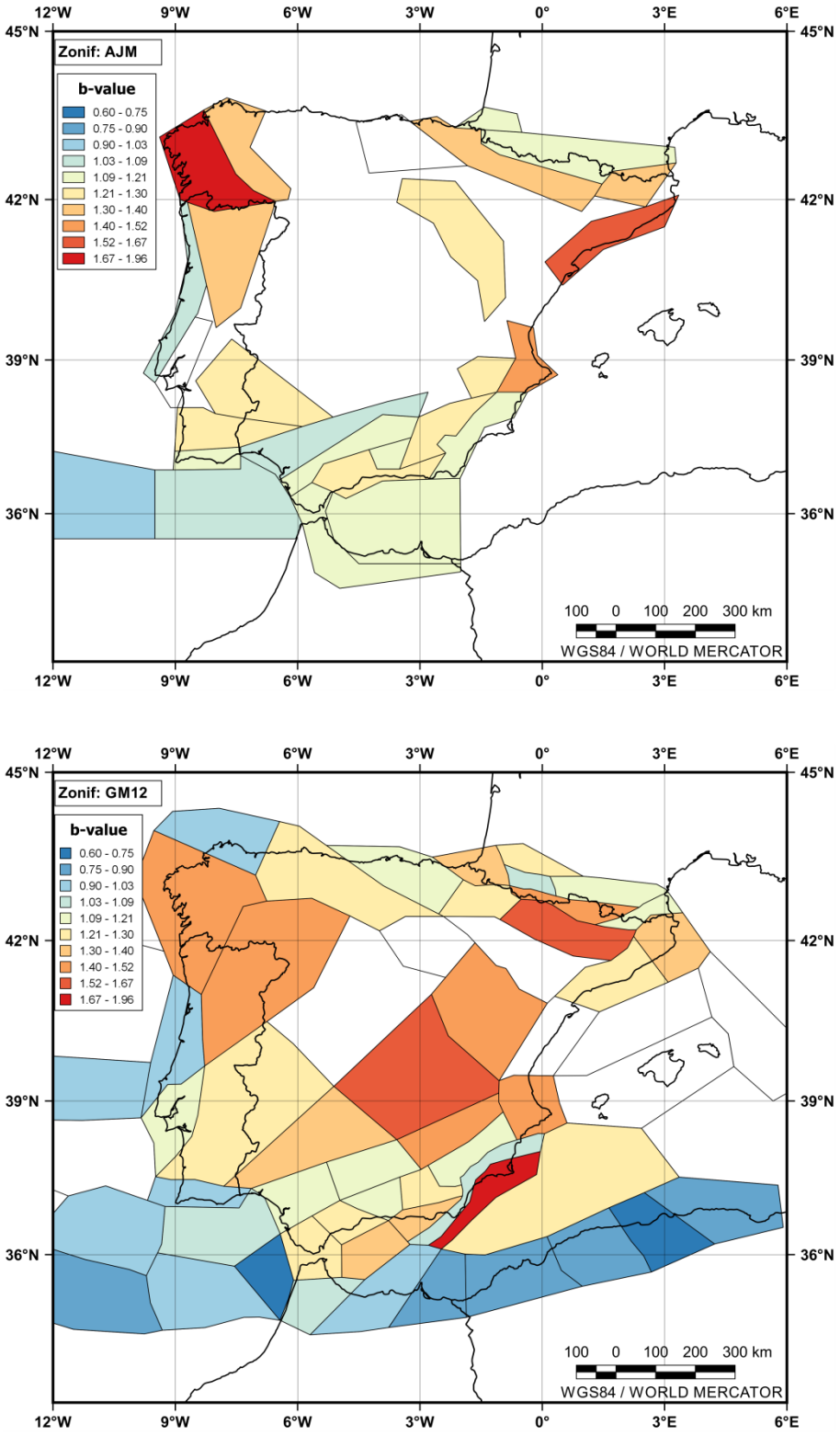

Figure 4.11. Color map to visualize the $\tilde{b}$-value for AJM (up) and GM12 (down) zonings. Source: Amaro-Mellado et al. (2017)

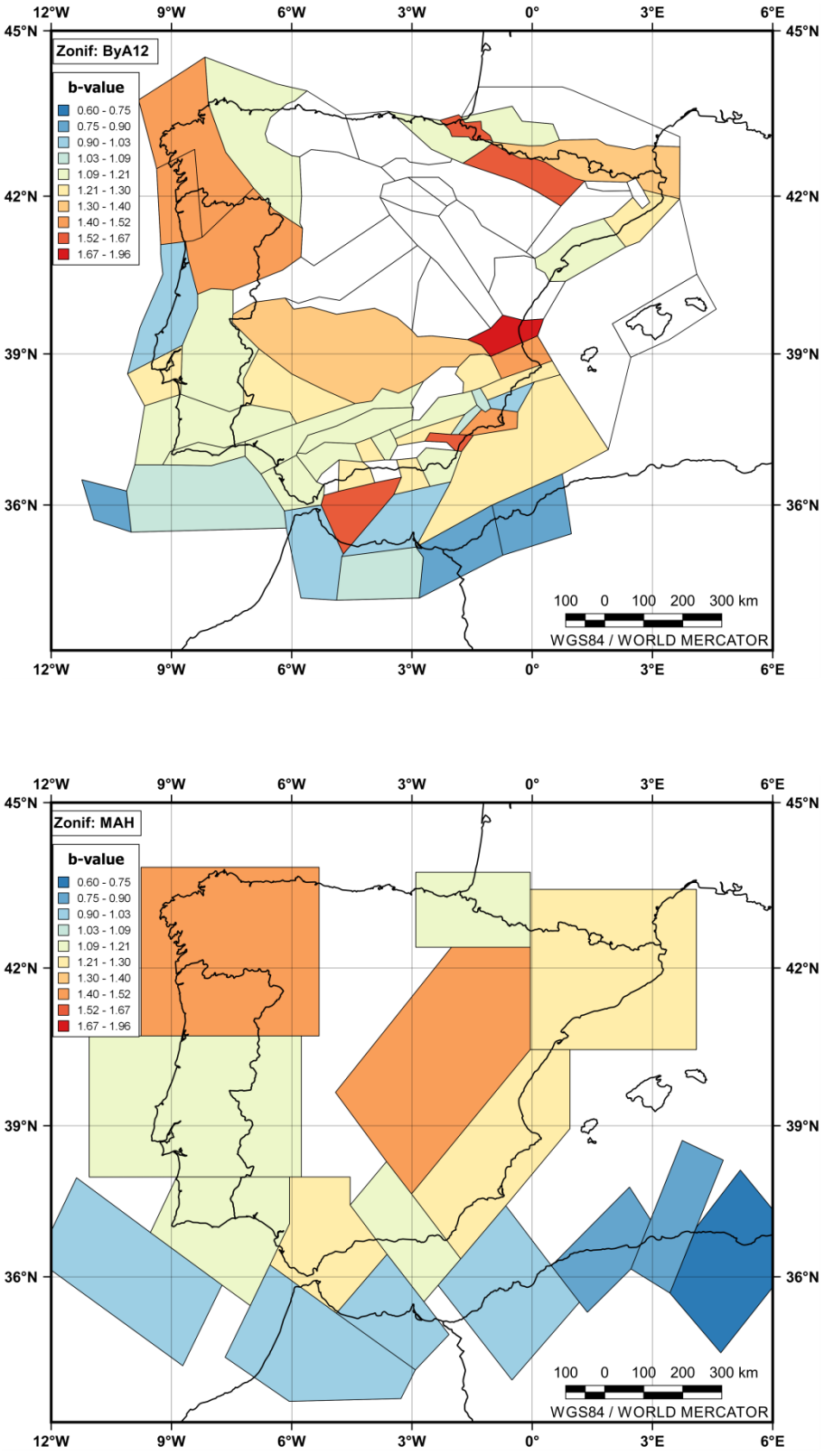

Figure 4.12. Color map to visualize the $\widetilde{b}$-value for ByA12 (up) and MAH (down) zonings. Source: Amaro-Mellado et al. (2017)

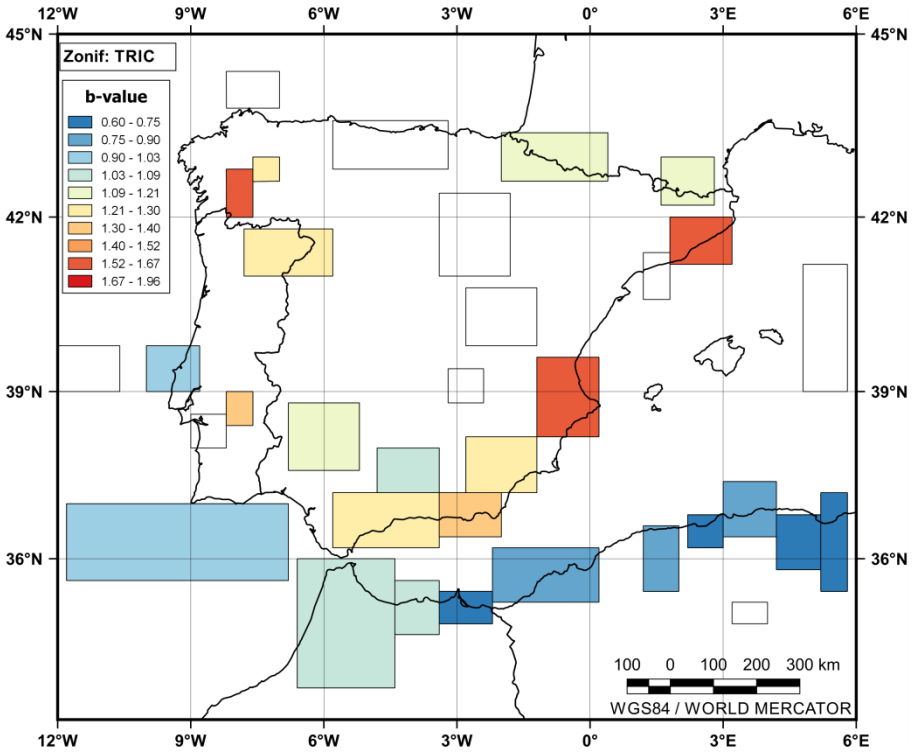

Figure 4.13. Color map to visualize the $\tilde{b}$-value for TRIC zoning. Source: Amaro-Mellado et al. (2017)

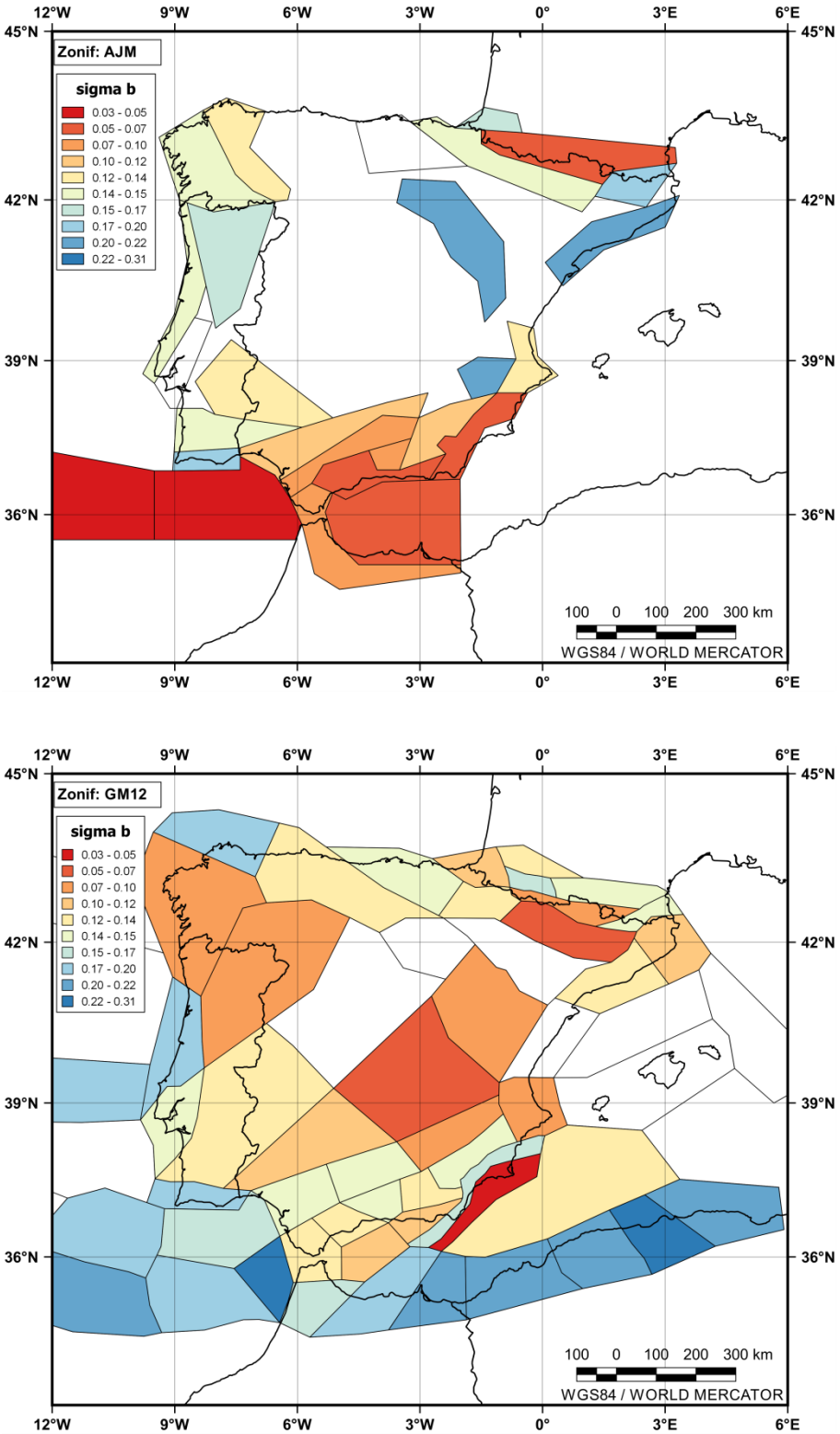

Figure 4.14. Color map to visualize the $\widetilde{b}$-value's standard deviation for AJM (up) and GM12 (down) zonings. Source: Amaro-Mellado et al. (2017)

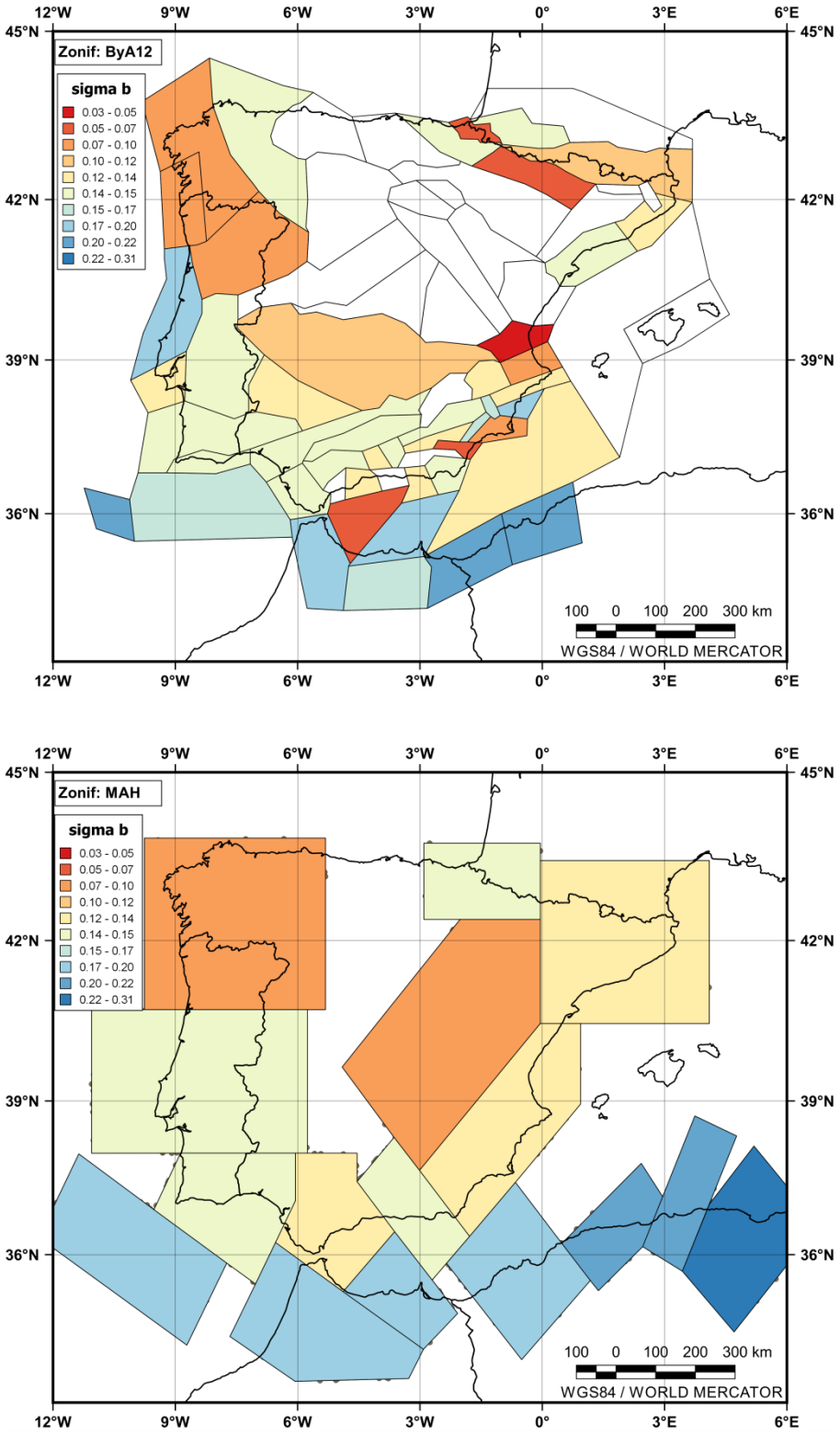

Figure 4.15. Color map to visualize the $\tilde{b}$-value's standard deviation for ByA12 (up) and MAH (down) zonings. Source: Amaro-Mellado et al. (2017)

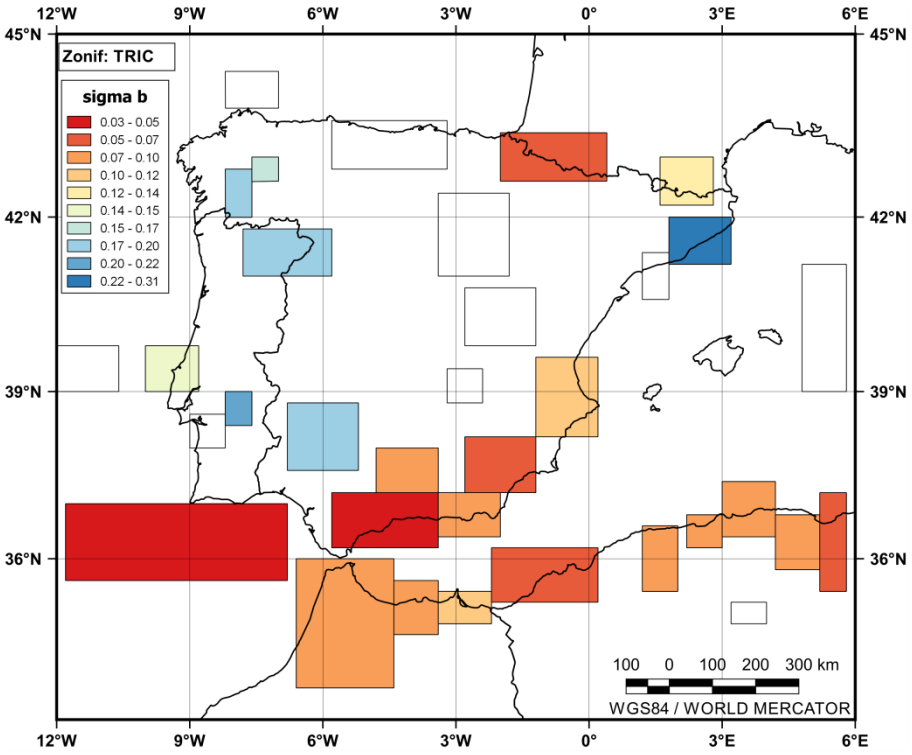

Figure 4.16. Color map to visualize the $\tilde{b}$-value's standard deviation for TRIC zoning. Source: Amaro-Mellado et al. (2017)

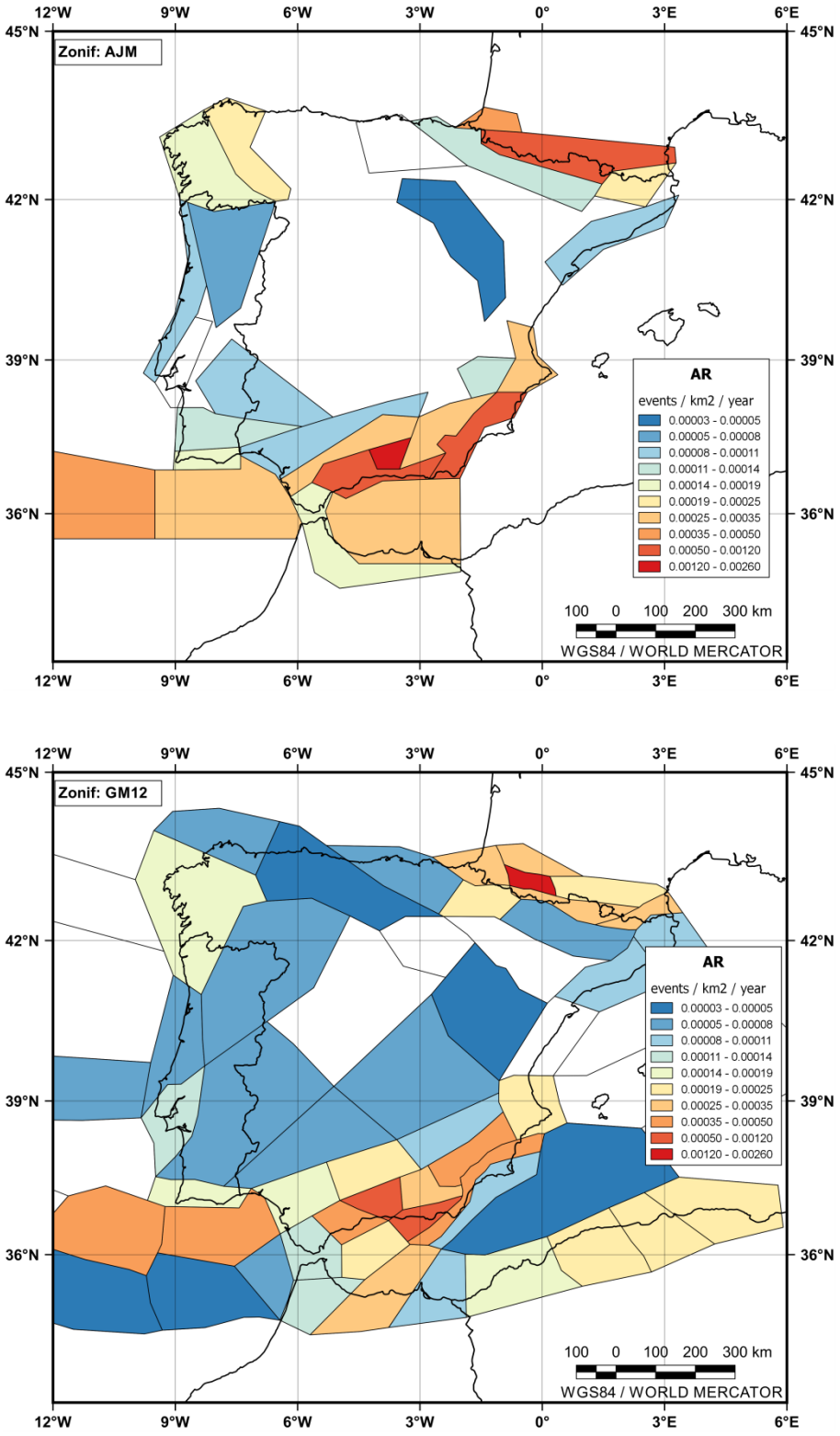

Figure 4.17. Color map to visualize *AR* for AJM (up) and GM12 (down) zonings. Source: Amaro-Mellado et al. (2017)

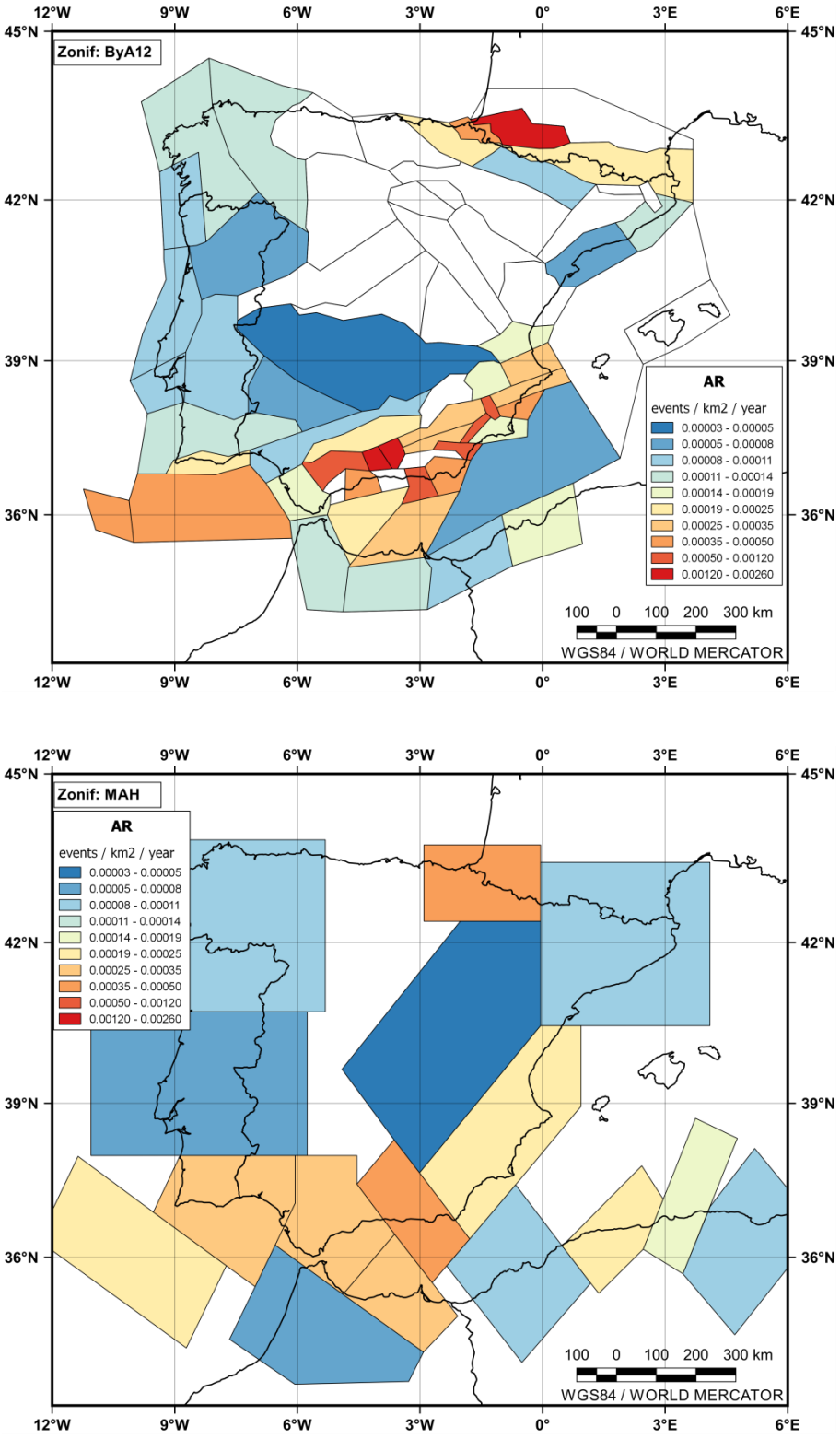

Figure 4.18. Color map to visualize *AR* for ByA12 (up) and MAH (down) zonings. Source: Amaro-Mellado et al. (2017)

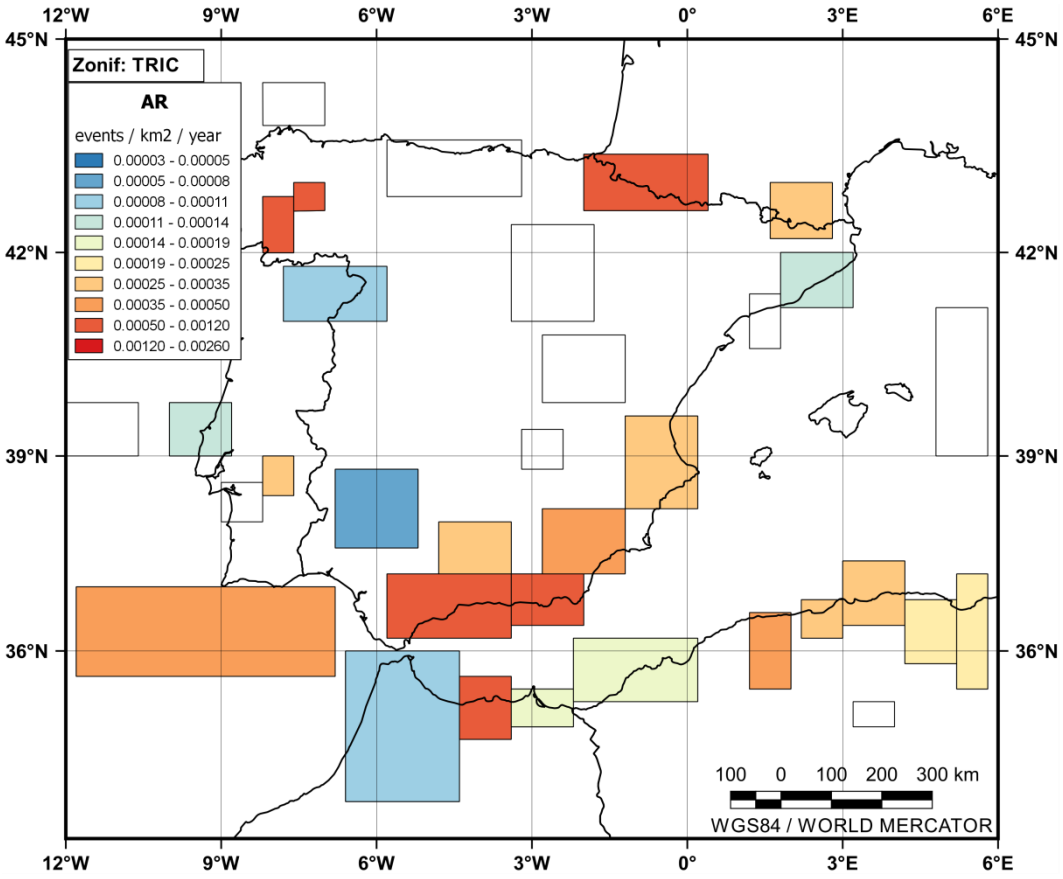

Figure 4.19. Color map to visualize *AR* for TRIC zoning. Source: Amaro-Mellado et al. (2017)

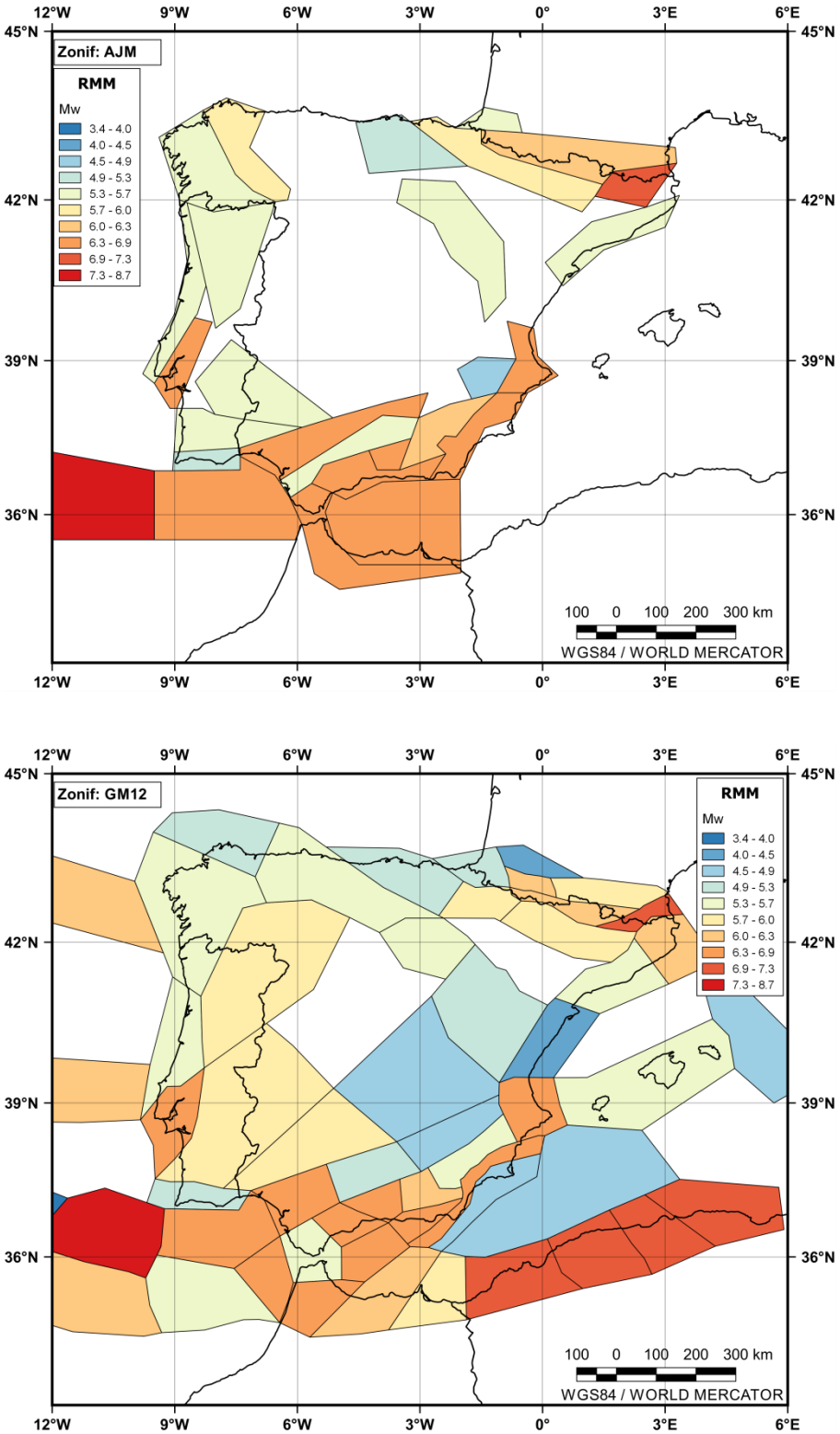

Figure 4.20. Color map to visualize *RMM* for AJM (up) and GM12 (down) zonings. Source: Amaro-Mellado et al. (2017)

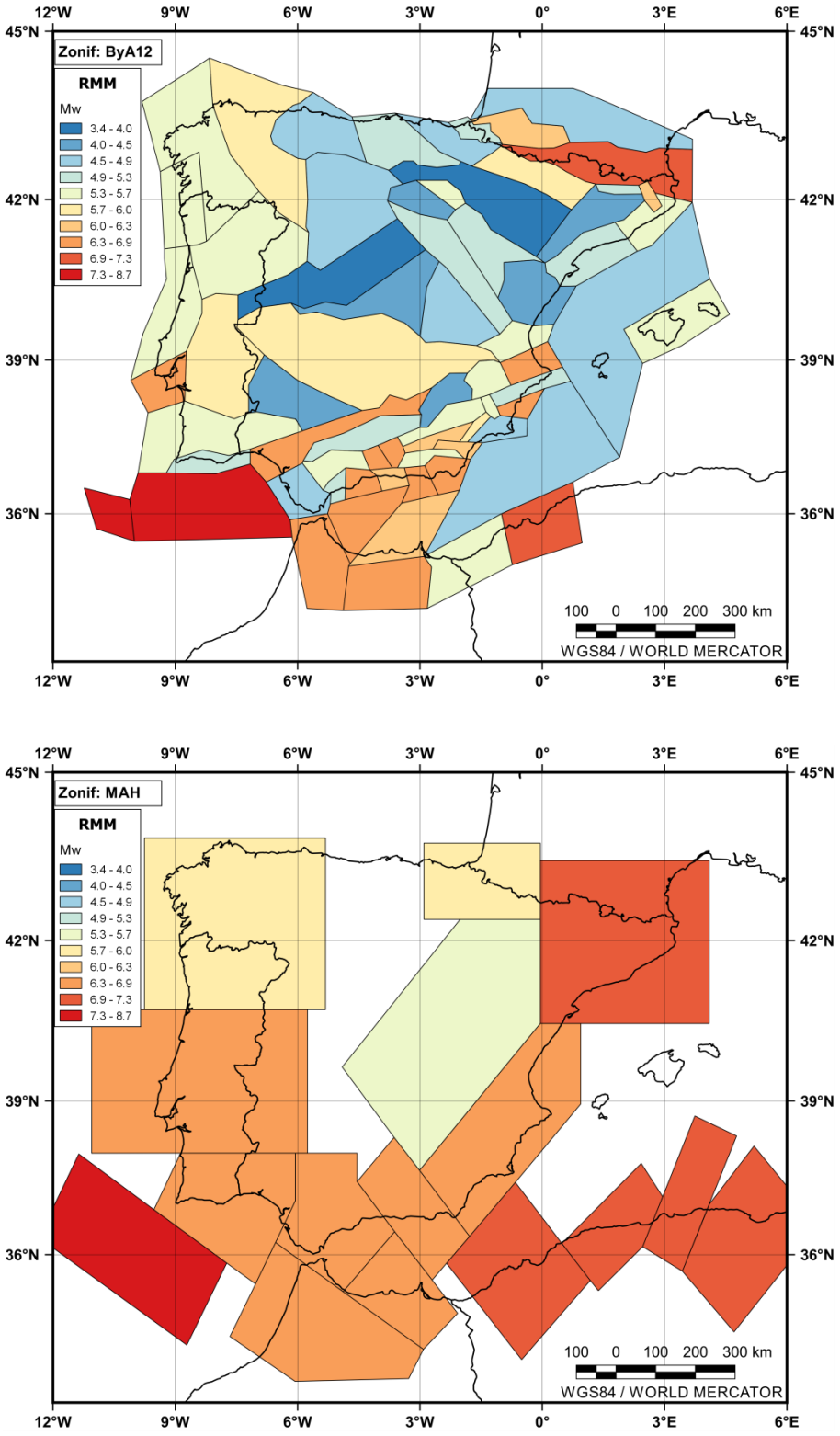

Figure 4.21. Color map to visualize *RMM* for ByA12 (up) and MAH (down) zonings. Source: Amaro-Mellado et al. (2017)

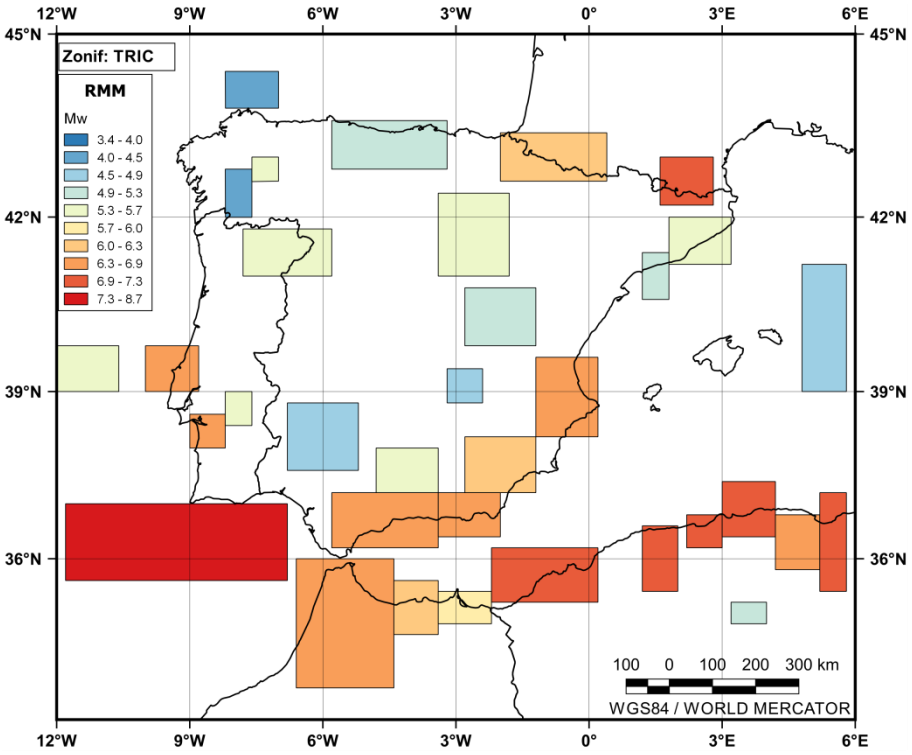

Figure 4.22. Color map to visualize *RMM* for TRIC zoning. Source: Amaro-Mellado et al. (2017)

4.4.3. Tectonic analysis

At present, it is clear that there is a net contact between the Eurasian and the North American plates (de Vicente et al., 2008). This becomes more diffuse towards the African Plate and within the IP. The IP is located between the African and the Eurasian plates. A slow convergence, mainly directed NW-SE, produces its seismicity. The Iberian Plate became part of the Eurasian Plate in the Lower Miocene (Srivastava et al., 1990). The movements between the Iberian, the African and the Eurasian Plates have generated its limits. It should be noted that the Iberian Plate formed part of the African Plate from the Upper Cretaceous to the Upper Eocene Roest and Srivastava, 1991, Srivastava et al., 1990. Most of the IP is under a strike-slip regime that coexists with an extensive regime to the East and to the North.

The Azores-Gibraltar Fault limits the Iberian Plate to the south. It presented a small movement till the Lower Oligocene. From then onward, it has shown an extension regime near the Azores, a strike-slip regime in the Gloria Fault and a compression regime to the East of the Gorringe Bank. In this study, the higher *RMM* and *FMM* have been found in the Azores-Gibraltar Fault. This is consistent with the predominant interplate seismicity of the IP that has produced very large earthquakes in the past.

The stress trajectory curves in the northeastern part of the IP. It moves from NW-SE to N-S and NE-SW. The Pyrenees, the Ebro Basin and the Valencia Basin are affected (de Vicente et al., 2000). The lowest *AR* has been found in the west of the Pyrenees. However, the north of the Pyrenees presents a high *AR*. It should be noted that, currently, there is no clear seismotectonic model for this area (Lacan and Ortuoño, 2012). In the Gulf of Cadiz and in the north of Algeria compressional stresses are predominant. In this study the seismicity in the Gulf of Cadiz is characterized by a *b*-value around 1.0 whereas the north of Algeria presents an outstanding seismicity with values around 0.7–0.8. In the Betics, the Alboran Sea and the Rif a strike-slip regime is principal (de Vivente et al., 2008) which coexists with reverse faults. In the Granada Basin the highest *AR* has been determined. In the Penibetic Area and the East of the Betics System a high *AR* is also shown.

4.4.4. Final remarks

The analysis of the $\tilde{b}$-value shows that the following minimum and maximum values have been obtained: AJM (0.98–1.68), GM12 (0.73–1.96), ByA12 (0.78–1.85), MAH (0.70–1.50) and TRIC (0.60–1.57). The lowest values have been achieved for the zones located in the Tell Atlas: zone 33 for TRIC. Such low $\tilde{b}$-value are hard to imagine. This which might show that the catalog is not complete for that zone, even having considered a regionalized years of completeness. The $\tilde{b}$-value is not far from 1.0 to 1.4 for all zones, except for GM12, where one zone has a value about 2.0. The standard deviations of the $\hat{b}$-value ranges are as follows: AJM (0.05–0.22), GM12 (0.04–0.31), ByA12 (0.04–0.29), MAH (0.04–0.11) and TRIC (0.03–0.24). With regards to the *AR*, the following zones have the highest values within the zonings: AJM (zone 1, 2, 3 and 22), GM12 (zone 16, 35, 38 and 37), ByA12 (zone 51, 52, 15, 60, 55, 40, 42 and 50), MAH (zone 10) and TRIC (zone 3, 6, 20, 18, 2, and 26). The maximum *RMM* ranges between 3.5 and 8.7. The maximum *RMM* is 8.7 for all the zonings. Regarding the maximum *FMM*, it varies from 4.9 to 8.6. The maximum *RMM* and the maximum *FMM* matches for all zonings, except for the GM12 zoning. In this case, the maximum *RMM* is 8.7 for zone 50 and the maximum *FMM* is 8.6 for zone 53.

Comparing these results with other studies, and considering just the *b*-value as a different cut-off magnitude that leads to non-comparable values for *AR*, authors can assess the following. They are a bit higher (0.2) in the mainland and a bit lower (0.3) in the north of Africa than those calculated by Hiemer et al., 2014, Woessner et al., 2015. The later found 0.9 as a global *b*-value for crustal seismicity in Europe. This work shows similar results to Jiménez et al. (1999), who obtained lower values for the North of Africa (0.4–0.9). However, lower values were found for the mainland (approximately 1.0), in contrast to the new results of about 1.2. By comparison to Jiménez et al (1989), the values obtained are pretty high as they calculated values between 0.37 and 0.58 for Southern and East of the IP and Pyrenees by applying Kijko and Sellevoll (1987) method. Vilanova and Fonseca (2007) found values about 1.0 for all Portugal and SW of Cape St. Vincent and this paper computes higher values the further to the North: *b*-values in Portugal up to about 1.5.

The results obtained are very similar, inside a (0.1–0.2) interval, to Mezcua et al. (2011), with the exception in the zones including the M8.7 Lisbon Earthquake, where higher values (about 0.4) were calculated in that research.

To conclude, the results of the *b*-value calculated in this thesis have been compared with those obtained by the authors proposing the zoning which have been analyzed in this doctoral thesis. The annual rate is not comparable, since the cut-off magnitudes are not the same.

- ✓ Martín (1984) worked with macroseismic intensities so the values calculated in this thesis have been considered to not be comparable with this source.
- ✓ When comparing the values that GM12 (García-Mayordomo et al., 2012b) give for their zones, there is important agreement in the southern part (within the uncertainties of the calculation). Even so, there are several areas of the Levant with significant differences (of more than 0.4): in the area that covers most of Galicia and in areas of the Levant, GM12 gets much lower values and the northern part of Galicia much higher.
- ✓ ByA12 (Bernal, 2011) calculates very similar values, although discrepancies are found in some of the areas of the Levant where fewer major earthquakes have occurred. In the northwestern part of Algeria, lower values can be seen in this thesis.
- ✓ MAH (Morales-Esteban et al., 2014) do not present *b*-value parameter values in their research.
- ✓ The results are consistent with those reached by TRIC (Martínez-Álvarez et al., 2015), although these obtain higher values by more than 0.3 in the Tell Atlas area, undoubtedly due to the lack of completeness regarding small earthquakes, especially in the TRIC. Similarly, in the areas of the Levant and eastern Catalonia they give higher values.

Chapter 5.
Seismic parameter analysis of zonings based on regular multiresolution grids

After analyzing the seismic parameters obtained for the zones of several seismic zonings proposed by the experts, this chapter starts from multiresolution grids (0.5º x 0.5º, 1º x 1º, 2º x 2º), purely geometric, and the parameters for each of the cells (which are the equivalent to the seismic zones) of these are obtained. In the introduction

5.1. INTRODUCTION

As can been seen in in previous chapters, some parameters are particularly relevant in this analysis: the *b*-value (the frequency–magnitude relation) that represents the relation between small and large earthquakes, the maximum possible magnitude and, finally, the annual rate of events exceeding a given magnitude threshold.

This research follows the mainstream which holds that the *b*-value can be regarded as a stress-meter. The aim is to obtain a *b*-value map for the Iberian Peninsula using a homogeneous, reviewed and updated catalog lasting more than 600 years. Moreover, different declustering methods, magnitudes of completeness and other restrictions have been considered. It should be noted that the maximum possible magnitude is an outstanding parameter in a seismic analysis (Kijko, 2012). In this research the maximum recorded magnitude (M_{max}) has been used as the maximum possible magnitude. Besides, the M_{max} and the annual rate have been calculated, and subsequently, depicted in maps. In order to properly integrate all the information required and to make the graphic representation easier, a Geographic Information System (GIS) has been used. GIS has also been successfully employed in other geological works (Torrecillas et al. 2006; Ghedhoui et al. 2016).

The GIS has enabled obtaining only the data for the selected area (longitude 12ºW−5ºE, latitude 34ºN−44ºN). Data homogenization has also been conducted by it. To select the data for every zone, for the M_{max}, *b*-value, *AR*, the data have been obtained from the GIS. It has also permitted the determination of the correct areas for the *AR*. It should also be noted that for calculations, the combination of graphical and numerical data has been possible thanks to the

GIS. Moreover, in this study more than 650 different cells have been used. Also, all the grids have been generated in it.

As was stated in Chapter 3, different values proposed by IGN-UPM WG (2013) and Peláez et al. (2007) to decluster the catalog through Gardner and Knopoff method have been employed.

The results of declustering, carried out with the *ZMAP* software (Wiemer 2001), with both methods, has been summarized in Table 5.1.

Table 5.1. Results of declustering

	Peláez et al. (2007)	**IGN-IPM WG (2013)**
Number of events	30,074	30,074
Number of clusters of earthquakes	2554	2098
Number of events removed	12,456	12,264
Number of mainshocks	17,618	17,810
Seismic moment released by clusters (%)	0.24	0.27

5.2. SEISMIC PARAMETERS

In a PSHA, one of the main parameters to define the seismic hazard is to establish the maximum possible magnitude, as this parameter can provide an idea of the seismicity of the area studied. For that purpose, a 0.5º x 0.5º grid, covering the Iberian Peninsula, has been established. As has been previously stated, different methods to estimate the maximum possible magnitude and its uncertainty can be found in the literature. In this study, given the temporal extent of the catalog (more than 600 years), the maximum recorded magnitude has been considered as the maximum possible magnitude. This is a simplification, not lacking error, although the catalog lasts for more than 600 years.

Other very important parameter is the *b*-value, the slope of the FMD in a log-log plot and it may reflect the physics of the area studied, as has been

mentioned. The method proposed by Kijko and Smit (2012), with the Ogata and Yamashina (1986) correction, has been used for its calculation as it is ideal for incomplete or inhomogeneous catalogs as NGIS earthquake one (despite of the effort to minimize this irregularities) because is rigorous but simple and easy to apply. Besides, it allows to compute the mean seismic activity rate easily, once the *b*-value has been obtained.

In this research, multiple M_c couples of values (M_c-year of completeness) have been used according to IGN-UPM WG (2013) regionalized (four areas) values, slightly modified. These values are consistent with the seismic detection network configuration changes (González 2017) for the Iberian Peninsula. In Table 3.2, it can be observed that there are important differences depending on the area considered, depicted in Figure 3.4.

Regarding the minimum number of events, it is clear that the lower the number of events (*N*), the greater the uncertainty of the *b*-value calculation. On the one hand, there is a trade-off between accuracy and coverage. On the other hand, the larger the radius, the smaller the spatial resolution is.

Similarly to Mousavi (2017), two maps with different *N* have been depicted in this research. Mousavi (2017) considered a different radius for Iran: N_{min} = 50, R_{max} = 170km (for high-coverage-low-accuracy) and N_{min} = 80 and R_{max} = 80 km (for high-resolution-low-uncertainty).

In this research, the method assessed by Mapa Sismotectónico WG (1992) has been used for the whole Iberian Peninsula: four 2º x 2º overlapped grids (the original; one shifted 1º to the East; another displaced 1◦ to the South; and finally, one moved both 1ºE and 1ºS). For the most seismic areas, the size of the grid has been reduced to 1º x 1º, with displacements of 0.5º instead of 1º. In this research, two maps have been produced. To do so, 25 events (Bender 1983; Bachmann et al. 2012) and 50 events (Amorese et al. 2010; Singh and Singh 2015; Mousavi 2017) have been considered. Also, the values determined by Nava et al. (2017) have been studied, considering that the Iberian Peninsula has a low-moderate seismicity, with aseismic areas. Likewise, the above cited studies have been examined.

For every cell, average geographical coordinates have been computed. Prior to computing the *b*-value, a completeness area is necessary for every cell.

Besides, the computed *b*-value and the mean seismic activity rate have been assigned to this average location, not to the cell center. Then, the method by Kijko and Smit (2012) has been used to calculate the *b*-value in every cell of every grid. Where *N* was lower than 25, its associated *b*-value has not been considered for mapping. Therefore, further analysis must be considered.

Finally, four color maps (Figure 5.2, Figure 5.3, Figure 5.4 and Figure 5.5) have been depicted for every option [N_{min} = 25; N_{min} = 50; decluster parameters suggested by IGN-UPM WG (2013); decluster parameters suggested by Peláez et al. (2007)], in all cases, the M_c has been regionalized as IGN-UPM WG (2013) as was pointed out in Chapter 3.

After calculating the *b*-value, the mean seismic activity rate of events have been computed from the as previously stated.

5.3. RESULT AND ANALYSIS

Three of the main seismic parameters: the M_{max}, *b*-value and (normalized) mean seismic activity rate (*AR*) have been calculated for the Iberian Peninsula. In particular, for *b*-value and *AR*, the methodology applied follows the method proposed by Kijko and Smit (2012). This enables computing the *b*-value and allows considering the incompleteness of the seismic catalog. This is especially relevant given the seismicity pattern and the configuration of the seismic network over time of the area. Besides, once the *b*-value has been calculated, the *AR* has been easily obtained.

5.3.1. The maximum recorded magnitude

The first parameter depicted is the M_{max}, which is useful for observing the size-distribution (Bod'a 2017) over the Iberian Peninsula. A 0.5º x 0.5º grid has been considered (Figure 5.1).

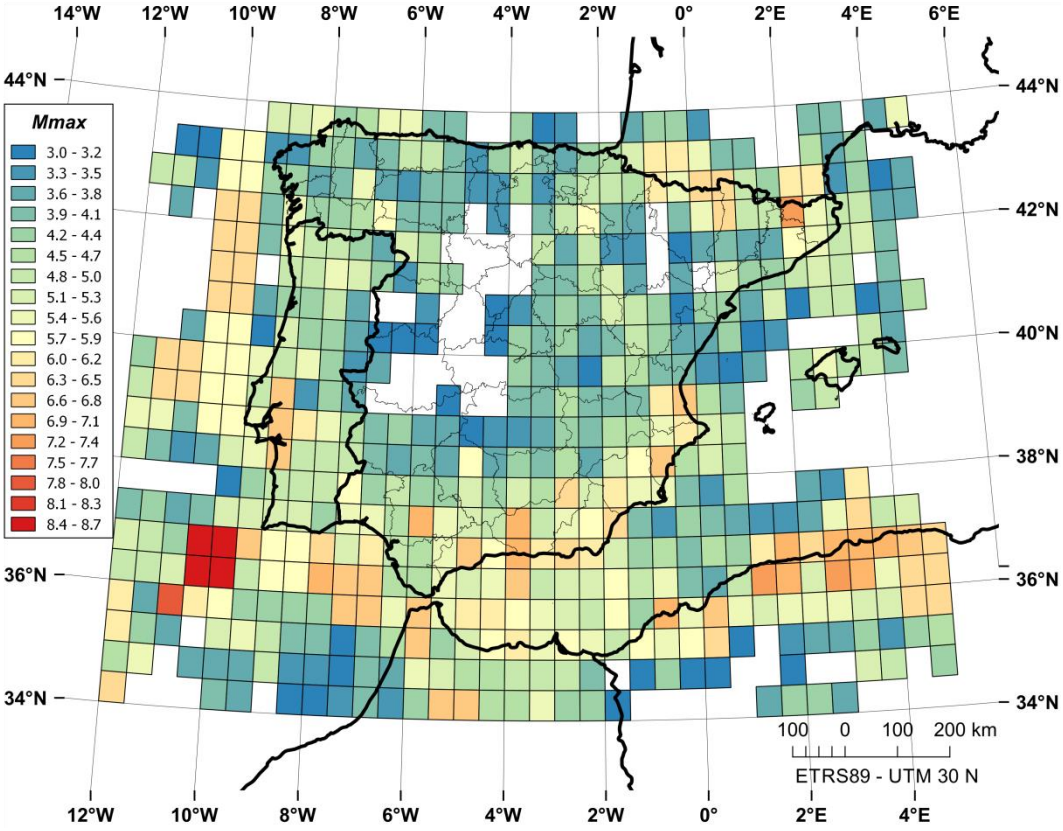

Figure 5.1. Maximum recorded magnitude (M_{max}). Grid 0.5º x 0.5º. Source: Amaro-Mellado et al. (2018)

The map shows that the largest earthquakes have a marine epicenter (100–200 km of the SW of Iberian Peninsula) and have reached up to M8.7. Also in the Alboran Sea area, there have been earthquakes of more than 6.0 and in the north of Algeria there have been earthquakes of a magnitude greater than 7.0, the effects of the latter on the Iberian Peninsula being almost negligible given the distance (Mezcua et al. 2011), but sometimes felt in the Balearic Islands. When studying the continental part of the Iberian Peninsula, earthquakes of considerable magnitudes (greater than 6.5) have been found in the Pyrenees and in the southeastern part of the peninsula (regions of eastern Andalusia, Murcia and southern Valencia) or even in the west (the Lisbon area), as well as other intraplate phenomena, such as those produced in Galicia, with M_w>5.5, which are worthy of mention.

As a summary, it can be stated that, although in much of the interior peninsular, especially in the Meseta, M4.0 has been infrequently exceeded (there are even regions where there are no events with M_w greater than 3.0 recorded),

there are a considerable number of areas that have exceeded magnitude 6.0, especially in the interior to the south of it.

5.3.2. The size-distribution (*b*-value)

This is a parameter of the utmost importance in seismic studies and it is related to the physics of the area. In this research, different variables (declustering parameters and number of events) have been used. This has allowed generating multiple maps. The results can be compared and a relevant value for every area of the area analyzed is provided.

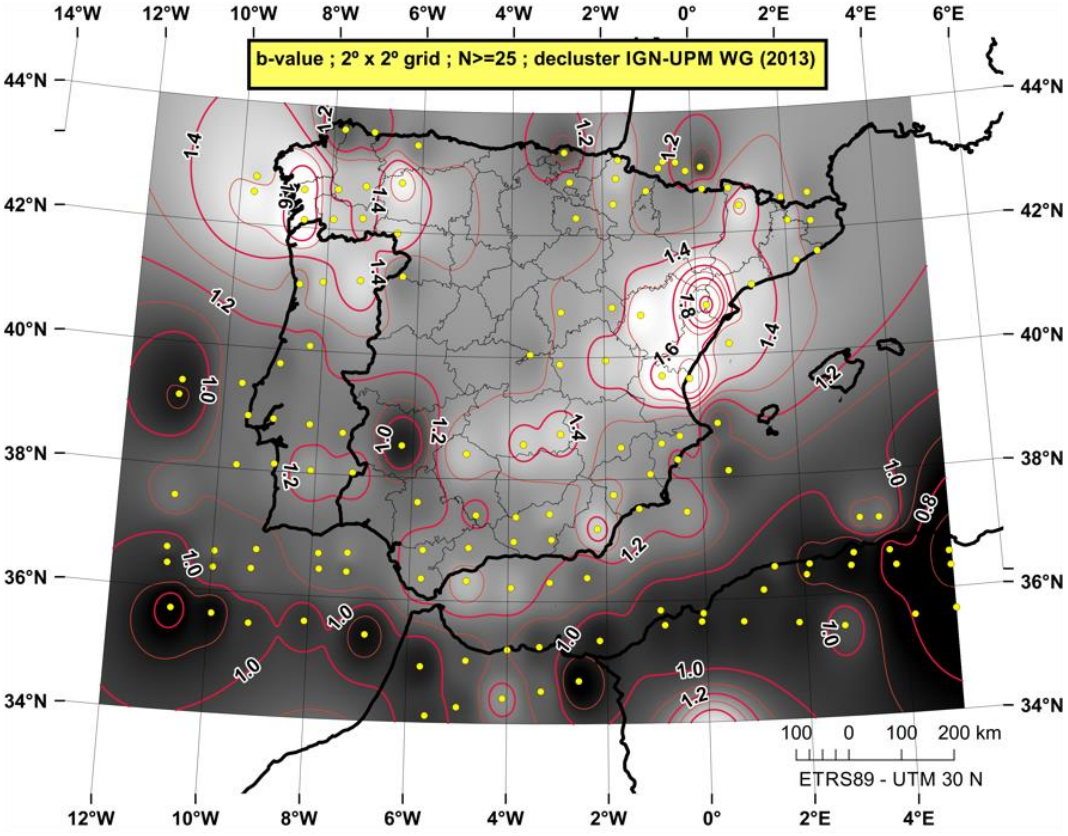

Figure 5.2. *b*-value map considering a grid of 2º x 2º, at least 25 events, M_c regionalized (IGN-UPM WG 2013) and the declustering parameters by IGN-UPM WG (2013). Source: Amaro-Mellado et al. (2018)

These maps can be found in Figure 5.2, Figure 5.3, Figure 5.4 and Figure 5.5, where yellow points are the points (representing a cell) where the number of events is at least 25 or 50, respectively. This means that if the distance between

the closest points is very high in a region, contour lines are not representative. This fact is more evident dealing with more than 50 events.

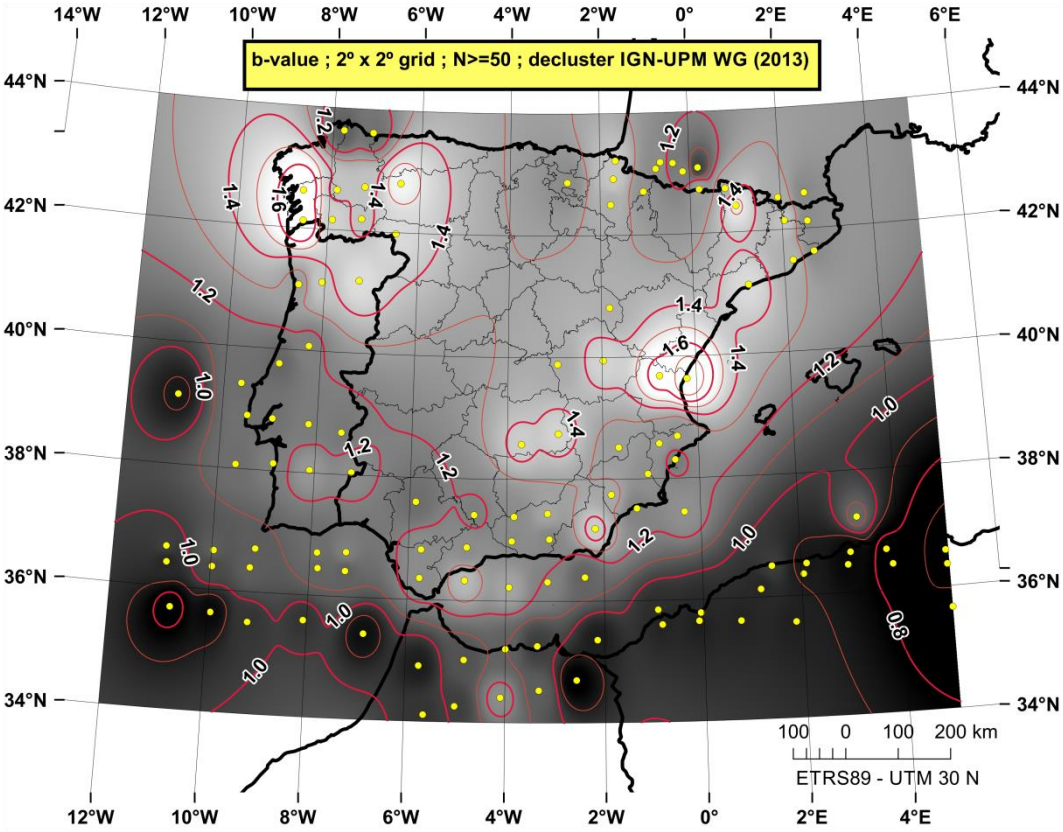

Figure 5.3. *b*-value map considering a grid of 2º x 2º, at least 50 events, M_c regionalized (IGN-UPM WG 2013) and the declustering parameters by IGN-UPM WG (2013). Source: Amaro-Mellado et al. (2018)

In the mainland, values higher than 1.2 are predominant. In the contact area between the African and the Eurasian plates the *b*-value is around 1.0. In the most active area in the S and SE, values are about 1.3 and in the Pyrenees values about 1.4 with higher dispersion are found. In Galicia (NW), higher values, of approximately 1.5 are found.

After computation, a reference *b*-value for the Iberian Peninsula can be set at 1.2–1.4, with some occasional 0.2 variations. This *b*-value decreases to about 1.0 (0.1) in the contact limit, the north of Africa and the Gorringe Bank. This means that the stress gets more accumulated in this area causing larger earthquakes.

These results are consistent with other *b*-value maps such as Crespo et al. (2012), but those authors calculated a *b*-value around 0.8–1.0 for the aseismic central west area.

If the results are compared to other authors proposal, similar findings to the Chapter 4 can be the drawn. In the continental zone the values are approximately 0.2 higher than those obtained by Hiemer et al. (2014) and Woessner et al. (2015), and, on the contrary, these are 0.3 higher for North Africa. Likewise, these authors calculated a reference value for the *b*-value of 0.9, somewhat lower than that obtained in this doctoral thesis.

If the work of Mezcua et al. (2011) is established as a reference, the results are very similar, within the range of expected errors (0.1-0.2), except in the area southwest of Cape St. Vincent, where values of 0.3-0.4 higher have been obtained.

When comparing the results with those obtained by Vilanova and Fonseca (2007), it should be mentioned that they obtained values close to 1.0 for Portugal and Cape St. Vincent, compared to the highest values obtained in this thesis (up to 1.5 in some areas of Portugal).

Something similar to what happened with the works of Hiemer et al. (2014) and Woessner et al. (2015), occurs in the comparison with the results of Jiménez et al. (1999), which for North Africa obtained values between 0.4 and 0.9 (consistent with this thesis), but lower in the peninsular zone: about 1.0 as opposed to the 1.2 that could be taken as a mean value according to this thesis.

Finally, if the work of Jiménez et al. (1989) is taken as a reference, the differences are appreciable, since they calculated much lower values (0.37-0.58) for the east and south of the Iberian Peninsula, and for the Pyrenees.

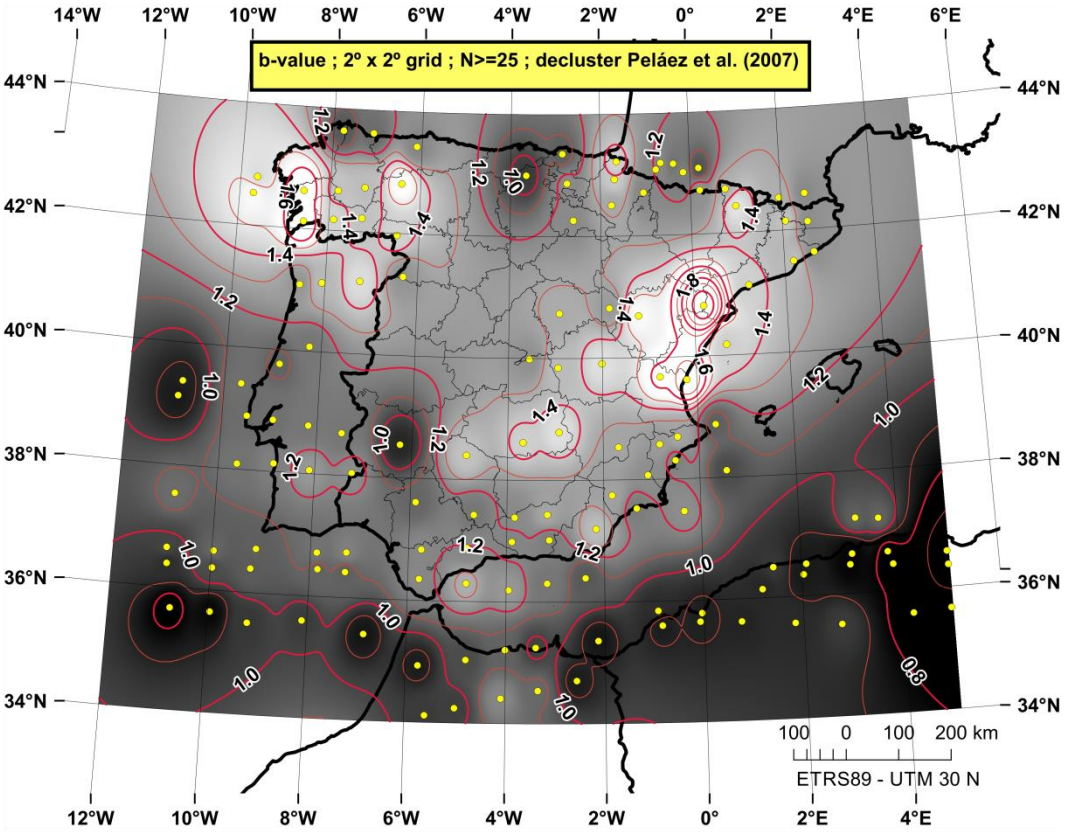

Figure 5.4. *b*-value map considering a grid of 2º x 2º, at least 25 events, *Mc* regionalized (IGN-UPM WG 2013) and the declustering parameters by Peláez et al. (2007). Source: Amaro-Mellado et al. (2018)

Regarding the decluster comparison, the results are very similar. Nevertheless, it can be checked that the *b*-value obtained is higher in IGN-UPM WG (2013), particularly in the North of Africa. This could be due to the fact that Peláez et al.'s (2007) parameters eliminate more small events, so the small/large proportion decreases, i.e., lower *b*-values.

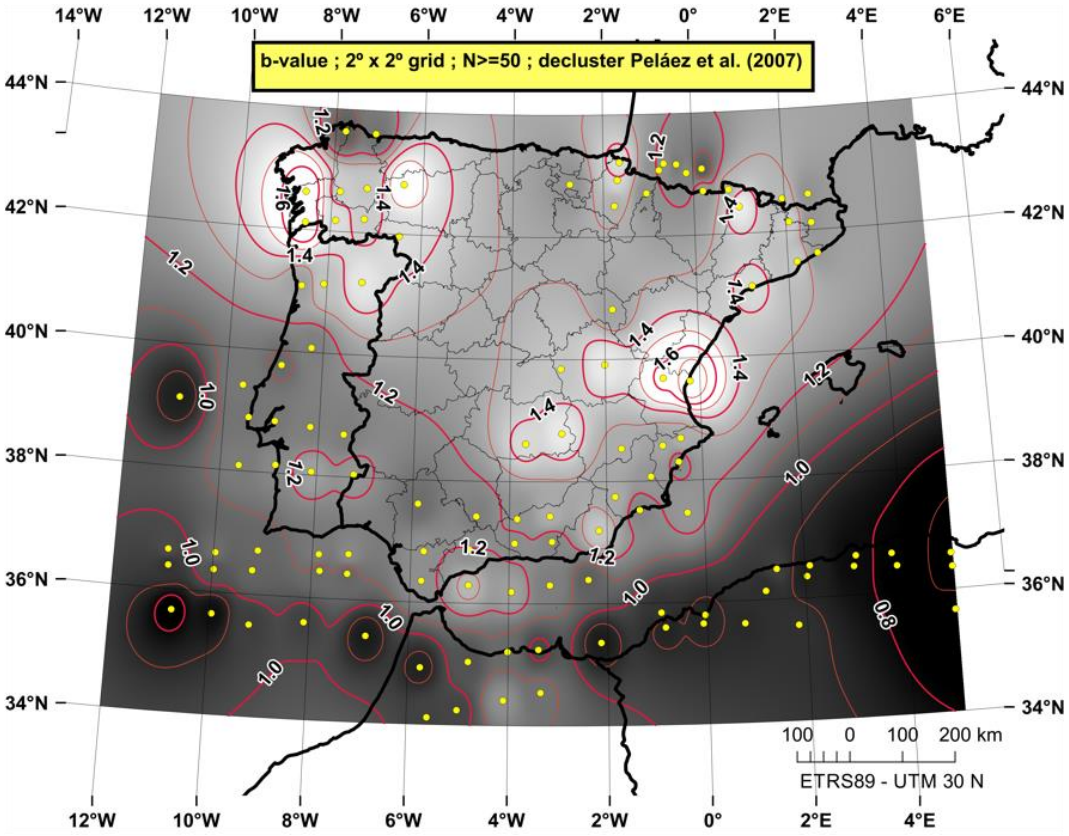

Figure 5.5. *b*-value map considering a grid of 2º x 2º, at least 50 events, M_c regionalized (IGN-UPM WG 2013) and the declustering parameters by Peláez et al. (2007). Source: Amaro-Mellado et al. (2018)

Finally, a more detailed map showing both M_{max} and the *b*-value has been depicted in Figure 5.6. The most seismic area in the mainland has been depicted using a 1º x 1º grid and at least 50 events have been considered (for *b*-value calculation).

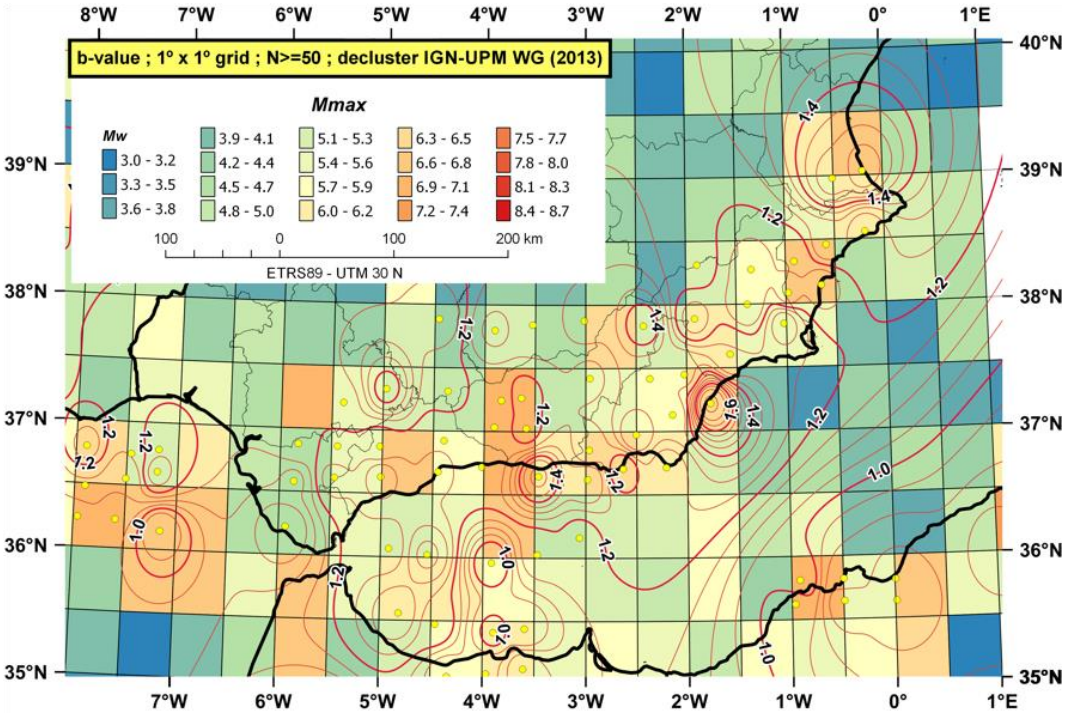

Figure 5.6. M_{max} (0.5º x 0.5º grid) and b-value (1º x 1º grid and at least 50 events). Declustering by IGN-UPM WG (2013). Source: Amaro-Mellado (2018)

5.3.3. The mean seismic activity rate

Finally, the mean seismic activity rate has been determined. This has been provided per area and not as an absolute value. In order to define de size of the grid, several resolutions have been tested. Finally, the 1º x 1º has been chosen, as it presents an optimal trade-off between the amount of data and the resolution. The results with different variables (declustering parameters and number of events) are pretty similar, so, M_c regionalized (IGN-UPM WG 2013) and declustering parameters by IGN-UPM WG (2013) have been depicted.

The *AR* value is strongly dependent on the size of the grid and the cut-off magnitude. It can be stated that the results with $M_w \geq 3.0$ are consistent with the studies by IGN-UPM WG (2013) ($M_w \geq 4.0$) and Mezcua et al. (2011) ($M_w \geq 3.5$) that used zonations. The results are also similar to studies that use continuous maps such as Crespo et al. (2012) ($M_w > 3.5$).

The highest values have been found in the Granada Basin and in the Pyrenees—more than 9 x 10^{-4} earthquakes / km^2. In the SW of the Cape St. Vincent, close to Huelva, in the NW (Galicia) and in the southern part of the east

extreme the values obtained are higher than 1 x 10^{-4} earthquakes / km^2. Most areas present values higher than 1 x 10^{-5} earthquakes / km^2, although some regions present a lower value.

Similarly to Figure 5.7, a more detailed map (Figure 5.8), for the most seismic area in the mainland, showing the *AR* and the *b*-value, has been depicted.

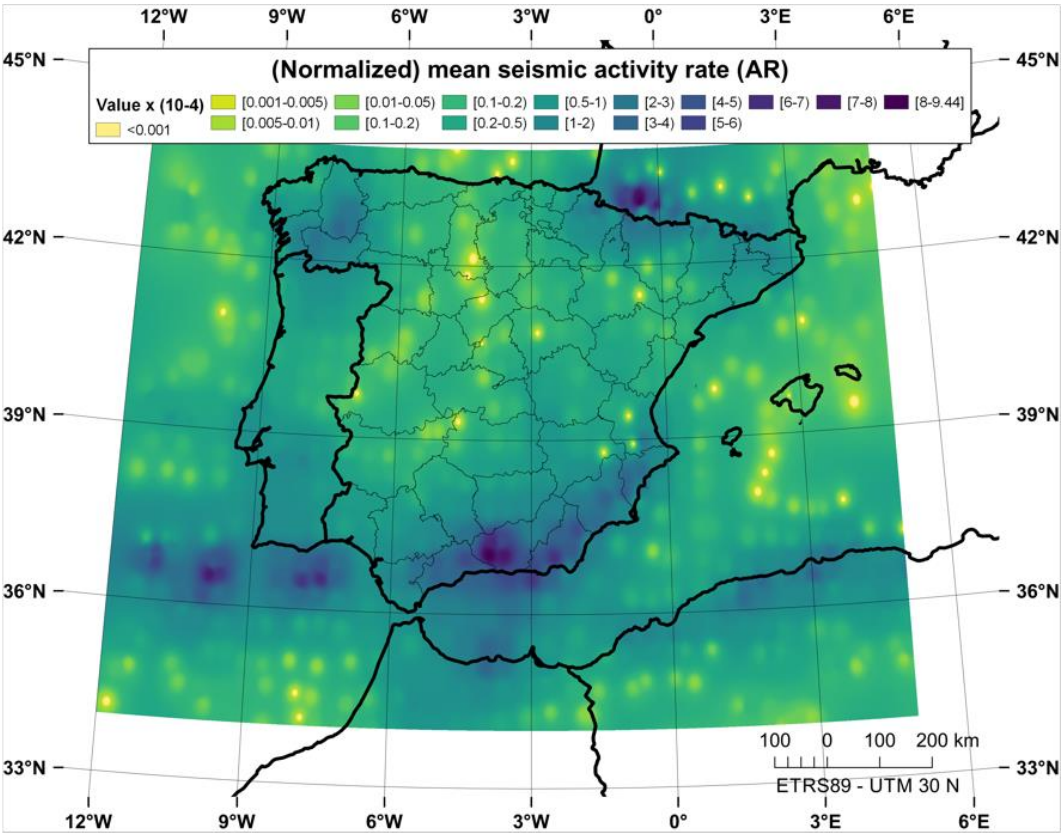

Figure 5.7. Mean seismic activuty rate by km^2 (values x 10^{-4}), considering a grid of 1º x 1º, *Mc* regionalized (IGN-UPM WG 2013) and the decluster parameters by IGN-UPM WG (2013). Source: Amaro-Mellado et al. (2018)

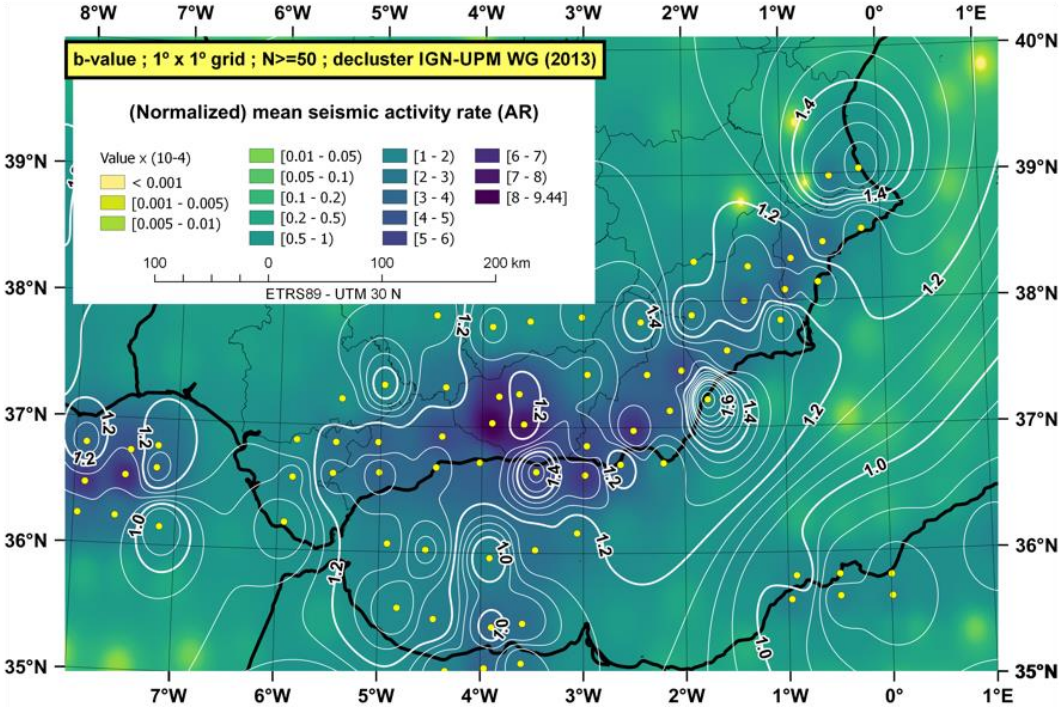

Figure 5.8. *AR* (1º x 1º grid) and *b*-value (1º x 1º grid and at least 50 events). Declustering parameters by IGN-UPM WG (2013). Source: Amaro-Mellado et al. (2018)

Chapter 6.
Conclusions / Conclusiones

6.1. CONCLUSIONS

The main objective of this doctoral thesis has been the study of some of the parameters considered most influential for the determination of seismic hazard in the Iberian Peninsula and its surroundings by means of the usage of a GIS.

This general objective has in turn been based on the achievement of a number of more specific objectives.

Firstly, to generate a new catalog of earthquakes, as extensive as possible given the information available, reviewed, homogeneous, in which only independent events for the study area are considered.

As a second objective, the calculation of the seismic parameters corresponding to a series of seismic zonings previously defined by different researchers, of a different nature, proposed for the Iberian Peninsula has been made: some taken as a reference for the seismic-resistant regulations; others based on criteria as objective as possible and mathematically robust.

The third objective, closely linked to the previous one, is the analysis of the parameters obtained in the calculation for each of the zonings proposed.

Finally, it has also been sought to calculate and represent the parameters of seismic hazard, but in this case starting not from predefined areas, but from a division of the territory by multiresolution grids (2º x 2º, 1º x 1º, 0.5º x 0.5º). The following can be concluded from the results achieved:

1. The generation of a new independent, homogeneous and as complete as possible catalog is a fundamental starting point for the analysis of seismic hazard parameters. In this doctoral thesis, a new seismic catalog has been compiled, which undoubtedly constitutes a valuable contribution. This compilation entails a series of steps that, in the end, give solidity to the study of seismic parameters, and are the re-evaluation of the intensity of earthquakes with a marine epicenter: the review of other seismic catalogs and other specific studies; the transformation of all events to the same type of magnitude (M_w, magnitude moment in this work); the

elimination of non-main events (declustering); and, given the heterogeneity in space and time of the seismic detection networks within the study area, a regionalization of the completeness date according to each magnitude considered.

2. The catalog compiled is a very satisfactory result of this work; even so, despite the efforts made, there are areas (although distant) that may not be considered complete, such as the Tell Atlas area.

3. When treating the results of the seismic parameters, in quite a few of the areas set out in the zoning proposed by Bernal (2011) there have not been more than 30 events according to the intervals of magnitude and time considered. This is understood as a negligible hazard and in more than a few the number is around that figure, so the uncertainties of the parameters are not the most desirable. This fact, although to a lesser extent, also occurs with the zoning proposed by GM12.

4. There are adjacent areas with similar parameters, which suggests that it would be reasonable to merge them. This fact is especially noticeable in the GM12 and ByA12 zoning. These two circumstances make it seem reasonable to consider fewer and larger zones, although the seismotectonic aspects of these zones should be carefully studied.

5. In general, there is consistency between the maximum magnitude values, both those recorded and the potential from QAFI faults. For future research, considering the maximum potential magnitude will become more important the more spatially complete the database from which it is extracted, since the step of integrating this information into the calculations has already been taken.

6. In addition, the map of maximum magnitudes recorded according to a grid of 0.5º x 0.5º gives very visual and intuitive information on the geographical distribution of earthquakes.

7. The use of a calculation method (of the *b*-value and of the seismic activity rate) that considers different pairs of dates and magnitudes of completeness makes it possible to work in a more correct way with non-homogeneous catalogs (of more than 600 years of temporal scope), such

as that of this work, which means another contribution of this doctoral thesis.

8. This thesis has confirmed the usefulness of GIS for studies involving both databases and the geographical phenomena associated with them. This fact is especially relevant when the sources of information are diverse, but the coherence of the data, both geometric and alphanumeric, is essential.
9. The use of GIS for managing, filtering, analyzing and, of course, representing geographical information has proved essential for the emergence of latent information within the baseline data. The strength provided by a quality graphical representation means that GIS play a fundamental role in decision making related to almost any area of society (including engineering and the environment).
10. The work with these systems has allowed the elaboration of a calculation and representation of parameters in a quite intuitive and agile way, being able to consider the territory of study as a continuum in a quite considerable extension of land, thanks to the use of multiresolution grids.

The contribution of this doctoral thesis can be assessed in the development of a methodology for the calculation and representation of hazard parameters through the use of GIS so that the hazard can be evaluated. This methodology can be extrapolated to other seismic regions, in such a way that a reclassification of the zones in function of the similarities between hazard parameters can be approached. It is also worth mentioning not only the methodological development but also the results obtained, the catalog compiled being of special interest

Furthermore, according to technological advances and the evolution of GIS towards spatial data infrastructures, in the future it could be considered that the results obtained in this or similar research would be visible and graphically accessible in an integrated way through the Internet (Amaro-Mellado, 2014).

Another field in which to advance is the greater definition in the delimitation of zones. As a future line of research, it is proposed to start from a denser grid of points and work with overlapping circles (centered on those points), so that the number of zones would be huge. In any case, zones with an insufficient number of events must not be taking into account.

Finally, another line of research to explore is the consideration of other catalogs as a source of initial information, such as those registered by the Portuguesse Institute for Sea and Atmosphere (*Instituto Português do Mar e da Atmosfera , IPMA*) in order to compare the results obtained.

6.2. CONCLUSIONES

El principal objetivo de esta tesis doctoral ha sido el estudio de algunos de los parámetros considerados más influyentes para la determinación de la peligrosidad sísmica en la península ibérica y su entorno mediante el empleo de un SIG.

Este objetivo general a su vez se ha basado en la consecución de una serie de objetivos más específicos.

En primer lugar, generar un nuevo catálogo de terremotos, lo más extenso posible dada la información disponible, revisado, homogéneo, en el que solo se consideren eventos independientes para el área de estudio.

Como segundo objetivo se ha abordado el cálculo de los parámetros sísmicos correspondientes a una serie de zonificaciones sísmicas previamente definidas por distintos investigadores, de distinta naturaleza, propuestas para la Península ibérica: unas tomadas como referencia para las normas sismorresistentes; otras basadas en criterios lo más objetivos posibles y robustos matemáticamente.

El tercer objetivo, estrechamente ligado al anterior, es el análisis de los parámetros obtenidos en el cálculo para cada una de las zonificaciones propuestas.

Finalmente, también se ha buscado calcular y representar los parámetros de la peligrosidad sísmica, pero en este caso partiendo, no de zonas predefinidas, sino de una división del territorio mediante mallas multirresolución (2º x 2º; 1º x 1º; 0,5º x 0,5º).

De los resultados obtenidos se pueden concluir lo siguiente:

1. La generación de un nuevo catálogo independiente, homogéneo y lo más completo posible es un punto de partida fundamental para el análisis de los parámetros de peligrosidad símica. En esta tesis doctoral se ha compilado un nuevo catálogo sísmico, lo que, constituye, sin duda, una valiosa aportación de la misma. Dicha compilación conlleva una serie de pasos que, a la postre, dotan de solidez al estudio de los parámetros

símicos, y son la reevaluación de la intensidad de los terremotos con epicentro marino; la revisión de otros catálogos símicos y otros estudios específicos; la transformación de todos los eventos a un mismo tipo de magnitud (M_w, magnitud momento en este trabajo); la eliminación de eventos no principales (*declustering*); y, dada la heterogeneidad en espacio y tiempo de las redes de detección sísmica dentro del área de estudio, una regionalización de la fecha de completitud en función de cada magnitud considerada.

2. El catálogo compilado es un resultado muy satisfactorio de este trabajo, aun así, a pesar de los esfuerzos llevados a cabo, existen zonas (aunque lejanas) que quizá no se pueden considerar completas, como la zona del Tell Atlas.

3. Al tratar los resultados de los parámetros sísmicos, en bastantes de las zonas propuestas en la zonificación propuesta por Bernal (2011) no se han producido más de 30 eventos según los intervalos de magnitud y tiempo considerados, lo que se entiende como una peligrosidad despreciable y en no pocas el número ronda esa cifra con lo que las incertidumbres de los parámetros no son las más deseables. Este hecho aunque en menor medida también ocurre con la zonificación propuesta por GM12.

4. Existen zonas adyacentes con parámetros similares lo que lleva pensar que sería razonable la fusión de las mismas. Este hecho es especialmente notorio en las zonificaciones de GM12 y ByA12. Estas dos circunstancias dan lugar a que parezca razonable el considerar menos zonas y más amplias, aunque habría que estudiar detenidamente los aspectos sismotectónicos de las mismas.

5. Por lo general, hay coherencia entre los valores de magnitud máxima tanto la registrada como la potencial a partir de las fallas del *QAFI*. Para futuras investigaciones, el considerar la magnitud máxima potencial cobrará mayor importancia cuanto más completa espacialmente sea la base de datos de la que se extraiga, ya que el paso de integrar dicha información en los cálculos ya está dado.

6. Además, el mapa de magnitudes máximas generado según una cuadrícula de 0,5º x 0,5º da una información muy visual e intuitiva de la distribución geográfica de los terremotos.

7. El empleo de un método de cálculo (del *b*-value y de la tasa de actividad sísmica) que considera distintos parejas de fecha y magnitud de completitud hace que se pueda trabajar de una forma más correcta con catálogos no homogéneos (de más de 600 años de ámbito temporal), como el de este trabajo, lo que supone otra aportación de esta tesis doctoral.

8. La presente tesis ha permitido constatar la utilidad de los SIG para abordar estudios en los que están implicados tanto bases de datos como fenómenos geográficos asociados a estas. Este hecho es especialmente relevante cuando las fuentes de información son diversas pero es imprescindible la coherencia de los datos, tanto geométrica como alfanumérica.

9. El empleo de los SIG para gestionar, filtrar, analizar y, por supuesto, representar información geográfica ha demostrado ser esencial para aflorar información latente dentro de los datos partida. La fuerza que proporciona una representación gráfica de calidad hace que los SIG tengan un papel fundamental en la toma de decisiones relacionadas con casi cualquier ámbito de la sociedad (incluidos el ingenieril y el medioambiental).

10. El trabajo con estos sistemas ha permitido la elaboración de un cálculo y representación de parámetros de una forma bastante intuitiva y ágil, pudiendo considerar el territorio de estudio como un continuo en una extensión de terreno bastante considerable, gracias al empleo de mallas multirresolución.

La aportación de esta tesis doctoral puede valorarse en el desarrollo de una metodología para el cálculo y la representación de parámetros de peligrosidad mediante el empleo de los SIG de forma que dicha peligrosidad pueda ser evaluada. Esta metodología puede ser extrapolada a otras regiones sísmicas, de tal forma que pueda ser abordada una reclasificación de las zonas en función de las similitudes entre parámetros de peligrosidad. También es digno

de mención, no solo el desarrollo metodológico, sino los propios resultados obtenidos, siendo de especial interés el catálogo compilado.

Además, según los avances tecnológicos y la evolución de los SIG hacia las infraestructuras de datos espaciales, en un futuro se podría plantear que los resultados obtenidos en esta investigación u otras similares fueran visibles y accesibles gráficamente de forma integrada a través de Internet (Amaro-Mellado, 2014).

Finalmente, otra línea de investigación a escrutar es la consideración de otros catálogos como fuente de información de partida, como podrían ser los registrados por el *Instituto Português do Mar e da Atmosfera* (*IPMA*) con el fin de comparar los resultados obtenidos.

Chapter 7. Publications produced under this PhD Thesis

7.1. USE OF A GEOGRAPHIC INFORMATION SYSTEM FOR THE ANALYSIS OF THE EXISTING SEISMOGENIC ZONINGS

This is the first contribution related to this PhD Thesis, since allowed to integrate information from different sources (seismic catalogs, seismogenic zonings, fault databases, etc.). The goal was to unify all of this information into a geographic information system in order to make an approach to analyze seismogenic zonings.

The reference of this document is:

- ✓ **Amaro-Mellado JL**, Morales-Esteban A, Martínez-Álvarez (2014) Utilización de un sistema de información geográfica para el análisis de las zonificaciones sismogenéticas existentes. In: Actas del XII Congreso Internacional de Expresión Gráfica aplicada a la Edificación, pp 279-289.

7.2. IMPACT OF THE UTM PROJECTION ON THE CALCULATION OF THE SURFACE OF STATES

This contribution is related to this PhD Thesis regarding representation systems (as all of them are affected by distortion), since arose the impact of the location of a polygon when calculating its surface using UTM projection (conformal projection, where shapes are maintained but surfaces are not), in comparison with the value that could be considered “deformation-free”.

After this work, the use of an equivalent projection (surfaces are kept but shapes are not) representation was chosen due to one of the seismic parameters to be calculated (the normalized annual rate) is closely related to surface values. This fact is more significant because of the different between 12ºW and 6ºE longitudes which would involve meaningful inaccuracies.

The reference of this document is:

- ✓ Pérez-Romero AM, **Amaro-Mellado JL** (2014) Utilización de un sistema de información geográfica para el análisis de las zonificaciones sismogenéticas existentes. In: Actas del XII Congreso Internacional de Expresión Gráfica aplicada a la Edificación, pp 295-301.

7.3. A NOVEL METHOD FOR SEISMOGENIC ZONING BASED ON TRICLUSTERING. APPLICATION TO THE IBERIAN PENINSULA

This paper is important in this thesis because was the first JCR publication related to this PhD works. In this, data from different sources were integrated into a geographic information system to deal these data rigorously and make a proper representation.

This work can be found in:

- ✓ Martínez-Álvarez F, Gutiérrez-Avilés D, Morales-Esteban A, Reyes J, **Amaro-Mellado JL**, Rubio-Escudero C (2015) A novel method for seismogenic zoning based on triclustering. Application to the Iberian Peninsula. Entropy 17(7):5000–5021.

- ✓ Journal Impact Factor (JCR 2015): **1.743**
- ✓ Ranking JCR: **25/79 (Q2)**

7.4. COMPARING SEISMIC PARAMETERS FOR DIFFERENT SOURCE ZONE MODELS IN THE IBERIAN PENINSULA

This paper is one of the two publications that constitute the kernel of this PhD, as in it the seismic catalog is deeply studied and compiled and because a thorough study on the seismic hazard parameters *(b*-value, maximum magnitude and normalized annual rate of earthquakes) related to different sesmic zonations proposed by the experts is conducted by means of a GIS.

This work can be found in:

- ✓ **Amaro-Mellado JL**, Morales-Esteban A, Asencio-Cortés G, Martínez-Álvarez F (2017) Comparing seismic parameters for different source zone models in the Iberian Peninsula. Tectonophysics 717:449-47. https://doi.org/10.1016/j.tecto.2017.08.032

- ✓ Journal Impact Factor (JCR 2017): **2.686**
- ✓ Ranking: **32/85 (Q2)**

7.5. MAPPING OF SEISMIC PARAMETERS OF THE IBERIAN PENINSULA BY MEANS OF A GEOGRAPHIC INFORMATION SYSTEM

This is second paper of the core of this research. In contrast to the previous paper, seismic hazard parameters (*b*-value, maximum magnitude and normalized annual rate of earthquakes) are calculated, represented and analyzed from zonings generated from multiresolution grids, developed to his end in a GIS, instead of coming from experts' delineation.

This work can be found in:

- ✓ **Amaro-Mellado JL**, Morales-Esteban A, Martínez-Álvarez F (2018) Mapping of seismic parameters of the Iberian Peninsula by means of a geographic information system. Central European Journal of Operations Research 26:739-758. https://doi.org/10.1007/s10100-017-0506-7

- ✓ Journal Impact Factor (JCR 2017): **0.730**
- ✓ Ranking: **74/84 (Q4)**

REFERENCES

- ✓ Aki K (1965) Maximum likelihood estimate of *b* in the formula *logN=a-bM* and its confidence limits. Bull Earthq Res Inst 43:237-239
- ✓ Amaro-Mellado JL (2014) Aplicaciones de las Infraestructuras de Datos Espaciales. In: Actas del XII Congreso Internacional de Expresión Gráfica aplicada a la Edificación, pp 302-311 (in Spanish)
- ✓ Amaro-Mellado JL, Morales-Esteban A, Asencio-Cortés G, Martínez-Álvarez F (2017) Comparing seismic parameters for different source zone models in the Iberian Peninsula. Tectonophysics 717:449-472
- ✓ Amaro-Mellado JL, Morales-Esteban A, Martínez-Álvarez F (2018) Mapping of seismic parameters of the Iberian Peninsula by means of a geographic information system. Central European Journal of Operations Research 26:739-758
- ✓ Amorese D, Grasso JR, Rydelek PA (2010) On varying *b*-values with depth: Results from computer-intensive tests for southern California. Geophys J Int 180(1):347–360
- ✓ Bender B (1983) Maximum likehood estimation of *b* values for magnitude grouped data. Bull Seismol Soc Am 73(3):831-851
- ✓ Bachmann CE, Wiemer S, Goertz-Allmann BP, Woessner J (2012) Influence of pore-pressure on the event-size distribution of induced earthquakes. Geophys Res Lett 39, L09302
- ✓ Bakun WH, Wentworth CM (1997) Estimating earthquakes location and magnitude from seismic intensity data. Bull Seismol Soc Am. 87:1502–1521
- ✓ Batlló J, Stich D, Macià R, Morales J (2010) Moment tensor inversion for the 5 July 1930 Montilla earthquake (southern Spain). Seismol Res Lett 81 (5): 724–731
- ✓ Batlló J, Stich D, Palombo B, Macià R, Morales J (2008) The 1951 Mw 5.2 and Mw 5.3 Jaén, Southern Spain, earthquake doublet revisited. Bull Seismol Soc Am 98 (3):1535–1545
- ✓ Bernal A (2011). Anexo I del informe técnico IGN-PSE. ZF. P03. pdf file: ANEXO Idoc. 2.3.0. Descrip. Zon. B y A.pdf, 41 pp (in Spainsh)

- ✓ Buforn E, Bezzeghoud M, Udías A, Pro C (2004) Seismic sources on the Iberia-African plate boundary and their tectonic implications. Pure Appl Geophys 161:623–646
- ✓ Buforn E, Sanz de Galdeano C, Udías A (1995) Seismotectonics of the Ibero-Maghrebian region. Tectonophysics 248:247-261
- ✓ Cabañas L, Rivas-Medina A, Martínez-Solares JM, Gaspar-Escribano JM, Benito B, Antón R, Ruiz-Barajas S (2015) Relationships between Mw and other earthquake size parameters in the Spanish NGIS Seismic Catalog. Pure Applied Geophys 172(9):2397-2410
- ✓ Carreño E, Benito B, Martínez-Solares JM, Cabañas L, GinerRobles JL., Murphy P, López C, Del Fresno C, Alcalde JM, Gaspar-Escribano JM, Antón JG, Martínez-Díaz J, Cesca S, Izquierdo A, Sánchez-Cabañero JG, Expósito P (2008) The June 7, 2007 mbLg 4.2 Escopete earthquake: an event with significant ground motion in a stable zone (Central Iberian Peninsula). Seismological Research Letters 79(6):820-829
- ✓ Carreño E, López C, Bravo B, Expósito P, Gurría E, García O (2003) Seismicity of the Iberian Peninsula in the instrumental period: 1985–2002. Física de la Tierra 15:73–91
- ✓ Castellaro S, Mulargia F, Kagan YY (2006) Regression problems for magnitudes. Geophys J Int 165: 913–930
- ✓ Cheng QM, Sun HY (2018) Variation of singularity of earthquake-size distribution with respect to tectonic regime. Geoscience Frontiers 9 (2): 453-458
- ✓ Crespo MJ (2011) Análisis de la peligrosidad sísmica en la Península Ibérica con un método basado en estimadores de densidad Kernel. PhD Thesis. Polytechnical University of Madrid, Spain (in Spanish)
- ✓ Council of the European Union European Parliament (2007) Directive 2007/2/EC of the European Parliament and of the Council of 14 March 2007 establishing an Infrastructure for Spatial Information in the European Community (INSPIRE), L108. In: Official Journal of the European Union
- ✓ Crespo MJ, Martí J, Martínez F (2012) Seismic activity rates in the Iberian Peninsula. Proc 15 WCEE, Lisboa

- ✓ de Vicente G, Martín-Velázquez S, Rodríguez-Pascua MA, Muñoz-Martín A, Arcilla M, Andeweg B (2000) Características de los tensores de esfuerzos activos entre la dorsal centroatlántica y la península ibérica. Geotemas 1 (1):95–98 (in Spanish)
- ✓ de Vivente G, Cloethingh S, Muñoz-Martín A, Olaiz A, Stich D, Vegas R, Galindo-Zaldívar J, Fernández-Lozano J (2008) Inversion of moment tensor focal mechanisms for active stresses around the microcontinent Iberia: tectonic implications. Tectonics 27:1–22
- ✓ Ferrater M, Ortuño M, Masana E, Martínez-Díaz JJ, Pallàs R, Perea H, Baize S, García-Meléndez E, Echeverria A, and Rockwell T, Sharp WD, Arrowsmith R (2017) Lateral slip rate of Alhama de Murcia fault (SE Iberian Peninsula) based on a morphotectonic analysis: Comparison with paleoseismological data. Quaternary International 451:87-100
- ✓ Frohlich C, Davis SD (1993) Teleseismic *b* values; or, much ado about 1.0. J Geophys Res 98:631-644
- ✓ García-Mayordomo J (2007) Considering geological data and geologically based criteria in seismic hazard analysis of moderate activity regions: I. Definition and characterization of seismogenic sources. Geogaceta 41 (2):87–90.
- ✓ García-Mayordomo J, Insua-Arévalo J, Martínez-Díaz J, Jiménez-Díaz A, Martín-Banda R, Martín-Alfageme S, Álvarez-Gómez J, Rodríguez-Peces M, Pérez-López R, Rodríguez-Pascua M, Masana E, Perea H, Martín-González F, Giner-Robles J, Nemser E, Cabral J, *QAFI* Compilers Working Group (2012a) The Quaternary Active Faults database of Iberia (*QAFI* v.2.0). J. Iber. Geol. 38 (1):285–302
- ✓ García-Mayordomo J, Insua-Arévalo J, Martínez-Díaz JJ, Perea H, Álvarez-Gómez JA, Martín-González F, González A, Lafuente P, Pérez-López R, Rodríguez-Pascua, MA, Giner-Robles J, Azañón JM, Masana E, Moreno X (2010) Modelo integral de zonas sismogénicas de España. In: Resúmenes de la 1ª Reunión Ibérica sobre Fallas Activas y Paleosismología (in Spanish)
- ✓ García-Mayordomo J, Martínez-Díaz JJ, Capote R, Martín-Banda R, Insua-Arévalo JM, Álvarez-Gómez J, Perea H, González A, Lafuente P, Martínez-González F, Pérez-López R, Rodríguez-Pascua MA, Giner-Robles J,

Azañón J, Masana E, Moreno X, Benito B, Rivas A, Gaspar-Escribano JG, Cabañas L, Vilanova S, Fonseca J, Nemser E, Baize S (2012b) Modelo de zonas sismogénicas para el cálculo de la peligrosidad sísmica en España. In: Actas de la 7 Asamblea Geodesia y Geofísica (in Spanish)

- ✓ Gardner JK, Knopoff L (1974) Is the sequence of earthquakes in Southern California, with aftershocks removed, Poissonian? Bull Seism Soc Am 64(5):1363-1367
- ✓ Gaspar-Escribano JM, Jiménez Peña ME, Pastor JJ, Benito, B (2008) Sobre la medida del tamaño del terremoto y la peligrosidad sísmica en España. 6a Asamblea Hispano-Portuguesa de Geodesia y Geofísica (in Spanish)
- ✓ Gentil P, Justo JL (1983) Terremoto de Carmona de 1504. Sismicidad histórica de la región de la Península Ibérica. Asociación Española de Ingeniería Sísmica 9–16 (in Spanish)
- ✓ Gentil P, Justo JL (1985) Mapa de isosistas del terremoto de Málaga de 1680. Revista de Geofísica 1:65–70 (in Spanish)
- ✓ Ghedhoui R, Deffontaines B, Rabia MC (2016) Neotectonics of coastal Jeffara (southern Tunisia): State of the art. Tectonophysics 676:211-228
- ✓ Ghosh A, Newman AV, Thomas AM, Farmer GT (2008) Interface locking along the subduction megathrust from *b*-value mapping near Nicoya Peninsula, Costa Rica. Geophys Res Lett 35:L01301
- ✓ Giner-Robles JL, Pérez-López R, Silva PG, Jiménez-Díaz A, Rodríguez-Pascua MA (2012) Recent tectonic model for the Upper Tagus Basin (central Spain). Journal of Iberian Geology 38(1):113-126
- ✓ Gómez-Novell O, Ortuño M, García-Mayordomo J, Masana E, Rockwell T, Baize S, López R, Baguer A (2019) Fisrt paleoseismic evidence of the frontal branch of Alhama de Murcia fault zone (Eastern Betics, SE Spain) and its Holocene activity. In: Pre-Workshops Proceedings of the Fault2SHA 4th Workshop. Barcelona, 3-5 June.
- ✓ González Á (2017) The Spanish National Earthquake Catalog: Evolution, precision and completeness. J Seismol 21:435-471
- ✓ Gutenberg B, Richter CF (1941) Seismicity of the Earth. Geol Soc Am 32 (3):163–191

- ✓ Gutenberg B, Richter CF (1944) Frequency of earthquakes in California. Bull Seism Soc Am 34:185–188
- ✓ Gutenberg B, Richter CF (1954) Seismicity of the Earth. Princeton University
- ✓ Hamdache M, Peláez JA, Talbi A, López-Casado C (2010) A unified catalog of main earthquakes for Northern Algeria from A.D. 856 to 2008. Seismol Res Lett 81 (5):732–739
- ✓ Hanks TC, Kanamori H (1979) A moment magnitude scale. J Geophys Res 84(B5):2348-2350
- ✓ Hiemer S, Woessner J, Basili R, Danciu L, Giardini D, Wiemer S (2014) A smoothed stochastic earthquake rate model considering seismicity and fault moment release for Europe. Geophys J Int 198:1159–1172
- ✓ IGME (2015). *QAFI* v.3: Quaternary Faults Database of Iberia. http://info.igme.es/*QAFI*
- ✓ IGN – Instituto Geográfico Nacional (2019a) Terremotos más importantes. http://www.ign.es/web/ign/portal/terremotos-importantes
- ✓ IGN – Instituto Geográfico Nacional (2019b) Catálogo de terremotos. http://www.ign.es/web/ign/portal/sis-catalogo-terremotos
- ✓ IGN – Instituto Geográfico Nacional (2019c) Catálogo de terremotos. http://www.ign.es/web/ign/portal/sis-catalogo-terremotos
- ✓ IGN-UPM Working Group (2013) Actualización de mapas de peligrosidad sísmica en España 2012. Instituto Geográfico Nacional. Madrid, Spain (in Spainsh)
- ✓ Ishimoto M, Iida K (1939) Observations sur les seismes enregistrés par le microsismographe construit derniérement. Bull Earthquake Res Inst 17:443–478 (in French)
- ✓ Jiménez MJ, García-Fernández M, GSHAP Ibero-Maghreb Working Group (1999) Seismic hazard assessment in the Ibero-Maghreb region. Ann Geofis 42(6):1057–1065.
- ✓ Jiménez-Peña ME, Carrera E, Terrasa L, Benito B, Lázaro FJG (1998) Estimación de la peligrosidad sísmica utilizando un SIG. Aplicación al

sureste de la Península Ibérica. In: IX Asamblea Nacional de Geodesia y Geofísica (in Spanish)

- ✓ Johnston AC (1996a) Seismic moment assesment of earthquakes in stable continental regions-I. Instrumental seismicity. Geophys J Int 124:381–414
- ✓ Johnston AC (1996b) Seismic moment assesment of earthquakes in stable continental regions-III. New Madrid 1811–1812, Charleston 1886 and Lisbon 1755. Geophys J Int 126:314–344
- ✓ Justo JL, Gentil P (1983) La falla del terremoto de carmona de 1504. Sismicidad histórica de la región de la Península Ibérica. Asociación Española de Ingeniería Sísmica 20–25 (in Spanish)
- ✓ Justo, JL, Gentil P (1990) El terremoto peninsular del 24 de agosto de 1356. Ingeniería Civil 24, 24–30 (in Spanish)
- ✓ Justo, JL, Salwa C (1998) The 1531 Lisbon earthquake. Bull. Seismol Soc Am 18 (2):319–328
- ✓ Kagan YY (1999) Universality of the seismic moment-frequency relation. Pure Appl Geophys 155:537–573
- ✓ Kamer Y, Hiemer S (2015) Data-driven spatial *b*-value estimation with applications to California seismicity: To *b* or not to *b*. J Geophys Res Solid Earth 120(7):2191–5214
- ✓ Kasahara K (1981) Earthquake Mechanics. Cambridge University Press
- ✓ Kijko A, Sellevoll MA (1987) Estimation of earthquake hazard parameters from incomplete data files. In: Technical Report Seismo-Series. 11 Seismological Observatory, University of Bergen
- ✓ Kijko A, Sellevoll MA (1989) Estimation of earthquake hazard parameters from incomplete data files. Part I. Utilization of extreme and complete catalogs with different threshold magnitudes. Bull Seismol Soc Am 79:645–654
- ✓ Kijko A, Sellevoll MA (1992) Estimation of earthquake hazard parameters from incomplete data files. Part II. Incorporation of magnitude heterogeneity. Bull Seismol Soc Am 82:120–134

- ✓ Kijko A (2012) On Bayesian procedure for maximum earthquake magnitude estimation. Res Geophys 2(1):46-51
- ✓ Kijko A, Smit A (2012) Extension of the Aki-Utsu *b*-value estimator for incomplete catalogs. Bull Seismol Soc Am 102(3):1283-1287
- ✓ Lacan P, Ortuoño M (2012) Active tectonics of the Pyrenees: a review. J Iber Geol 38:9–30
- ✓ Lee K, Yang WS (2006) Historical seismicity of Korea. Bull Seismol Soc Am 71 (3):846–855
- ✓ Lombardi AM (2003) The maximum likelihood estimator of *b*-value for mainshocks. Bull Seismol Soc Am 93 (5):2082–2088
- ✓ Longley PA, Goodchild MF, Maguire DJ, Rhind DW (2015) Geographic Information Science and System. 4th edition. Wiley
- ✓ López C (2008) Nuevas fórmulas de magnitud para la Península Ibérica y su entorno. In: Master Thesis. Complutense University of Madrid, Spain (in Spanish)
- ✓ López-Arroyo A, Martín-Martín AJ, Mezcua-Rodríguez J, Muñoz D, Udías A (1981) El terremoto de Andalucía del 25 de diciembre de 1884. In: Technical report. Instituto Geográfico Nacional (in Spanish)
- ✓ López-Casado C, Sanz de Galdeano C, Delgado J, Peinado MA (1995) The *b* parameter in the Betic Cordillera, Rif and nearby sectors. Relations with the tectonics of the region. Tectonophysics 248:277–292
- ✓ López-Casado C, Molina-Palacios S, Delgado J, Peláez, JA (2000) Attenuation of the intensity with epicentral distance in the Iberian Peninsula. Bull Seismol Soc Am 90(1):34-47
- ✓ Mapa Sismotectónico Working Group (1992) Análisis sismotectónico de la Península Ibérica, Baleares y Canarias. Instituto Geográfico Nacional. Publ Tec 26 (in Spanish)
- ✓ Martín AJ (1984) Riesgo sísmico en la Península Ibérica. PhD Thesis. Instituto Geográfico Nacional, Spain (in Spanish)

- ✓ Martín R, Stich D, Morales J, Mancilla F (2015) Moment tensor solutions for Iberian-Maghreb region during the IberrArray deployment (2009–2013). Tectonophysics 663:261–274
- ✓ Martín-González F, Antón L, Insúa JM, de Vicente G, Martínez-Díaz JJ, Muñoz-Martín A, Heredia N, Olaiz A (2012) Seismicity and potentially active faults in the Northwest and Central-West Iberian Peninsula. Journal of Iberian Geology 38(1):52-69
- ✓ Martínez-Álvarez F, Gutiérrez-Avilés D, Morales-Esteban A, Reyes J, Amaro-Mellado JL, Rubio-Escudero C (2015) A novel method for seismogenic zoning based on triclustering. Application to the Iberian Peninsula. Entropy 17(7):5000–5021
- ✓ Martínez-Solares JM, Mezcua J (2002) Catálogo sísmico de la Península Ibérica (800 a C. - 1900). Instituto Geográfico Nacional, Madrid, Spain (in Spanish)
- ✓ Masana E, Moreno X, Gràcia E, Pallàs R, Ortuño M, López Escudero R, Gómez Novell O, Ruano P, Perea Manera H, Stepancikova P, Khazaradze G (2018) First evidence of paleoearthquakes along the Carboneras Fault Zone (SE Iberian Peninsula): Los Trance site. Geologica Acta 16(4):461-476
- ✓ Mezcua J, Martínez Solares JM (1983) Sismicidad del área Ibero-magrebí. In: Technical Report. 203 Instituto Geográfico Nacional (in Spanish)
- ✓ Mezcua J, Rueda J, García-Blanco, RM (2004) Reevaluation of historic earthquakes in Spain. Seismol Res Lett 75(1):189–204
- ✓ Mezcua J, Rueda J, García-Blanco RM (2011) A new probabilistic seismic hazard study of Spain. Nat Hazards 59(2):1087-1108
- ✓ Mignan A, Werner MJ, Wiemer S, Chen CC, Wu YM (2011) Bayesian estimation of the spatially varying completeness magnitude of earthquake catalogs. Bull Seismol Soc Ame 101(3):1371-1385
- ✓ Mignan A, Woessner J (2012) Estimating the magnitude of completeness for earthquake catalogs, Comm Online Resour Stat Seism Anal (available at http://www.corssa.org)

- ✓ Miguel FD, Payo G (1980) Cálculo de magnitudes de terremotos ocurridos en la península ibérica y áreas tectónicas adyacentes entre 1962 y 1975. In: Technical Report. 13 Instituto Geográfico Nacional (in Spanish)
- ✓ Miguel FD, Payo G (1983) Cálculo de magnitudes de terremotos ocurridos en la Península Ibérica y áreas tectónicas adyacentes entre 1948 y 1961. In: Technical Report. 15 Instituto Geográfico Nacional
- ✓ Ministerio de Fomento (Gobierno de España) (2002) Norma de la Construcción Sismorresistente Española (NCSE-02). In: Boletín Oficial del Estado (in Spanish)
- ✓ Ministerio de Obras Públicas Transporte y Medio Ambiente (Gobierno de España) (1994) Norma de la Construcción Sismorresistente Española (NCSE-94). In: Boletín Oficial del Estado (in Spanish)
- ✓ Molina S (1998) Sismotectónica y peligrosidad sísmica del área de contacto entre Iberia y África. PhD Thesis. University of Granada, Spain
- ✓ Morales-Esteban A, Martínez-Álvarez F, Reyes J (2013) Earthquake prediction in seismogenic areas of the Iberian Peninsula based on computational intelligence. Tectonophysics 593:121–134
- ✓ Morales-Esteban A, Martínez-Álvarez F, Scitovski S, Scitovski R (2014) A fast partitioning algorithm using adaptive Mahalanobis clustering with application to seismic zoning. Comput Geosci 73:132-141
- ✓ Morales-Esteban A, Martínez-Álvarez F, Troncoso A, de Justo JL, Rubio-Escudero C (2010) Pattern recognition to forecast seismic time series. Expert Syst Appl 37(12):8333–8342
- ✓ Mousavi, SM (2017) Mapping seismic moment and *b*-value within the continental-collision orogenic-belt region of the Iranian Plateau. J Geodynamics 103:26-41
- ✓ Nava FA, Márquez-Ramírez VH, Zúñiga FR, Ávila Barrientos L, Quinteros CB (2017) Gutenberg-Richter *b*-value maximum likelihood estimation and sample size. J Seismol 21:127-135
- ✓ Ogata Y, Yamashina K (1986) Unbiased estimate for *b*-value of magnitude frequency. J Phy Earth 34:187-194

- ✓ Olivera C, Redondo E, Lambert J, Riera A, Roca A (2006) Els terratrémols del segles XIV i XV a Catalunya. Institut Cartográfic de Catalunya
- ✓ Page MT, Elst Nvd, Hardebeck J, Felzer K, Michael AJ (2016) Three ingredients for improved global aftershocks forecast: tectonic region, time-dependent catalog incompleteness, and inter-sequence variability. Bull Seismol Soc Am 106(5):2290–2301
- ✓ Peláez JA, Chourak M, Tadili BA, Aït Brahim L, Hamdache M, López-Casado, C, Martínez-Solares JM (2007) A catalog of main Moroccan Earthquakes from 1045 to 2005. Seismol Res Lett 78(6):614-621
- ✓ Peláez JA, López-Casado C (2002) Seismic hazard estimate at the Iberian Peninsula. Pure Appl Geophys 159:2699–2713
- ✓ Pérez-Romero AM, Amaro-Mellado JL (2014) Repercusión del empleo de la proyección UTM en el cálculo de la superficie de fincas. In: Actas del XII Congreso Internacional de Expresión Gráfica aplicada a la Edificación, pp 295-301
- ✓ Reasenberg P (1985) Second-order moment of central California seismicity, 1969–1982. J Geophys Res 90(B7):5479–5495
- ✓ Reyes J, Morales-Esteban A, Martínez-Álvarez F (2013) Neural networks to predict earthquakes in Chile. Appl Soft Comput 13:1314–1328
- ✓ Richter CF (1935) An instrumental earthquake magnitude scale. Bull Seismol Soc Am 25(1):1–32
- ✓ Roberts NS, Bell AF, Main IG (2015) Are volcanic seismic *b*-values high, and if so when? J Volcanol Geotherm Res 308:127–141
- ✓ Rodríguez-Pascua MA, Silva-Barroso PG, Giner-Robles JL, Pérez-López R, Perucha MA, Martín-González F (2013) Arqueolosismología: una herramienta para la sismología y la protección del patrimonio. Revista Otarq 1:151–169
- ✓ Roest WR, Srivastava SP (1991) Kinematics of the plate boundaries between Eurasia, Iberia, and Africa in the north atlantic from the late cretaceous to the present. Geology 19:613–616

- ✓ Rueda J, Mezcua J (2002). Estudio del terremoto de 23 de septiembre de 2001 en Pego (Alicante). Obtención de una relación mbLg-Mw para la Península Ibérica. Rev Soc Geol España 15:159–173
- ✓ Rueda J, Mezcua J (2005) Near-real-time seismic moment-tensor determination in Spain. Seismol Res Lett 76(4):455–465
- ✓ Samardjieva E, Payo G, Badal J (1999) Magnitude formulae and intensity-magnitude relations for early instrumental earthquakes in the Iberian region. Nat Hazards 19:189–204
- ✓ Schorlemmer D, Wiemer S, Wyss M (2005) Variations in earthquake-size distribution across different stress regimes. Nature 437:539–542
- ✓ Secanell R, Goula X, Susagna T, Fleta J, Roca A (1999) Mapa de zonas sísmicas de Cataluña. In: Actas del 1 Congreso Nacional de Ingeniería Sísmica
- ✓ Shi Y, Bolt A (1982) The Standard error of the magnitude-frequency *b* value. Bull Seismol Soc Ame 72(5):1677-1687
- ✓ Singh C, Singh S (2015) Imaging *b*-value variation beneath the Pamir-Hindu Kush Region. Bull Seism Soc Am 105:808-815
- ✓ Srivastava SP, Roest WR, Kovacs LC, Oakey G, Levesque S, Verhoef J, Macnab R (1990) Motion of Iberia since the Late Jurassic: results from detailed aeromagnetic measurements in the Newfoundland Basin. Tectonophysics 184:229–260
- ✓ Stepp JC (1972) Analysis of completeness of the earthquake sample in the Puget Sound area and its effect on statistical estimates of earthquake hazard: Proceedings of the International Conference on Microzonation 2: 897-910
- ✓ Stich D, Ammon CJ, Morales J (2003) Moment tensor solutions for small and moderate earhquakes in the Ibero-Maghreb region. J Geophys Res 108(B3), 2148
- ✓ Stich D, Batlló J, Maciá R, Teves-Costa P, Morales J (2005) Moment tensor inversion with single-component historical seismograms: the 1909 Benavente (Portugal) and Lambesc (France) earthquakes. Geophys J Int 162(5):850–858

- ✓ Stich D, Batlló J, Morales J, Maciá R, Dineva S (2003) Source parameters of the Mw =6.1, 1910 Adra earthquake (southern Spain). Geophys J Int 155:539–546
- ✓ Stich D, Mancilla FL, Morales J (2005) Crust-mantle coupling in the Gulf of Cadiz (SW-Iberia). Geophys Res Lett 32, L13306.
- ✓ Stich D, Martín R, Morales J (2010) Moment tensor inversion for Iberia-Maghreb earthquakes 2005–2008. Tectonophysics 483:390–398
- ✓ Stucchi M, Rovida A, Gomez Capera AA, Alexandre P, Camelbeeck T, Demircioglu MB, Gasperini P, Kouskouna V, Musson RMW, Raduliana M, Sesetyan K, Vilanova S, Baumont D, Bungum H, Fäh D, Lenhardt W, Makropoulos K, Martínez-Solares JM, Scotti O, Őivcic M, Albini P, Batlló J, Papaioannou C, Tatevossian R, Locati M, Meletti C, Viganó D, Giardini D (2013) The SHARE European Earthquake Catalog (SHEEC) 1000–1899. J Seismol 17(2):523–544
- ✓ Talbi A, Yamazaki F (2009) Sensitivity analysis of the parameters of earthquake recurrence time power law scaling. J Seismol 13(1):53-72
- ✓ Teves-Costa P, Batlló J, Cabral J (2017) The Lower Tagus Valley (Portugal) earthquakes: Lisbon 26 January 1531. Física de la Tierra 29:61-84
- ✓ and Benavente 23 April 1909
- ✓ Tinti S, Mulargia F (1987) Confidence intervals of *b*-values for grouped data. Bull Seismol Soc Am 77:2125-2134
- ✓ Tormann T, Wiemer S, Mignan A (2014) Systematic survey of high-resolution *b*-value imaging along Californian faults: Inference on asperities. J Geophys Res Solid Earth 119:5830–5833
- ✓ Torrecillas C, Berrocoso M, García-García A (2006) The Multidisciplinary Scientific Information Support System (SIMAC) for Deception Island. In: Fütterer D, Damaske D, Kleinschmidt G, Miller H, Tessensohn F (eds) Antarctica. Springer, Berlin Heidelberg, pp. 397-402
- ✓ Utsu T (1965) A method for determining the value of *b* in a formula *log n = a - bM* showing the magnitude-frequency relation for earthquakes. Geophys Bull Hokkaido Univ 13:99-103

- ✓ Veith KF, Clawson GE (1972) Magnitude from short period p-wave data. Bull Seismol Soc Am 62(2):435–452
- ✓ Vilanova SP, Fonseca JFBD (2007) Probabilistic seismic hazard assessment for Portugal. Bull Seismol Soc Am 97(5):1702–1717
- ✓ Weichert DH (1980) Estimation of the earthquake recurrence parameters for unequal observation periods for different magnitudes. Bull Seismol Soc Am 70:1337–1346
- ✓ Weichert DH (1980) Estimation of the earthquake recurrence parameters for unequal observation periods for different magnitudes. Bull Seismol Soc Am 70:1337-1346
- ✓ Wiemer S (2001) A software package to analyze seismicity: ZMAP. Seismol Res Lett 72:373–382
- ✓ Wiemer S, Wyss M (2000) Minimum magnitude of complete reporting in earthquake catalogs: Examples from Alaska, the Western United States, and Japan. Bull Seismol Soc Am 90(4):859–869
- ✓ Wiemer S, Wyss M (2002) Mapping spatial variability of the frequency-magnitude distribution of earthquakes. Adv Geophys 45:259–302
- ✓ Woessner J, Danciu L, Giardini D, Crowley H, Cotton F, Grünthal G, Valensise G, Arvidsson R, Basili R, Demircioglu MN, Hiemer S, Meletti C, Musson RW, Rovida AN, Sesetyan K, Stucchi M, SHARE Consortium (2015) The 2013 European seismic hazard model: key components and results. Bull Earthq Eng 13(12):3553–3596
- ✓ Zhao YZ, Wu ZL (2008) Mapping the *b*-values along the Longmenshan fault zone before and after the 12 May 2008, Wenchuan, China, MS 8.0 earthquake. Nat Hazards Earth Syst Sci 8:1375-1385